Lecture Note #2 (Fall, 2022)

Surface and Adsorbate Structure

1. Surface geometric structure
2. Surface electronic structure
3. Surface vibrational structure

Including HW #1(1-4) due: Sept. 21
#2(1-4) due: Sept. 28

Reading: Kolasinski, ch.1

Surface science

3-dimemsional world vs. 2-D world

Edwin Abbott Abbott, *Flatland: A Romance of Many Dimensions*(플랫랜드: 다차원 세계의 이야기) (1884)

chemical reaction,
catalysis, synthesis…

Geometric structure → geometric effect

Electronic structure → electronic effect

} ensemble effect

Vibrational structure → vibrational effect (phonon, plasmon…)

Clean surfaces

- Ultra-high vacuum (UHV) conditions → atomically clean surfaces

the Flux, F, of molecules striking the surface of unit area at pressure P

$$F = \frac{N_A P}{\sqrt{2\pi MRT}} \qquad (1.2)$$

Z_w in (1.0.1) in textbook

or

$$F\ (\text{atoms}^{-1}\,\text{cm}^{-2}\,\text{s}^{-1}) = 2.63 \times 10^{20} \frac{P\ (\text{Pa})}{\sqrt{M\ (\text{g mol}^{-1})T(\text{K})}} \qquad (1.3)$$

or

$$F\ (\text{atoms}\,\text{cm}^{-2}\,\text{s}^{-1}) = 3.51 \times 10^{22} \frac{P\ (\text{Torr})}{\sqrt{M\ (\text{g mol}^{-1})T(\text{K})}} \qquad (1.4)$$

M: average molecular weight of gases species, N_A: Avogadro's number
$m = M/N_A$, $k_B = R/N_A$

$$Z_w = P/(2\pi m k_B T)^{1/2}$$

(1.0.1) in textbook

The collision flux (F or Z_w) (from Atkins' Phys. Chem.)

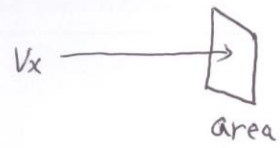

time interval

All molecules in the volume, $Av_x \cdot \Delta t$
(striking A)

Total # of collisions, $N \cdot Av_x \Delta t$

N: # density of molecules

Considering a range of velocities and the probability distribution of velocities

$$\# \text{ of collisions} = N A \Delta t \int_0^\infty v_x f(v_x)\, dx$$

where $f(v_x) = \left(\frac{M}{2\pi RT}\right)^{1/2} e^{-Mv_x^2/2RT}$ —(1)

The collision flux (F or Z_w): # of collision divided by A and Δt

$$Z_w = N \int_0^\infty v_x f(v_x)\, dx$$

Using (1), $\int_0^\infty v_x f(v_x)\, dv_x = \left(\frac{m}{2\pi kT}\right)^{1/2} \int_0^\infty v_x e^{-mv_x^2/2kT} \cdot dv_x = \left(\frac{kT}{2\pi m}\right)^{1/2}$

$\left(\because \left(\frac{M}{2\pi RT}\right)^{1/2} = \left(\frac{m}{2\pi kT}\right)^{1/2}\right)$

and using $\int_0^\infty x e^{-ax^2} dx = \frac{1}{2a}$

Therefore

$$Z_w = N\left(\frac{kT}{2\pi m}\right)^{1/2} = \left(\frac{P}{kT}\right)\left(\frac{kT}{2\pi m}\right)^{1/2} = \frac{P}{(2\pi m kT)^{1/2}}$$

$\left(\because N = \frac{nN_A}{V} = \frac{P}{kT}\right)$

Fundamental Constants

Constant	Symbol	Value
Speed of light	c	2.998×10^{10} cm/sec $= 2.998 \times 10^{8}$ m/sec
Planck's constant	h	6.626×10^{-27} erg · sec $= 6.626 \times 10^{-34}$ J · sec
Avogadro's number	N_A	6.022×10^{23} molecules/mole
Electron charge	e	1.602×10^{-21} coulombs $= 4.803 \times 10^{-10}$ esu
Gas constant	R	1.987 cal/deg/mole $= 8.315$ J/deg/mole
Boltzmann's constant	k_B	1.381×10^{-16} erg/deg $= 1.381 \times 10^{-23}$ J/deg $= R/N_A$
Gravitational constant	g	9.807 m/sec^2
Permittivity of vacuum	ϵ_0	8.854×10^{-12} C^2/J/m

Other Conversion Factors

1 atm	=	1.013×10^5 kg/m/sec^2
	=	1.013×10^5 N/m^2
	=	1.013×10^5 Pa
1 torr	=	133.3 N/m^2 =133.3 Pa
1 debye	=	3.336×10^{-30} C · m

1 atm = 1013 mbar = 1.013 bar

1 Pa = 1 N/m^2 = 10^{-5} bar =
7.5 x 10^{-3} torr = 9.8692 x 10^{-6} atm

1 hPa(hecto) = 100 Pa = 1 mbar
1 atm = 1013.25 hPa

Energy Conversion Table[a]

	erg	joule	cal	eV	cm^{-1}
1 erg	1	10^{-7}	2.389×10^{-8}	6.242×10^{11}	5.034×10^{15}
1 joule	10^7	1	0.2389	6.242×10^{18}	5.034×10^{22}
1 cal	4.184×10^7	4.184	1	2.612×10^{19}	2.106×10^{23}
1 eV	1.602×10^{-12}	1.602×10^{-19}	3.829×10^{-20}	1	8066.0
1 cm^{-1}	1.986×10^{-16}	1.986×10^{-23}	4.747×10^{-24}	1.240×10^{-4}	1

[a] For example, 1 erg $= 2.389 \times 10^{-8}$ cal.

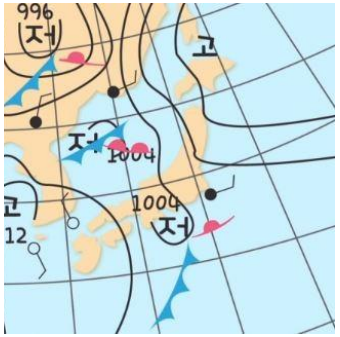

strong typoon <950 hPa

- UHV (ultra-high vacuum, <1.33 x 10^{-7} Pa = 10^{-9} Torr) → to maintain a clean surface for ~ 1h

P = 4 x 10^{-4} Pa (3 x 10^{-6} torr), M = 28 g/mole (N_2), T = 300 K
→ Z_w (or F) = 10^{15} molecules/cm^2·sec
→ surface ~10^{15}/cm^2 (bulk density(ρ) ~1 g/cm^3 = 5 x 10^{22} (ice 18g = 6 x 10^{23}) → surface density, $\rho^{2/3}$ ~ 10^{15}/cm^2)

→ 1sec for 1 monolayer on surface (100% covered)

1 x 10^{-6} torr → 1sec to cover monolayer if sticking coefficient s = 1

Unit of gas exposure is 1.33 x 10^{-4} Pa-sec (10^{-6} torr-sec) = "L (Langmuir)"

1 L exposure in 1sec → 1 monolayer if s = 1 (each incident gas molecule "sticks")

1.33 x 10^{-7} Pa (10^{-9} torr) → 10^3 sec before a surface is covered completely
(1h = 3600 s)

HW #1(1)

Ultra-high vacuum (UHV)

The earth's average atmospheric pressure is 1 bar (101.3kPa)

In outer space, the pressure is 1.322×10^{-11} Pa – essentially zero, since there is very little air

The moon has 3×10^{-10} Pa

Mars has mostly of carbon dioxide, 750 Pa or about 1/100 of the Earth's

1. Surface geometric structure

1st layer of close-packed spheres

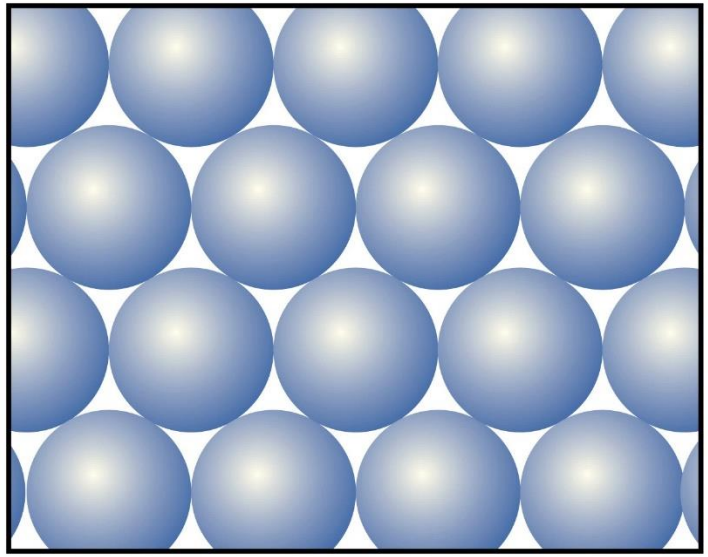

Figure 20-32
Atkins Physical Chemistry, Eighth Edition

2nd layer of close-packed spheres

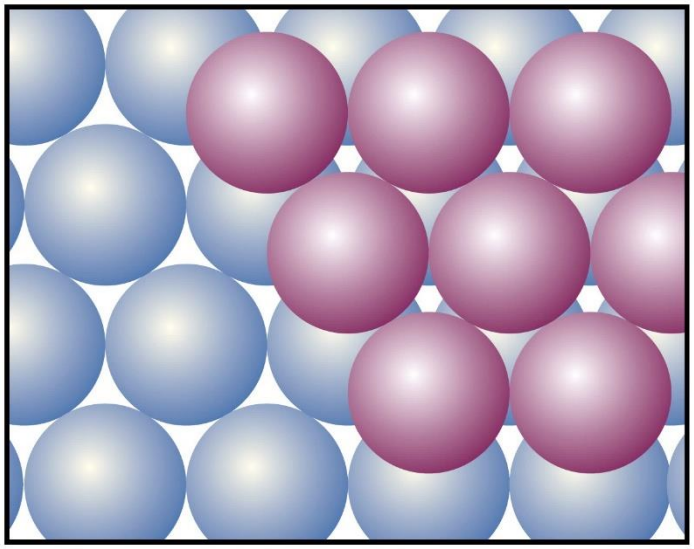

Figure 20-33
Atkins Physical Chemistry, Eighth Edition

3rd layer of close-packed spheres: ABA (hexagonal close-packed)
ABC (cubic close-packed, e.g. fcc(face-centered cubic))

hcp: ABABAB…
ccp: ABCABC…

Atkins, *Physical Chemistry*

hcp

fcc (one example of ccp)

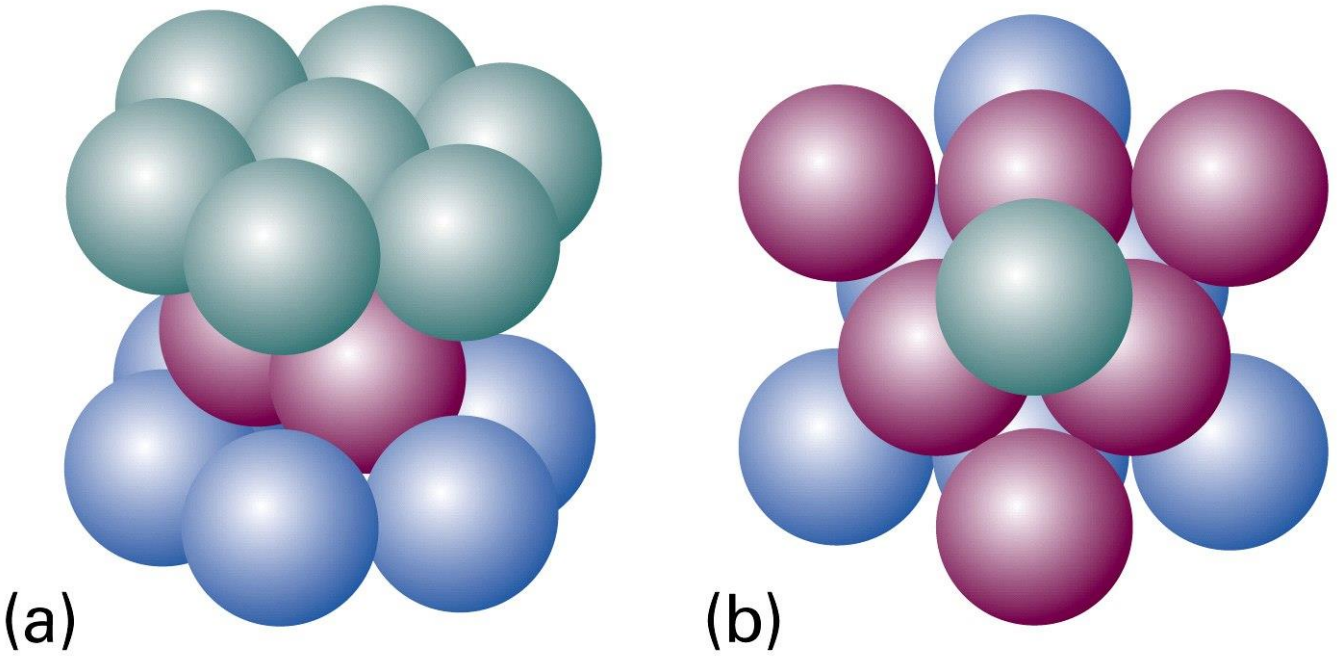

Figure 20-35
Atkins Physical Chemistry, Eighth Edition

fcc (face-centered cubic)

Atkins, *Physical Chemistry*

close-packed spheres (hcp, ccp)

coordination numbers = 12
packing fraction: 0.740 (26% empty space)

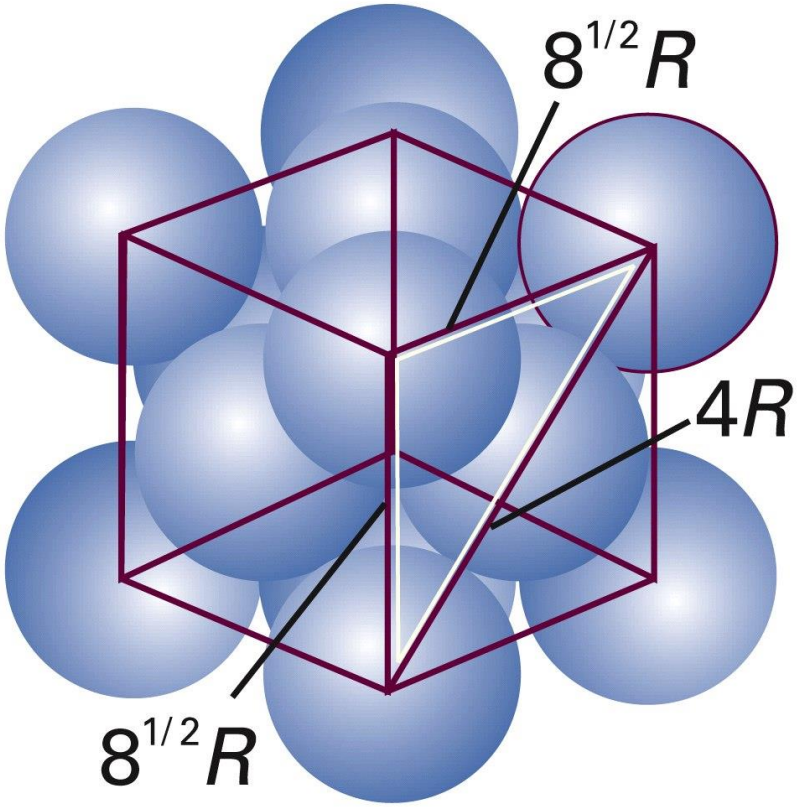

Figure 20-36
Atkins Physical Chemistry, Eighth Edition

a (or a_0): bulk lattice parameter (or lattice constant) in unit cell

$a = 2\sqrt{2}R$
Volume of unit cell = a^3
Each cell = 4 spheres
Volume of each sphere = $(4/3)\pi R^3$
Fraction = $[4 \times (4/3)\pi R^3] / a^3 = 0.740$

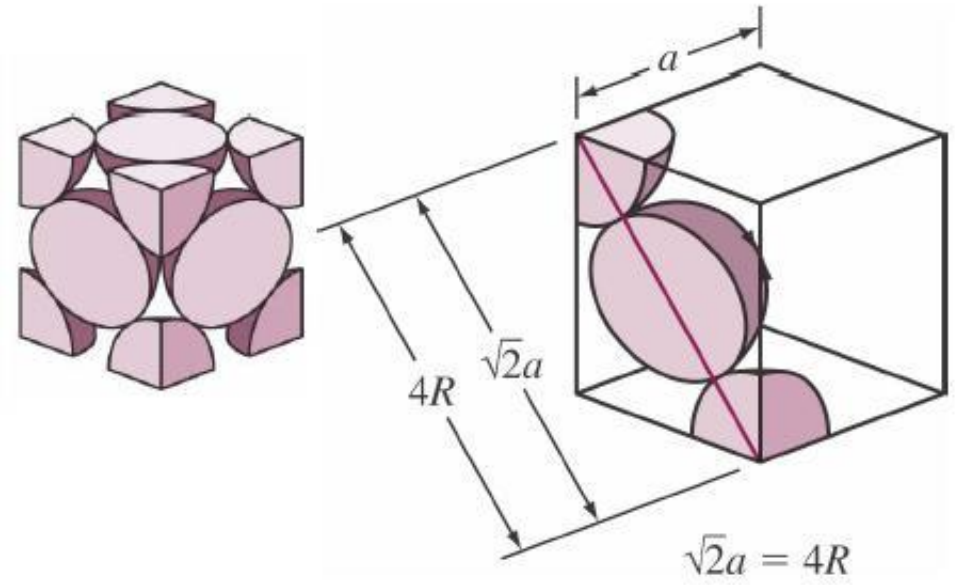

Table 20.2 The crystal structures of some elements

Structure	Element
hcp*	Be, Cd, Co, He, Mg, Sc, Ti, Zn Ru
fcc* (ccp, cubic F)	Ag, Al, Ar, Au, Ca, Cu, Kr, Ne, Ni, Pd, Pb, Pt, Rh, Rn, Sr, Xe
bcc (cubic I)	Ba, Cs, Cr, Fe, K, Li, Mn, Mo, Rb, Na, Ta, W, V
cubic P	Po

* Close-packed structures.

bcc (body-centered cubic)
coordination numbers = 8
packing fraction: 0.680 (32% empty space)

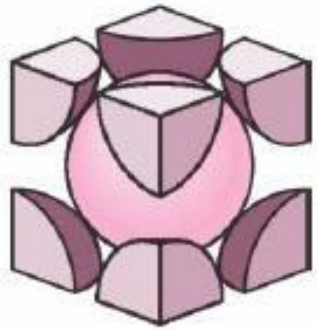

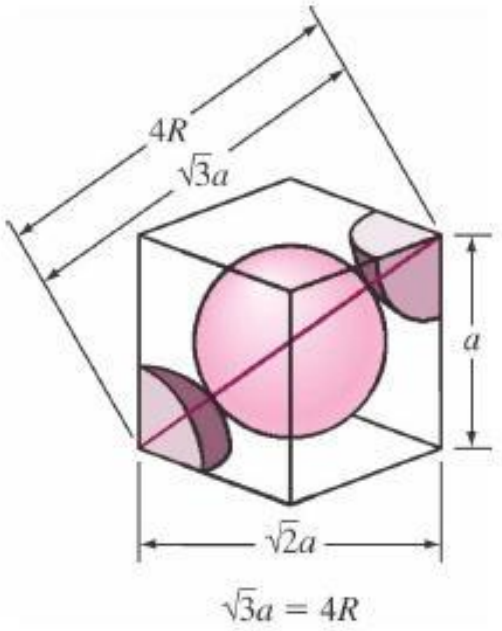

Atkins, *Physical Chemistry*

Miller index: crystal planes

plane (hkl): reciprocals of intersection distances, set {001} = (100), (010), (001)

direction [hkl]: direction normal to a plane (hkl) (면에 수직방향)

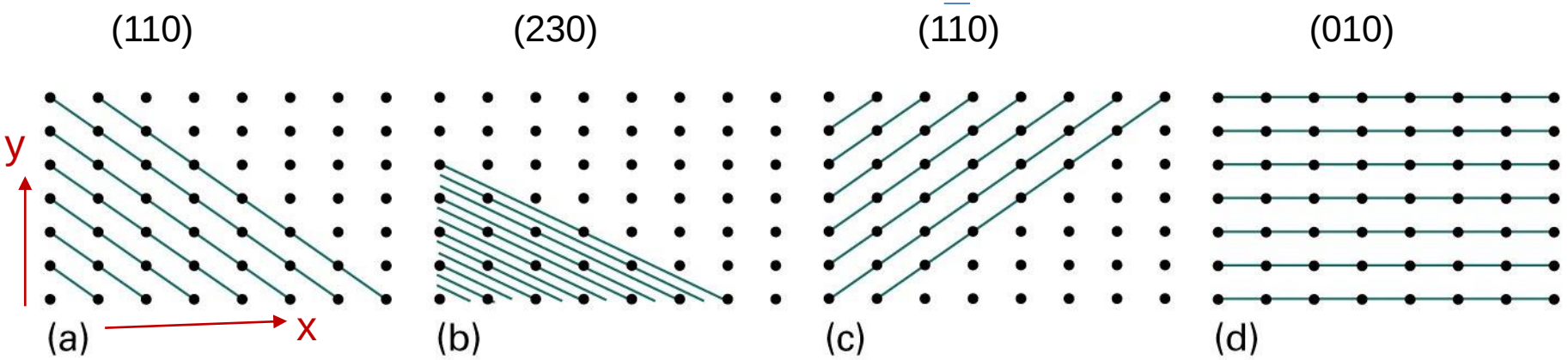

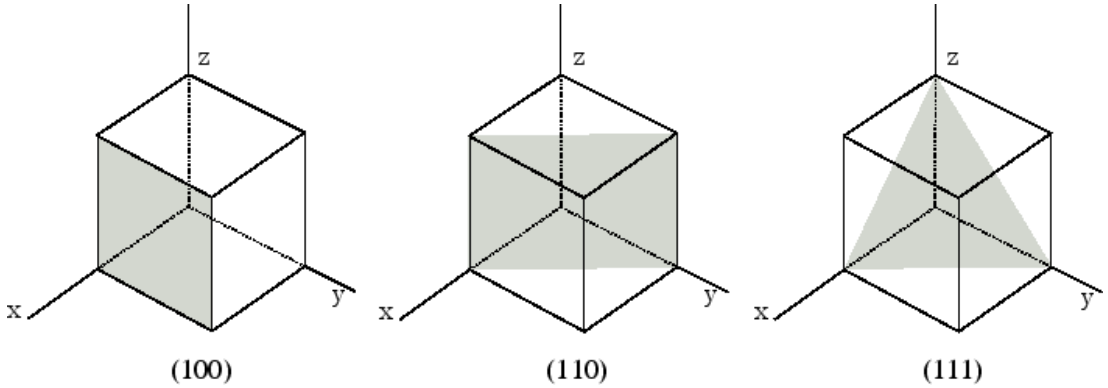

Plane and direction

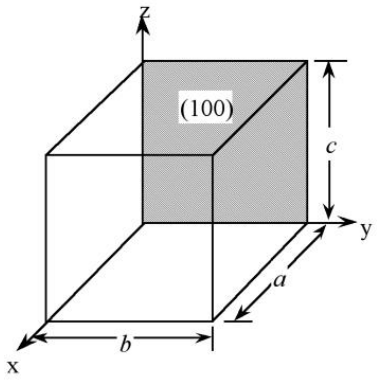

$$\frac{h}{1}, \frac{k}{\infty}, \frac{l}{\infty} = (100)$$

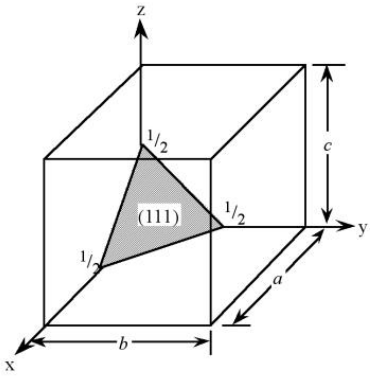

$$\frac{h}{1}, \frac{k}{1/2}, \frac{l}{1/2} = (222) = (111)$$

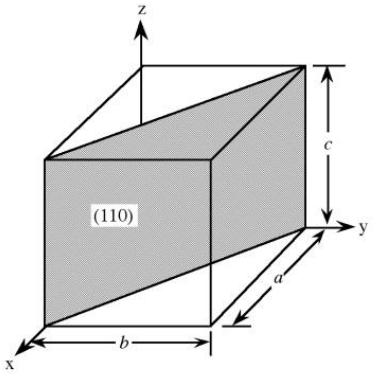

$$\frac{h}{1}, \frac{k}{1}, \frac{l}{\infty} = (110)$$

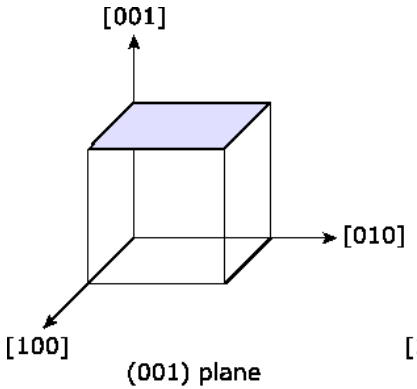

(001) plane

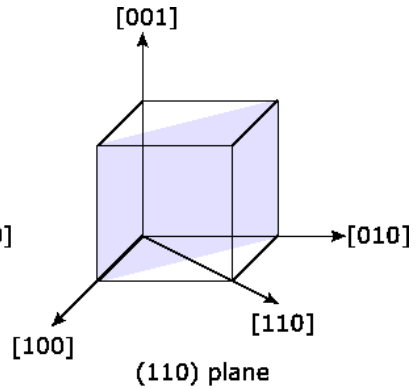

(110) plane

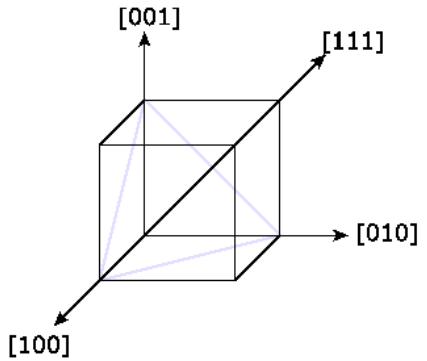

(111) plane

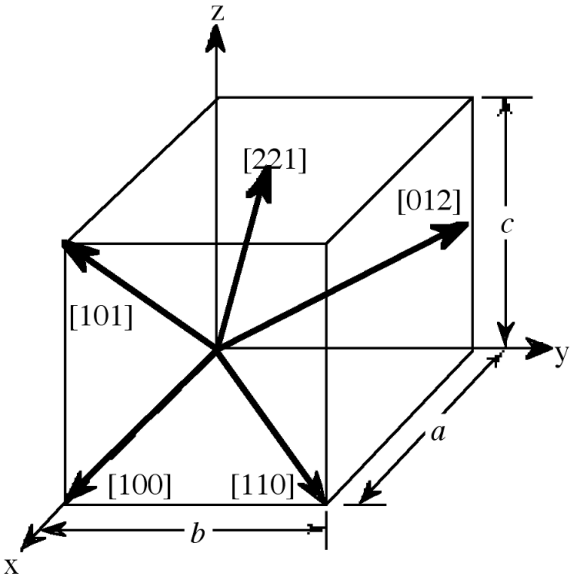

fcc

a_0

lattice constant

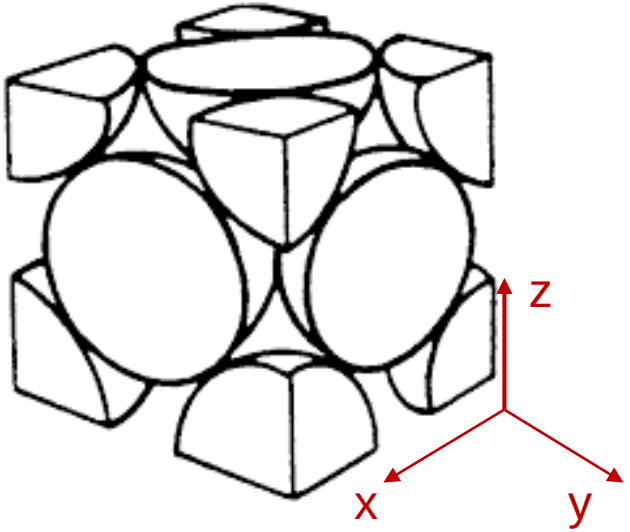

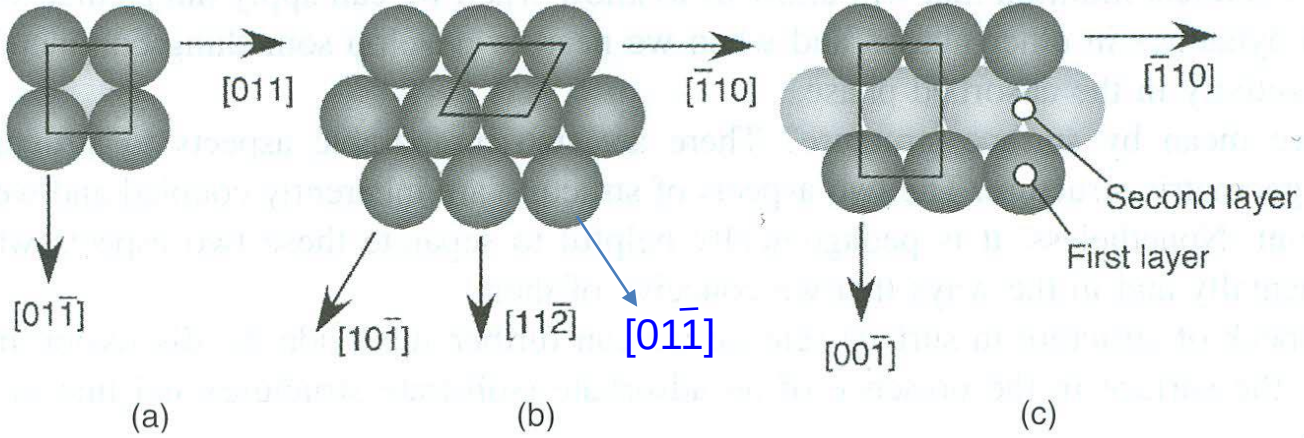

Figure 1.1 *Hard sphere representations of face-centred cubic (fcc) low index planes: (a) fcc(100); (b) fcc(111); (c) fcc(110).*

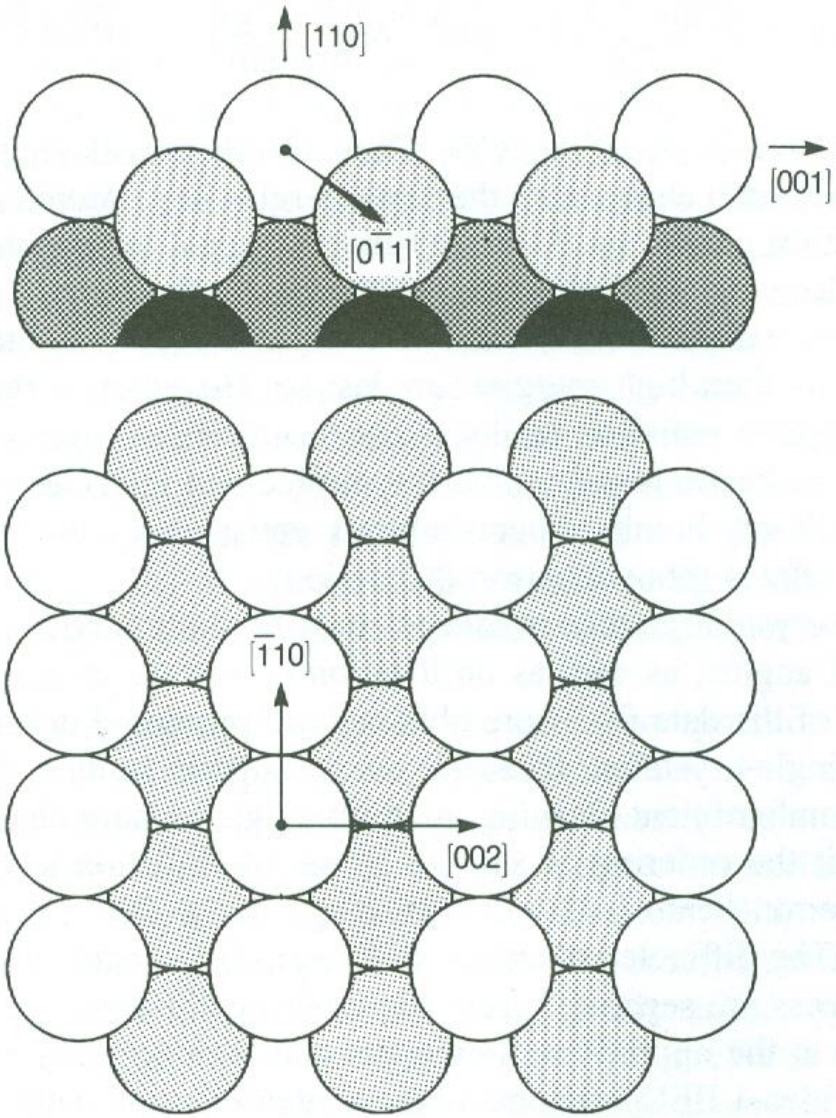

Figure 2.8. Top views and side views of the face-centered cubic (fcc) crystal surfaces: (**a**) (110), (**b**) (100), and (**c**) (111)

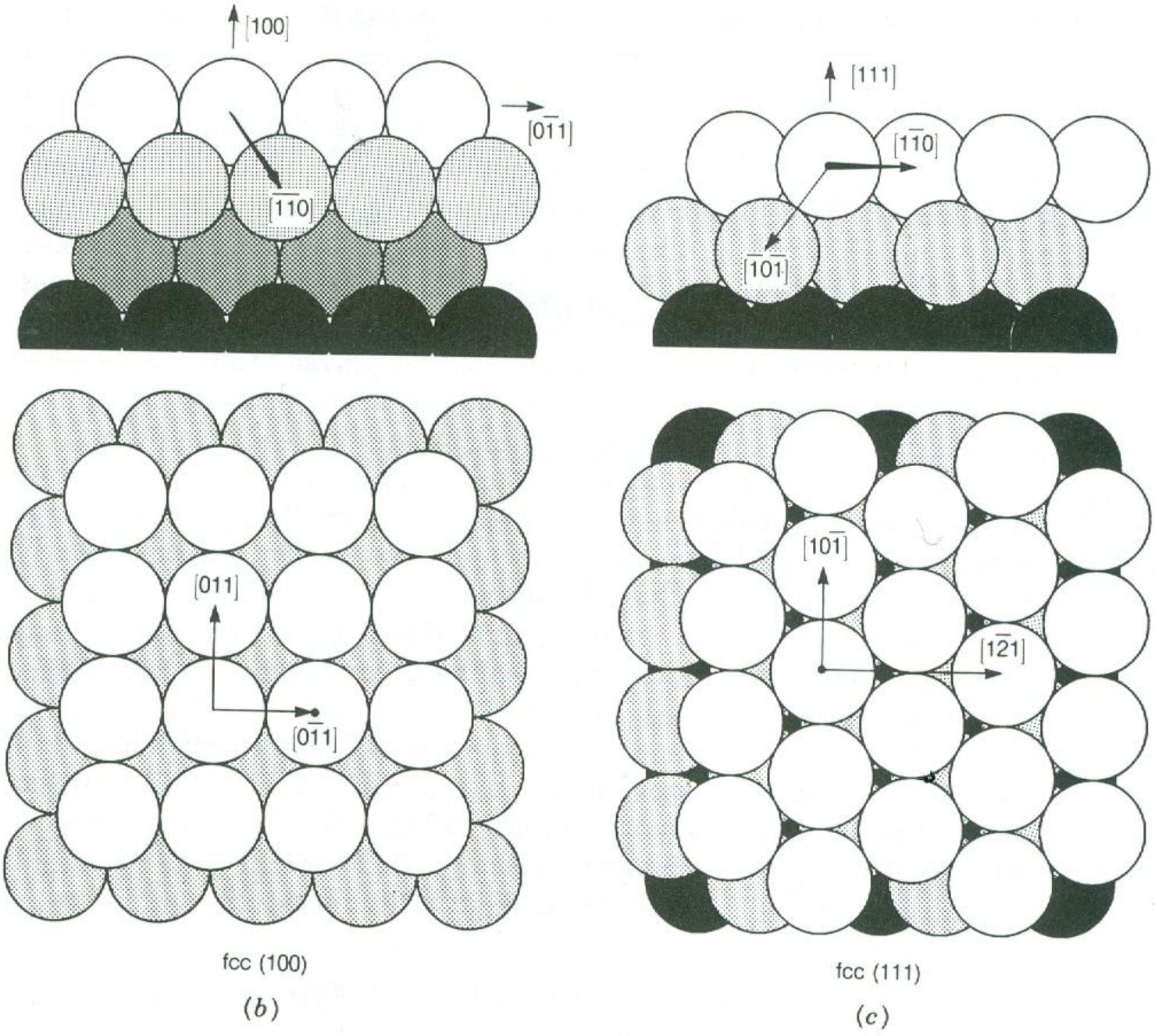

Figure 2.8. (*Continued*)

- Ideal structure of low-Miller-index surfaces of face-centered cubic (fcc)

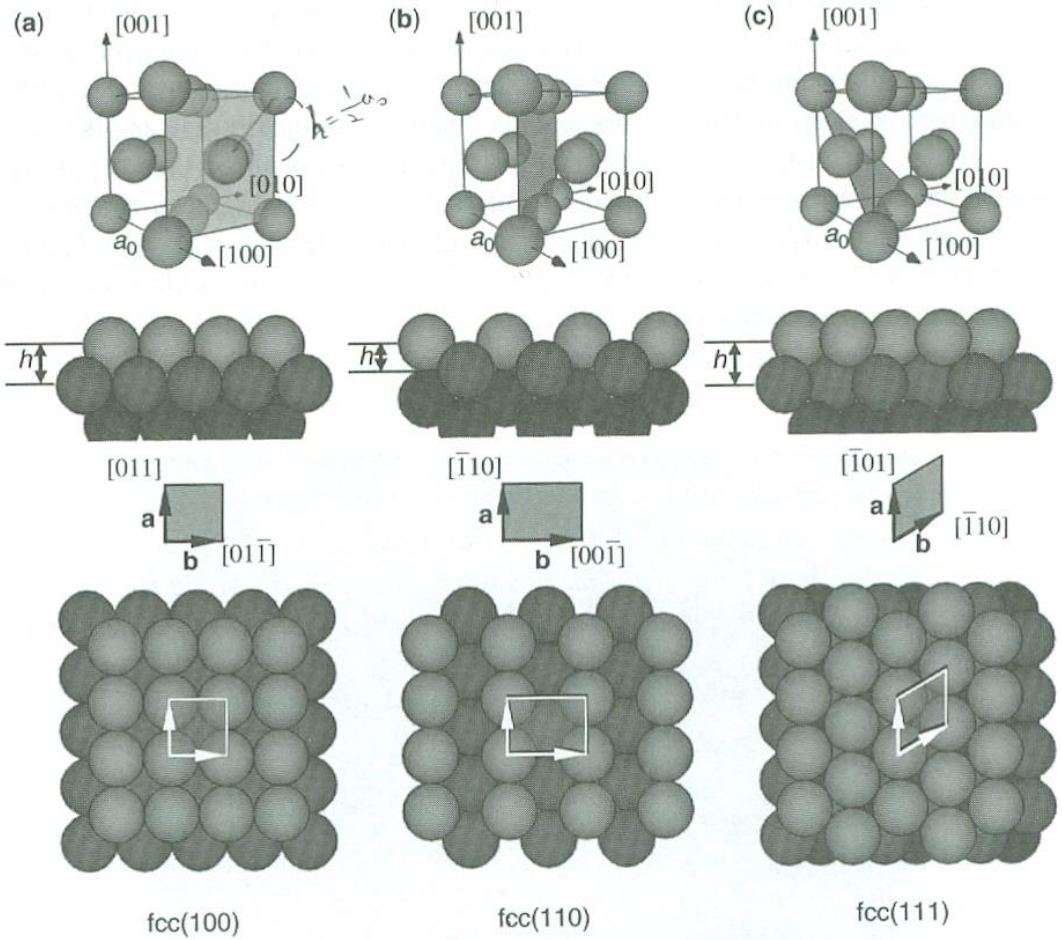

Figure 2.8. Unreconstructed surfaces of the fcc crystal surfaces, where a_0 is the lattice constant of the crystal, **a** and **b** are the unit-cell vectors, and h is the distance between the first and the second layer. (a) fcc(100): $|\mathbf{a}| = |\mathbf{b}| = (\sqrt{2}/2)a_0$, and $h = \frac{1}{2}a_0$. To obtain the second layer, shift the first layer by $\frac{1}{2}\mathbf{a} + \frac{1}{2}\mathbf{b}$ in the plane, then $\frac{1}{2}a_0$ in the $[\bar{1}00]$ direction. (b) fcc(110): $|\mathbf{a}| = (\sqrt{2}/2)a_0$, $|\mathbf{b}| = a_0$, and $h = (\sqrt{2}/4)a_0$. To obtain the second layer, shift the first layer by $\frac{1}{2}\mathbf{a} + \frac{1}{2}\mathbf{b}$ in the plane, then $(\sqrt{2}/4)a_0$ in the $[\bar{1}\bar{1}0]$ direction. (c) fcc(111): $|\mathbf{a}| = |\mathbf{b}| = (\sqrt{2}/2)a_0$, and $h = (\sqrt{3}/3)a_0$. To obtain the second layer, shift the first layer by $\frac{1}{3}\mathbf{a} + \frac{1}{3}\mathbf{b}$ in the plane, then $(\sqrt{3}/3)a_0$ in the $[\bar{1}\bar{1}\bar{1}]$ direction. (See color insert.)

HW #1(2)

bcc

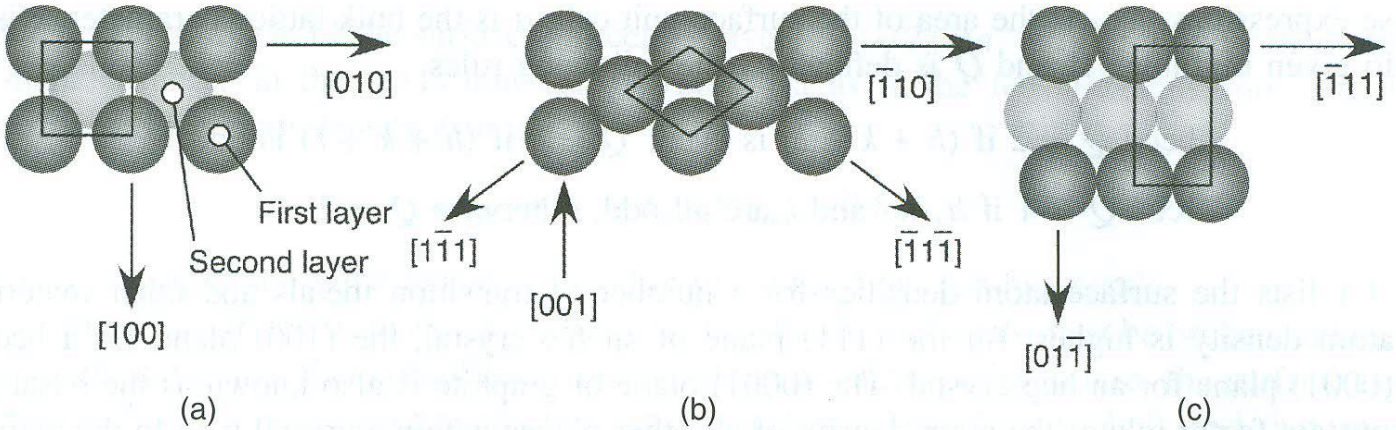

Figure 1.2 *Hard sphere representations of body-centred cubic (bcc) low index planes: (a) bcc(100); (b) bcc(110); (c) bcc(211).*

hcp(hexagonal close-packed)

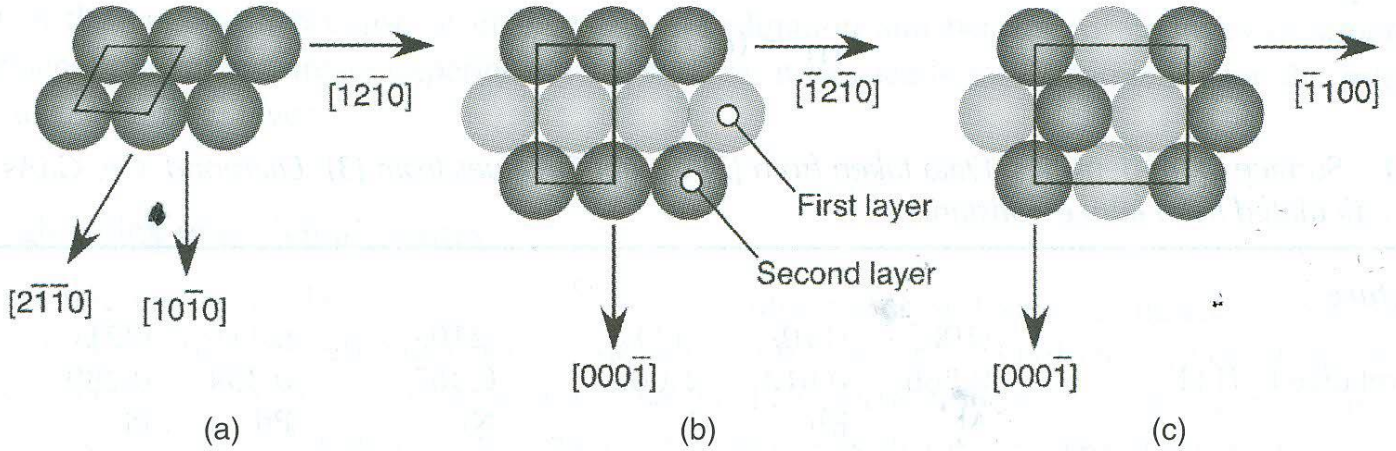

Figure 1.3 *Hard sphere representations of hexagonal close-packed (hcp) low index planes: (a) hcp*(001) = (0001)*; (b) hcp*(10$\bar{1}$0) = *hcp*(100)*; (c) hcp*(11$\bar{2}$0) = *hcp*(110)*.*

HW #1(3)

hcp $(a_1\ a_2\ a_3\ c) = (a_1\ a_2\ c)$

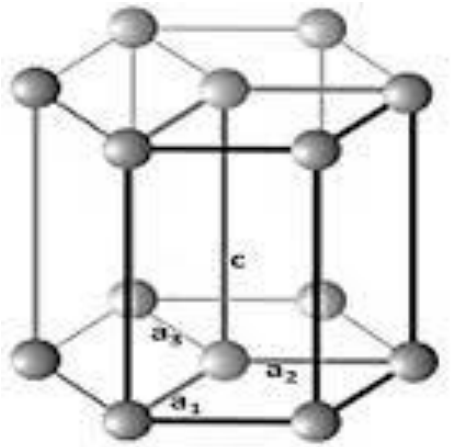

(a)

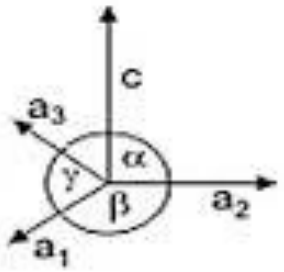

$a_1=a_2=a_3\neq c$

$\alpha=\gamma=90°\ \beta=120°$

(b)

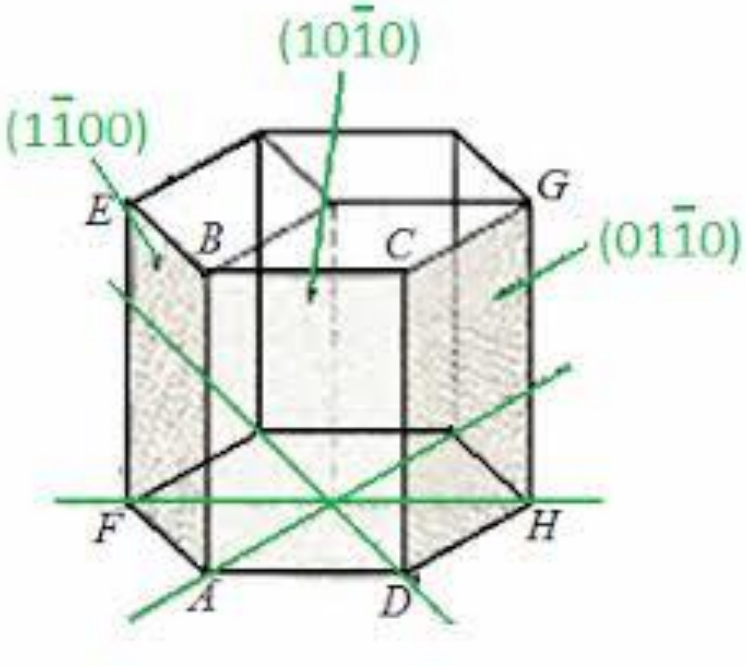

α: angle a_2 and c

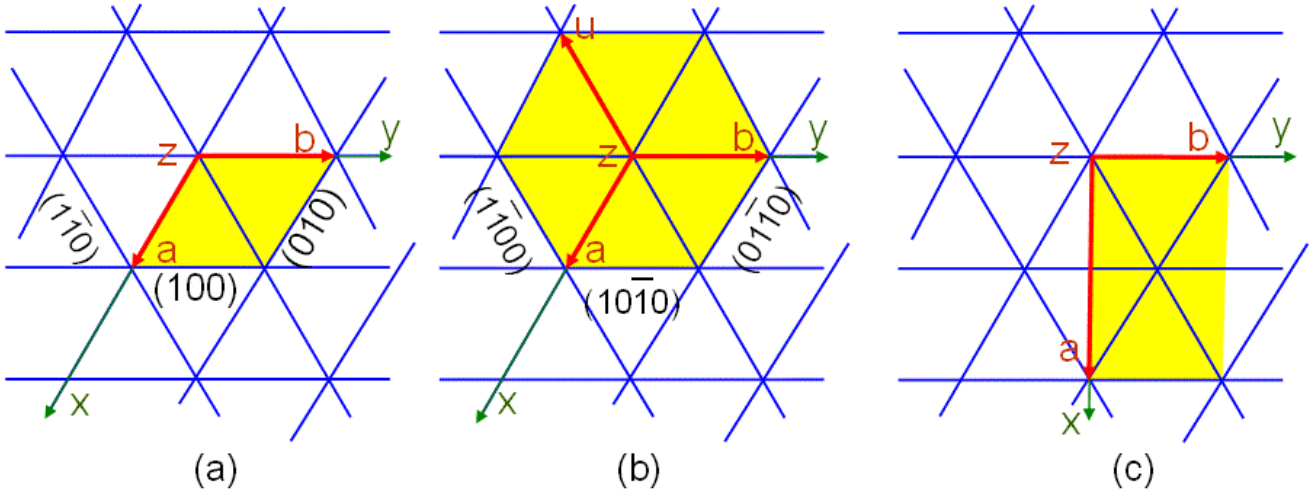

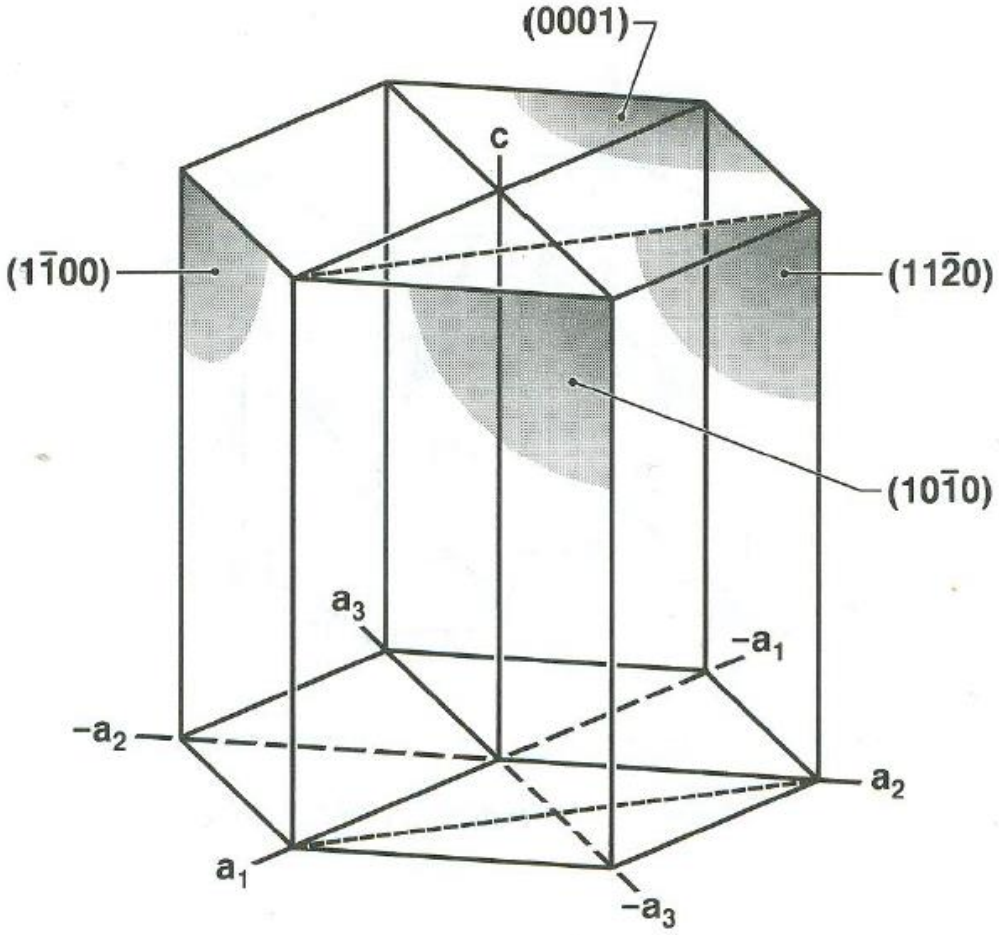
(0001)
c
(1$\bar{1}$00)
(11$\bar{2}$0)
(10$\bar{1}$0)
a_3
$-a_1$
$-a_2$
a_2
a_1
$-a_3$

- Ideal structure of low-Miller-index surfaces of body-centered cubic (bcc)

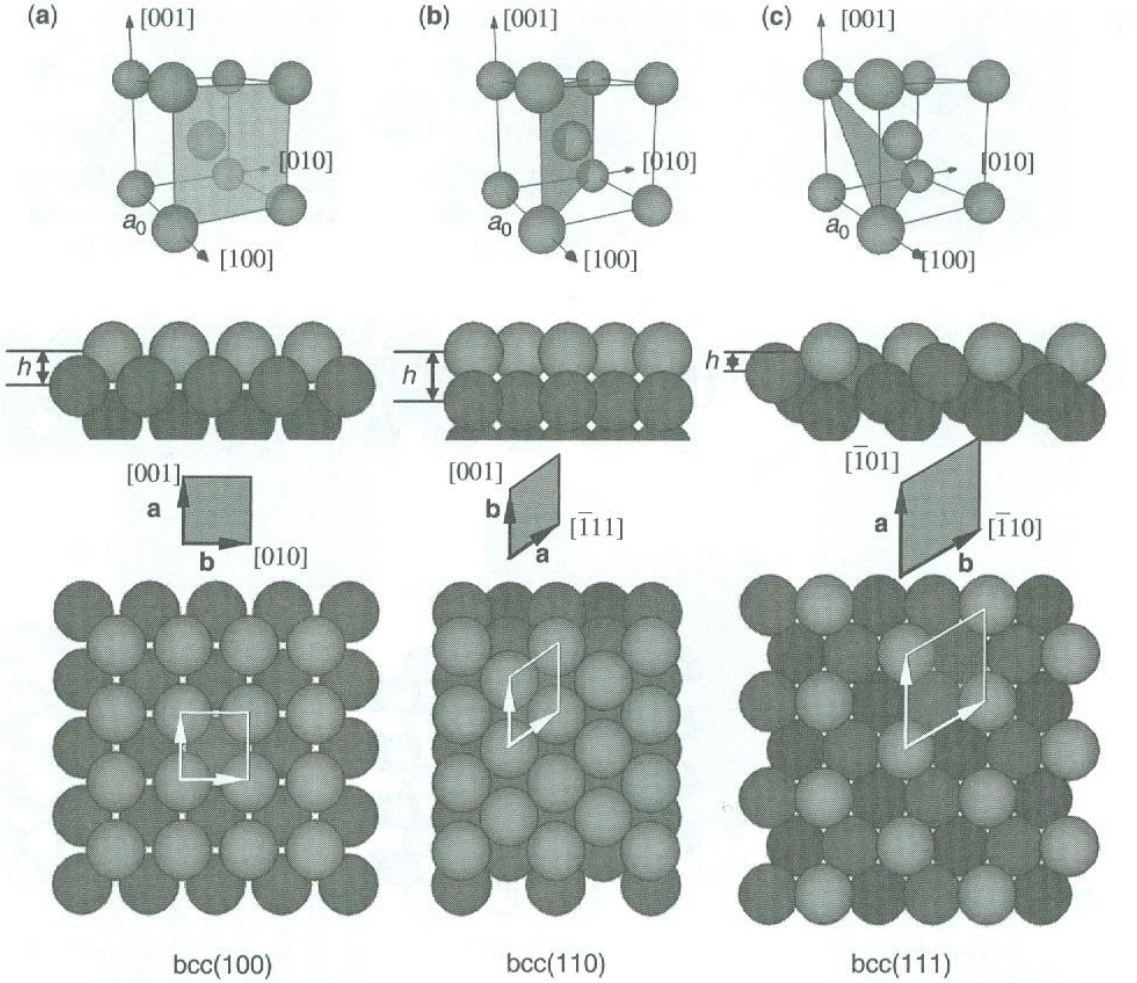

Figure 2.9. Unreconstructed surfaces of the bcc crystal surfaces, where a_0 is the lattice constant of the crystal, **a** and **b** are the unit-cell vectors, h is the distance between the first and the second layer. (a) bcc(100): $|\mathbf{a}| = |\mathbf{b}| = a_0$, and $h = \frac{1}{2}a_0$. To obtain the second layer, shift the first layer by $\frac{1}{2}\mathbf{a} + \frac{1}{2}\mathbf{b}$ in the plane, then $\frac{1}{2}a_0$ in the $[\bar{1}00]$ direction. (b) bcc(110): $|\mathbf{a}| = (\sqrt{3}/2)a_0$, $|\mathbf{b}| = a_0$, and $h = (\sqrt{2}/2)a_0$. To obtain the second layer, shift the first layer by $\frac{1}{2}\mathbf{b}$ in the plane, then $\frac{1}{2}a_0$ in the $[\bar{1}\bar{1}0]$ direction. (c) bcc(111): $|\mathbf{a}| = |\mathbf{b}| = \sqrt{2}a_0$, and $h = (\sqrt{3}/6)a_0$. To obtain the second layer, shift the first layer by $\frac{1}{3}\mathbf{a} + \frac{1}{3}\mathbf{b}$ in the plane, then $(\sqrt{3}/6)a_0$ in the $[\bar{1}\bar{1}\bar{1}]$ direction. (See color insert.)

HW #1(4)

Diamond cubic crystals

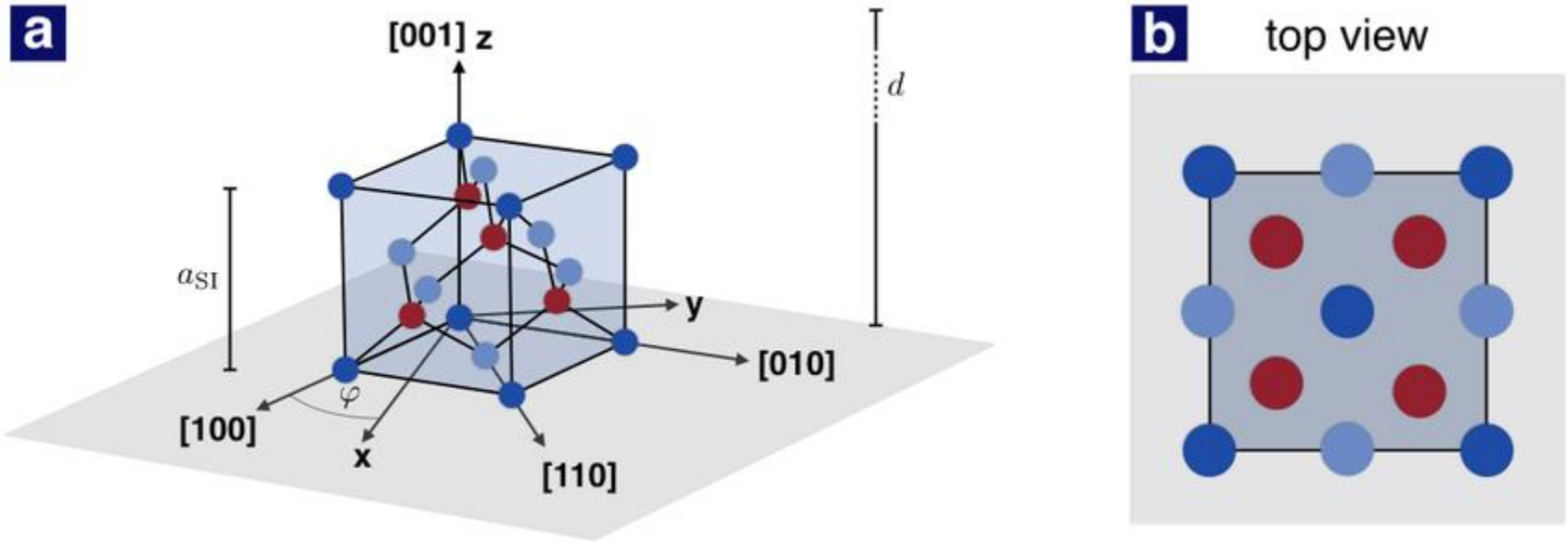

7 -(a) Face-centered diamond cubic crystal structure of silicon. The dark blue atoms are located at the edges of the unit cell, whereas the atoms depicted in light blue are positioned at the center of the outer faces. The silicon atoms illustrated in red are centered around three light blue atoms and one dark blue atom. The slab's normal vector (z-direction) is parallel to the [001]-direction of the silicon lattice, resulting in one degree of freedom; the orientation between the silicon's [100]-direction and the x-axis of the slab, which is quantified by the angle ϕ. The lattice constant of silicon (a SI ≈ 0.5 nm) is significantly smaller the slab's thickness (d = 220 nm) such that the unpatterend silicon slab features a C 4 symmetry (b).

Source: researchgate.net

- Ideal structure of low-Miller-index surfaces of diamond cubic crystals

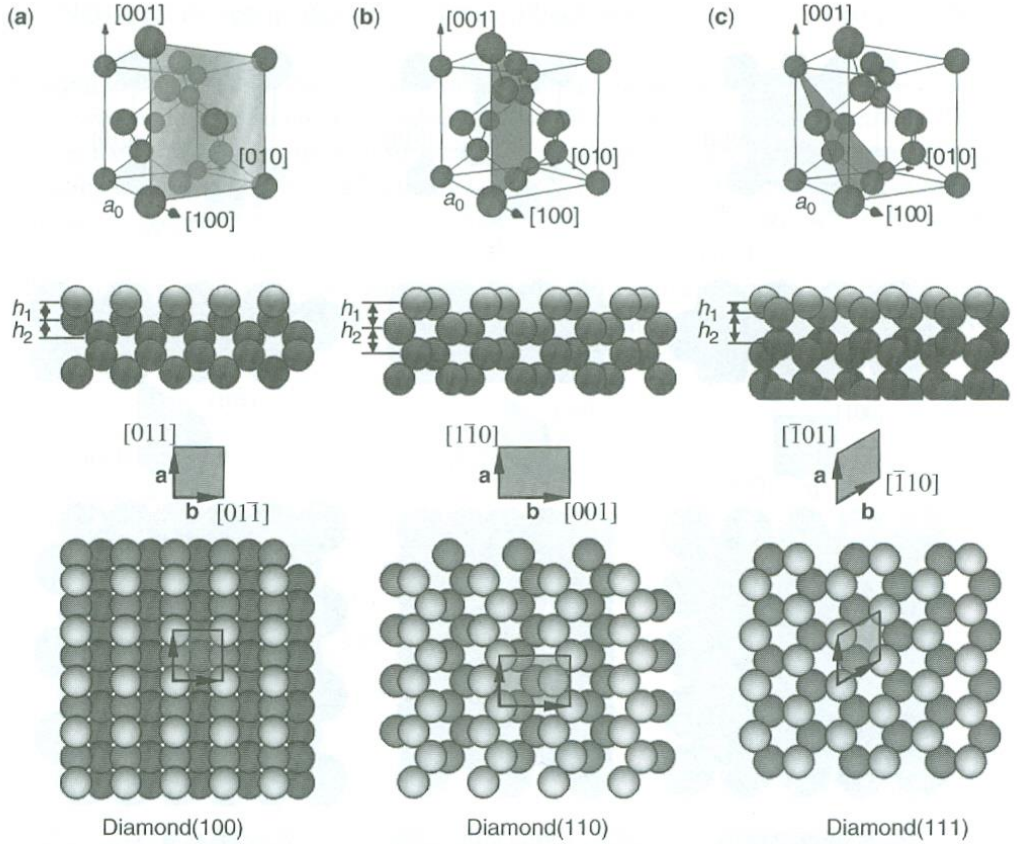

Figure 2.10. Unreconstructed surfaces of the diamond crystal surfaces, where a_0 is the lattice constant of the crystal, **a** and **b** are the unit-cell vectors, h_1 and h_2 are the distances between the first and the second layer, and the second and the third layer, respectively. (a) Diamond(100): $|\mathbf{a}| = |\mathbf{b}| = (\sqrt{2}/2)a_0$, and $h_1 = h_2 = \frac{1}{4}a_0$. To obtain the second layer, shift the first layer by $\frac{1}{2}\mathbf{a}$ in the plane, then $\frac{1}{4}a_0$ in the $[\bar{1}00]$ direction. To obtain the third layer, shift the first layer by $\frac{1}{2}\mathbf{a} + \frac{1}{2}\mathbf{b}$ in the plane, then $\frac{1}{2}a_0$ in the $[\bar{1}00]$ direction. (b) Diamond(110): $|\mathbf{a}| = (\sqrt{2}/2)a_0$, $|\mathbf{b}| = a_0$, and $h_1 = h_2 = (\sqrt{2}/2)a_0$. To obtain the second layer, shift the first layer by $\frac{1}{2}\mathbf{a} + \frac{1}{2}\mathbf{b}$ in the plane, then $(\sqrt{2}/2)a_0$ in the $[\bar{1}\bar{1}0]$ direction. To obtain the third layer, shift the first layer by $\sqrt{2}a_0$ in the $[\bar{1}\bar{1}0]$ direction. (c) Diamond(111): $|\mathbf{a}| = |\mathbf{b}| = (\sqrt{2}/2)a_0$, $h_1 = (\sqrt{3}/12)a_0$, and $h_2 = (\sqrt{3}/4)a_0$. To obtain the second layer, shift the first layer by $\frac{1}{3}\mathbf{a} + \frac{1}{3}\mathbf{b}$ in the plane, then $(\sqrt{3}/12)a_0$ in the $[\bar{1}\bar{1}\bar{1}]$ direction. To obtain the second layer, shift the first layer by $\frac{1}{3}\mathbf{a} + \frac{1}{3}\mathbf{b}$ in the plane, then $(\sqrt{3}/3)a_0$ in the $[\bar{1}\bar{1}\bar{1}]$ direction. (See color insert.)

d_{hkl} Separation of planes

a (or a_0): bulk lattice parameter (or lattice constant) in unit cell

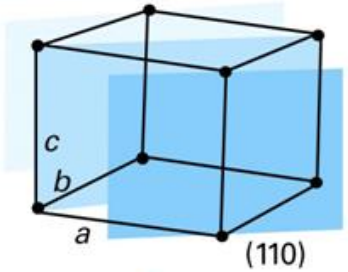

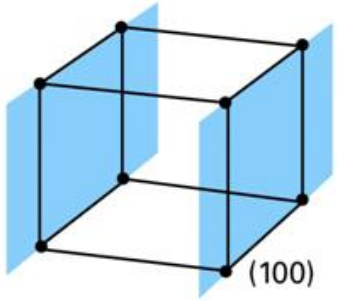

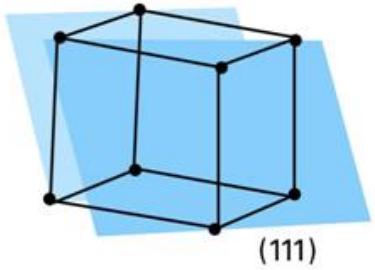

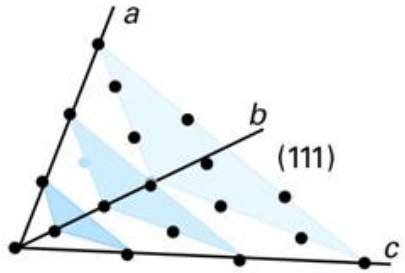

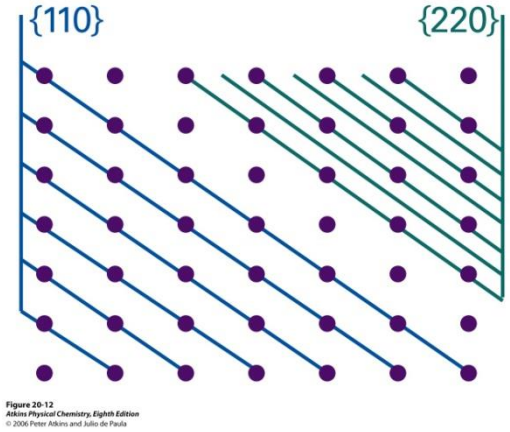

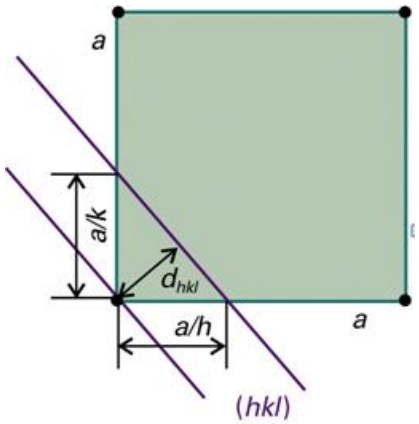

$$\frac{1}{d_{hkl}^2} = \frac{h^2 + k^2 + l^2}{a^2} \quad \text{or} \quad d_{hkl} = \frac{a}{(h^2 + k^2 + l^2)^{1/2}}$$

; cubic

$$\frac{1}{d_{hkl}^2} = \frac{h^2}{a^2} + \frac{k^2}{b^2} + \frac{l^2}{c^2}$$

; orthorhombic

$1/d_{hkl}^2 = (h^2 + k^2)/a^2 + l^2/c^2$; tetragonal

$1/d_{hkl}^2 = (4/3)(h^2 + hk + k^2)/a^2 + l^2/c^2$; hexagonal

Cubic	$a = b = c, \quad \alpha = \beta = \gamma = 90°$	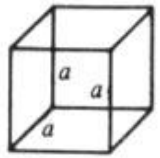
Tetragonal	$a = b \neq c, \quad \alpha = \beta = \gamma = 90°$	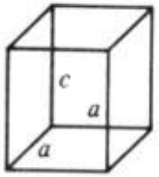
Orthorhombic	$a \neq b \neq c, \quad \alpha = \beta = \gamma = 90°$	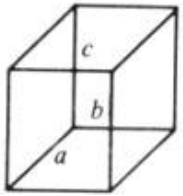
Rhombohedral	$a = b = c, \quad \alpha = \beta = \gamma \neq 90°$	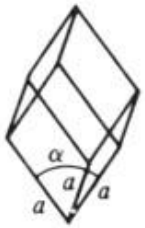
Hexagonal	$a = b \neq c, \quad \alpha = \beta = 90°, \gamma = 120°$	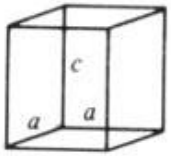
Monoclinic	$a \neq b \neq c, \quad \alpha = \gamma = 90° \neq \beta$	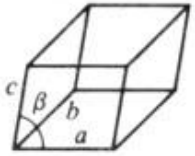
Triclinic	$a \neq b \neq c, \quad \alpha \neq \beta \neq \gamma \neq 90°$	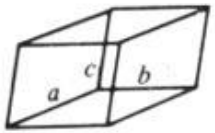

Diffraction

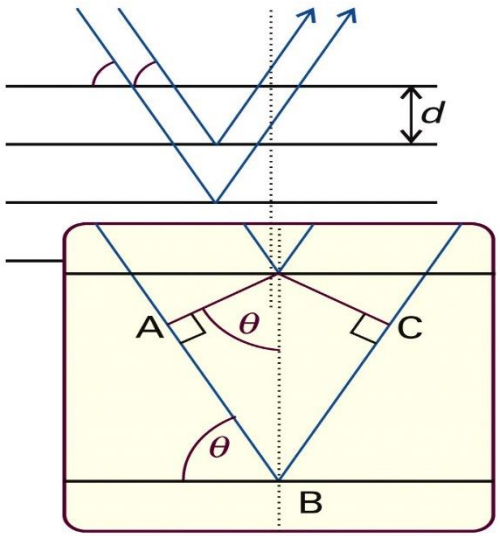

Figure 20-19
Atkins Physical Chemistry, Eighth Edition

X-ray powder diffraction

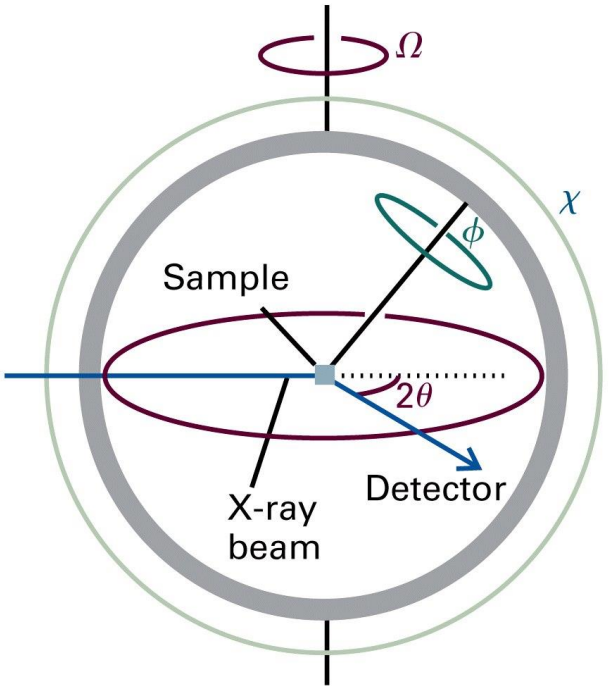

Figure 20-18
Atkins Physical Chemistry, Eighth Edition

Bragg's law

$$n\lambda = 2d\sin\theta,$$

$AB + BC = 2d\sin\theta = n\lambda$

→ θ (X-ray experiment) → d calculation (structure)

Atkins, *Physical Chemistry*

e.g. Cubic structure

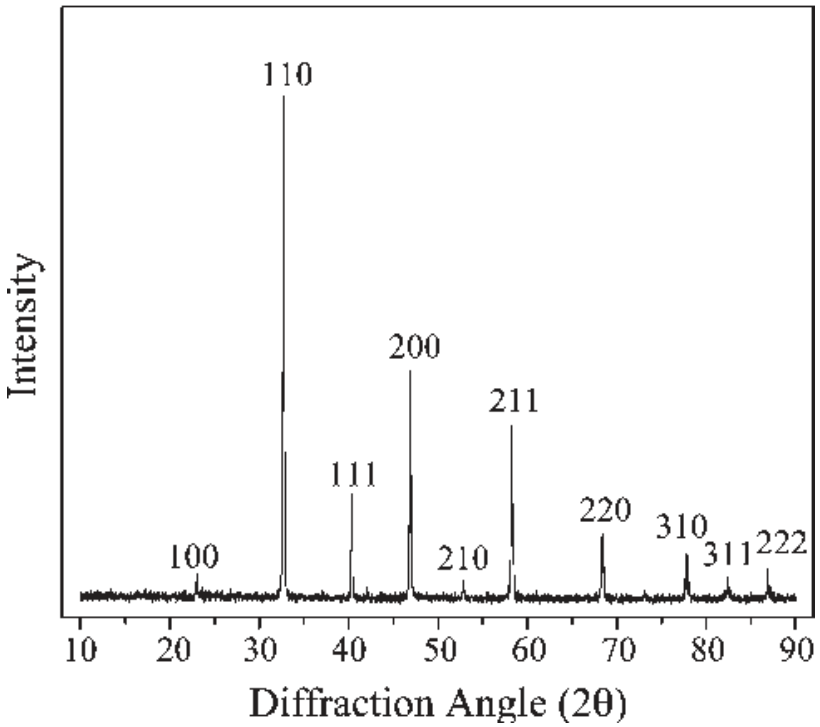

semanticscholar.org

Cubic

$$\frac{1}{d_{hkl}^2} = \frac{h^2+k^2+l^2}{a^2} \quad \text{or} \quad d_{hkl} = \frac{a}{(h^2+k^2+l^2)^{1/2}}$$

{hkl}:	(100)	(110)	(111)	(200)	(210)	(211)	(220)	(310)…
$h^2+k^2+l^2$:	1	2	3	4	5	6	8	10

→ 7, 9 missing (cubic!!)

$n\lambda = 2d\sin\theta \rightarrow \sin\theta = (h^2+k^2+l^2)^{1/2}(\lambda/2a)$

(111) plane of cubic crystal (CuK_α, λ=154pm), θ =20° → lattice parameter a?
→ $\sin 20 = (1+1+1)^{1/2}(154\text{pm}/2a)$ → a = 380 pm

(220) plane: HW #2(1)

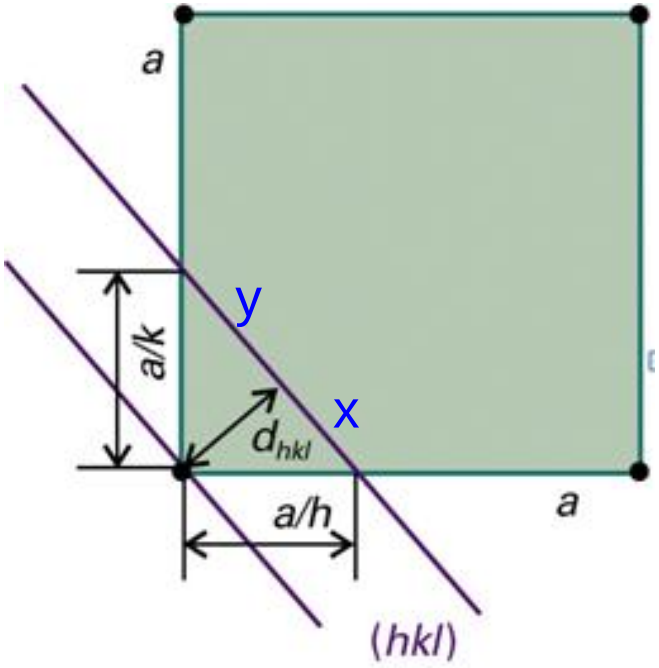

a/h : d = a/k : y → y = dh/k
a/h : x = a/k : d → x = dk/h
½[(a/h)·(a/k)] = ½(x+y)d
→ $1/d^2 = (h^2 + k^2)/a^2$
→ extend to 3-D

$$\frac{1}{d_{hkl}^2} = \frac{h^2 + k^2 + l^2}{a^2} \quad \text{or} \quad d_{hkl} = \frac{a}{(h^2 + k^2 + l^2)^{1/2}}$$

e.g. orthorhombic unit cell, a = 0.82 nm, b = 0.94 nm, c = 0.75 nm

{123} plane → $1/d_{123}^2 = 1^2/(0.82\ \text{nm})^2 + 2^2/(0.94\ \text{nm})^2 + 3^2/(0.75\ \text{nm})^2$
$= 0.22\ \text{nm}^{-2}$
→ d = 0.21 nm
{246} plane → d_{246} = 0.11 nm (½ of d_{123})

Surface atom density (σ_0) vs. Miller index *hkl*

$$\sigma_0 = \frac{1}{A_{hkl}} = \frac{4}{Q\,a^2\,(h^2 + k^2 + l^2)^{1/2}} \quad \text{for fcc and bcc} \qquad (1.1.1)$$

$$\sigma_0 = \frac{1}{A_{hkl}} = \frac{2}{a^2\,[4r^2(h^2 + h\,k + k^2) + 3l^2]^{1/2}} \quad \text{for hcp.} \qquad (1.1.2)$$

In these expressions, A_{hkl} is the area of the surface unit cell, a is the bulk lattice parameter, r is the hcp axial ratio given in Table 1.1 and Q is defined by the following rules:

bcc: $Q = 2$ if $(h + k + l)$ is even, $Q = 4$ if $(h + k + l)$ is odd

fcc: $Q = 1$ if h, k, and l are all odd, otherwise $Q = 2$.

Diamond, zincblende lattice:

$$A_{100} = a^2/2 \qquad (1.1.3)$$

$$A_{111} = (a^2/2)\sin 120^\circ \qquad (1.1.4)$$

because the length of a side of the surface unit cell is given by $(\sqrt{2}/2)a$, the (100) unit cell is rectangular and the included angle in the (111) unit cell is 120°, just as in the fcc unit cells shown in Figure 1.1. Therefore, the surface atom density ratio is

$$\frac{\sigma_{100}}{\sigma_{111}} = \frac{A_{111}}{A_{100}} = 0.866. \qquad (1.1.5)$$

Table 1.1 *Surface atom densities. Data taken from [2] except Si values from [3]. Diamond, Ge, GaAs and graphite calculated from lattice constants*

fcc structure							
Plane	(100)	(110)	(111)	(210)	(211)	(221)	
Density relative to (111)	0.866	0.612	1.000	0.387	0.354	0.289	
Metal	Al	Rh	Ir	Ni	Pd	Pt	Cu
Density of (111)/cm^{-2} $\times 10^{-15}$	1.415	1.599	1.574	1.864	1.534	1.503	1.772
Metal	Ag	Au					
Density of (111)/cm^{-2} $\times 10^{-15}$	1.387	1.394					
bcc structure							
Plane	(100)	(110)	(111)	(210)	(211)	(221)	
Density relative to (110)	0.707	1.000	0.409	0.316	0.578	0.236	
Metal	V	Nb	Ta	Cr	Mo	W	Fe
Density of (100)/cm^{-2} $\times 10^{-15}$	1.547	1.303	1.299	1.693	1.434	1.416	1.729
hcp structure							
Plane	(0001)	$(10\bar{1}0)$	$(10\bar{1}1)$	$(10\bar{1}2)$	$(11\bar{2}2)$	$(11\bar{2}2)$	
Density relative to (0001)	1.000	$\frac{3}{2r}$	$\frac{\sqrt{3}}{(4r^3+3)^1}$	$\frac{\sqrt{3}}{(4r^3+12)}$	$\frac{1}{r}$	$\frac{1}{2(r^3+1)^1}$	
Metal	Zr	Hf	Re	Ru	Os	Co	Zn
Density of (0001)/cm^{-2} $\times 10^{-15}$	1.110	1.130	1.514	1.582	1.546	1.830	1.630
Axial ratio $r = c/a$	1.59	1.59	1.61	1.58	1.58	1.62	1.86
Metal	Cd						
Density of (0001)/cm^{-2} $\times 10^{-15}$	1.308						
Axial ratio $r = c/a$	1.89						

	Diamond lattice			Zincblende	Graphite
Element	C	Si	Ge	GaAs	C
Areal Density/cm^{-2} $\times 10^{-15}$					basal plane
(100)	1.57	0.6782	0.627	0.626	3.845
(111)	1.82	0.7839	0.724	0.723	

fcc structure: cubic

bulk unit cell

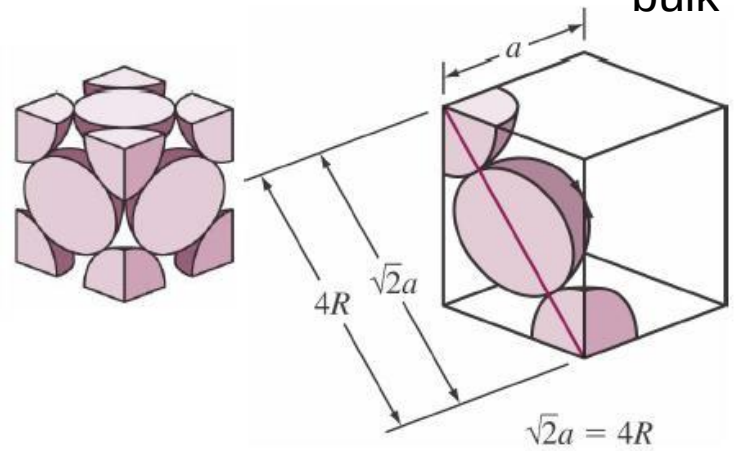

surface unit cell

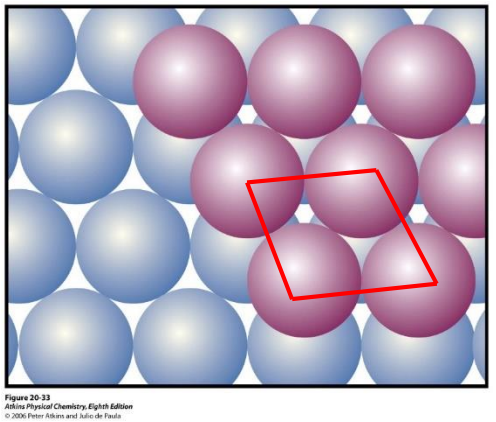

Q = 1 for hkl = (111)

Area(surface unit cell) $A_{hkl} = 2R \times \sqrt{3}R = 2\sqrt{3}R^2$

$\sigma_0 = 1/(2\sqrt{3}R^2) = 4/(1 \cdot a^2 \cdot \sqrt{3}) \rightarrow a = 2\sqrt{2}R$

Separation of planes $d_{hkl} = a/(h^2 + k^2 + l^2)^{1/2} = a/\sqrt{3}$

fcc(100) $\rightarrow A_{hkl} = 4R^2 \rightarrow \sigma_0 = 1/(4R^2)$

$\sigma_0(100)/\sigma_0(111) = (2\sqrt{3}R^2)/(4R^2) = \sqrt{3}/2 = 0.866$

fcc(110) $\rightarrow A_{hkl} = 2R \cdot a = 2R \cdot 2\sqrt{2}R = 4\sqrt{2}R^2 \rightarrow \sigma_0 = 1/(4\sqrt{2}R^2)$

$\sigma_0(110)/\sigma_0(111) = (2\sqrt{3}R^2)/(4\sqrt{2}R^2) = \sqrt{6}/4 = 0.612$

bcc:
HW #2(2)

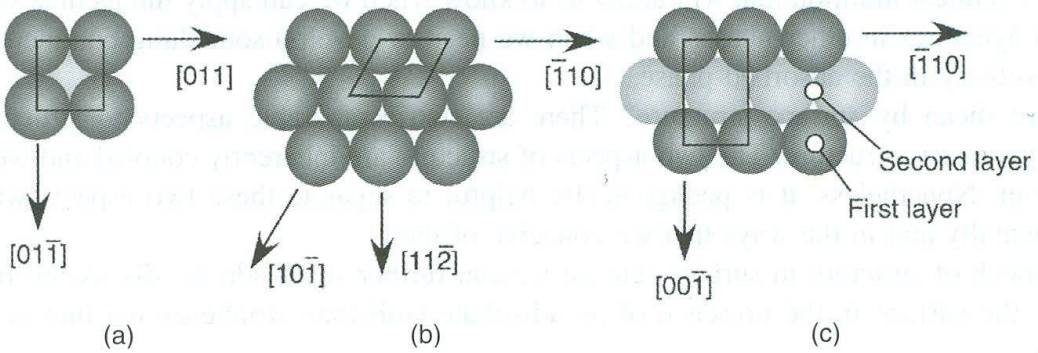

Figure 1.1 *Hard sphere representations of face-centred cubic (fcc) low index planes: (a) fcc(100); (b) fcc(111); (c) fcc(110).*

a: lattice parameter or lattice constant

Au: 0.408 nm(408 pm), Pt: 0.392 nm(3.92 Å), Ni: 0.352 nm
Pd: 0.389 nm, Cu: 0.362 nm, Ag: 0.409 nm

Pt, fcc, $a = 2\sqrt{2}R \rightarrow R = a/(2\sqrt{2}) = 0.392\ nm/(2\sqrt{2}) = 0.1387\ nm$

area $A_{hkl} = 2\sqrt{3}R^2 = 0.6664 \times 10^{-15}\ cm^2$

$\rightarrow$ density $= 1/A_{hkl} =$ 1.5 x 10^{15} Pt atoms/cm^2

Ni density: HW #2(3)

High index and vicinal planes

- Dislocation: mismatch of atomic planes

dislocation densities: ~10^6-10^8 cm^{-2} at metal or ionic crystal surfaces, 10^4-10^6 cm^{-2} in semiconductor or insulator crystals

surface concentration of atoms ~10^{15} cm^{-2} →each terrace contains roughly $10^{15}/10^6 = 10^9$ atoms

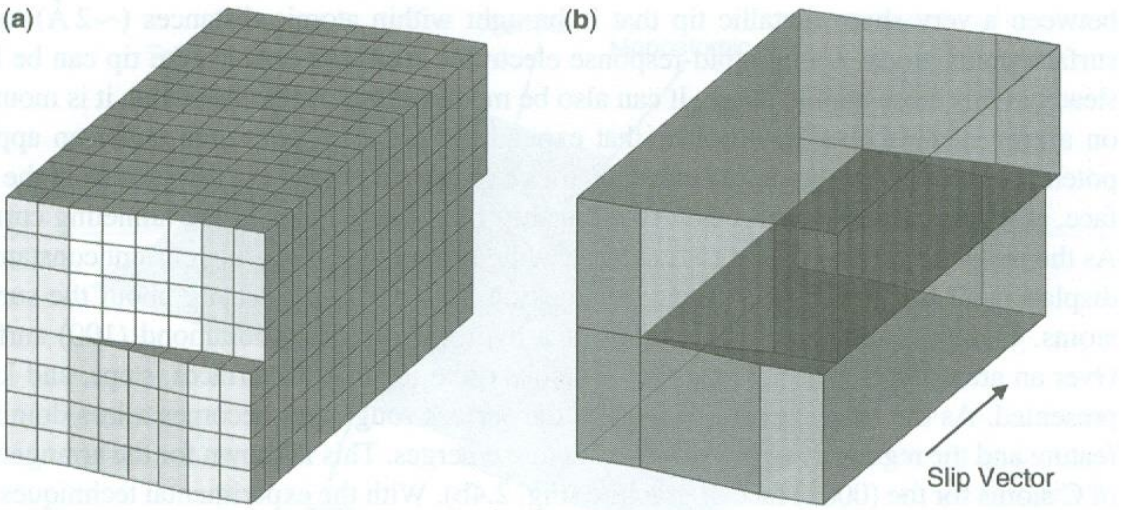

Figure 2.2. One type of screw dislocation giving rise to (a) atomic steps at the surface and (b) the slip plane that produces the dislocation (indicated by the dark plane) and, ultimately, the defects at the surface (steps and kinks).

- Model of surface structure of solids

Atoms in terraces are surrounded by the largest number of nearest neighbors. Atoms in steps have fewer neighbors, and atoms in kink sites have even fewer. Or line defects (steps and kinks) and point defects (atomic vacancies and adatoms)

On a rough surface, 10~20% steps, 5% kink, <1% point defects

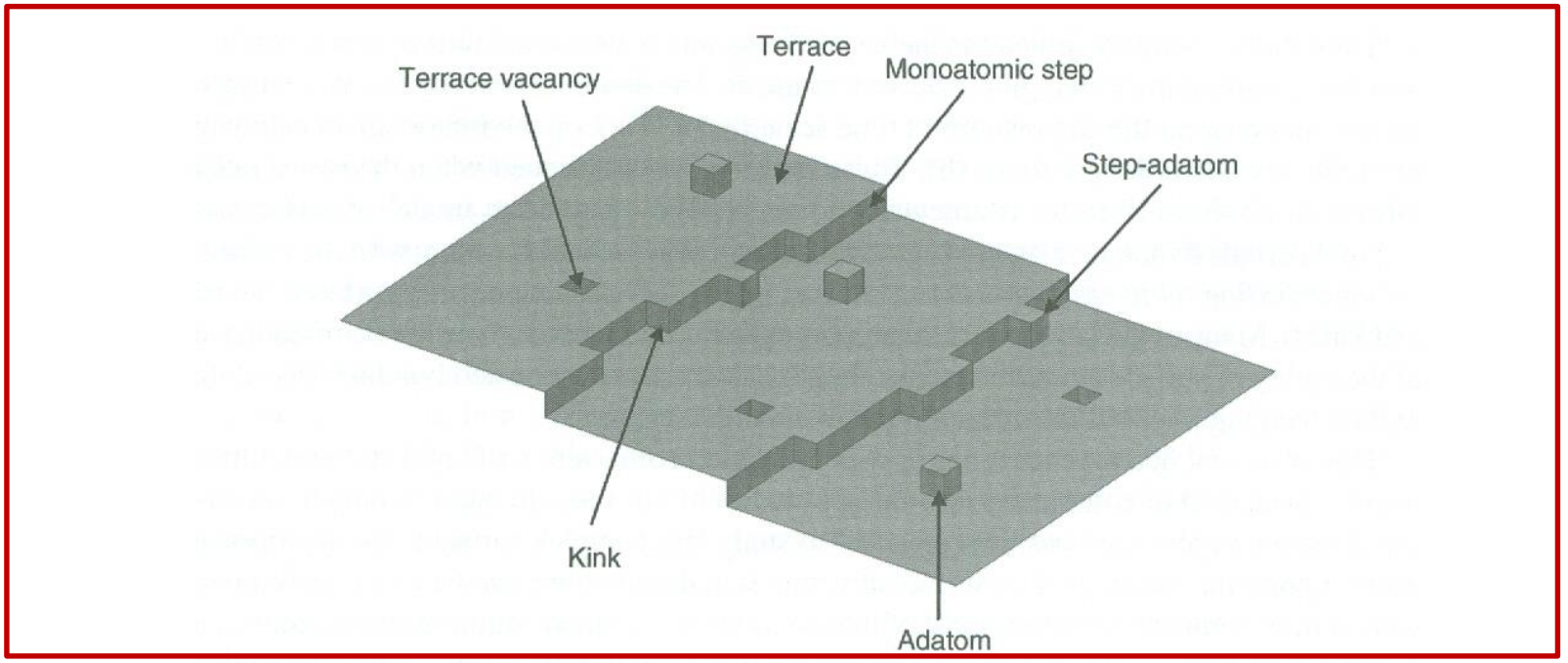

Figure 2.5. Model of a heterogeneous solid surface depicting different surface sites. These sites are distinguishable by their number of nearest neighbors.

- Notation of high-Miller-index, stepped surfaces

(755) Surface of fcc:
6 atoms wide (111) terrace,
1 atom height (100) step

Notation of terrace + step:
W(hkl) x ($h_s k_s l_s$)

Kinked surface
e.g., (10,8,7) =
7(111) x (310)

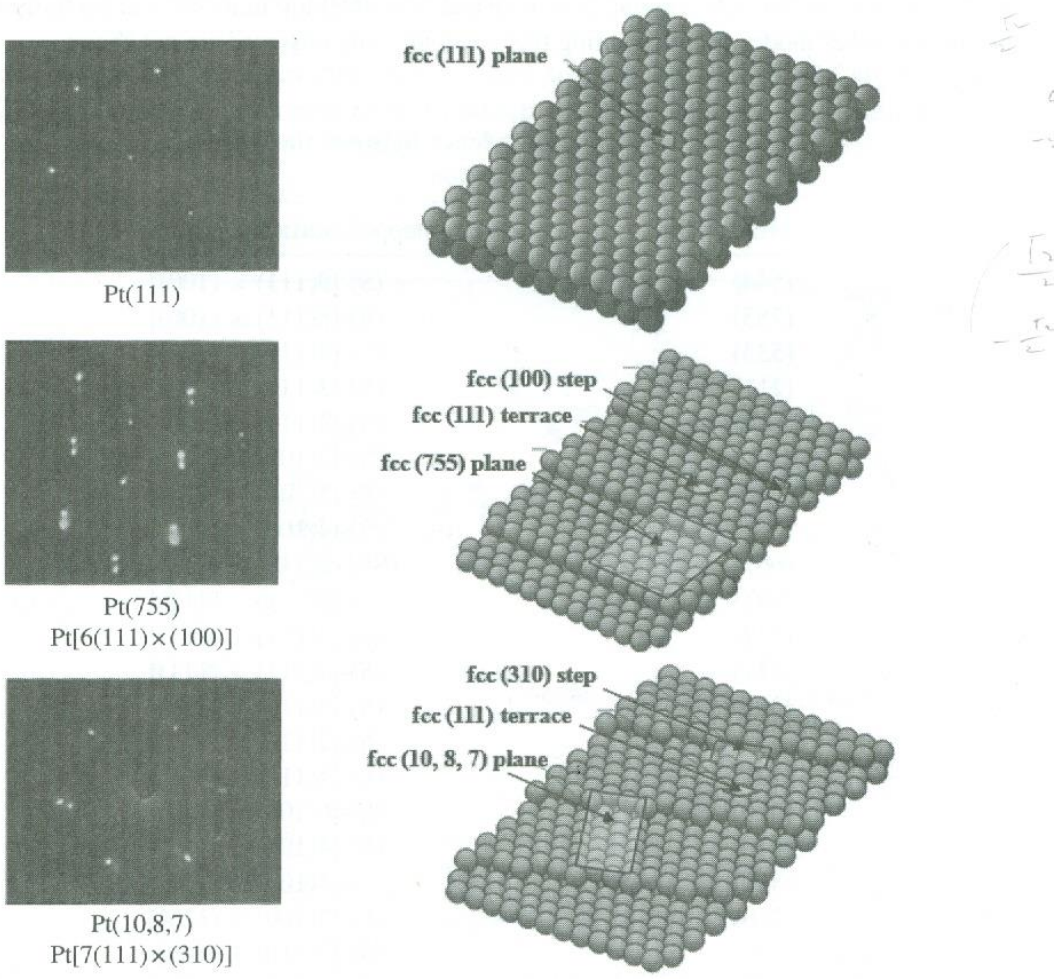

Figure 2.12. Surface structures in real space and LEED diffraction patterns of the flat Pt(111), stepped Pt(755), and kinked Pt(10,8,7) crystal faces.

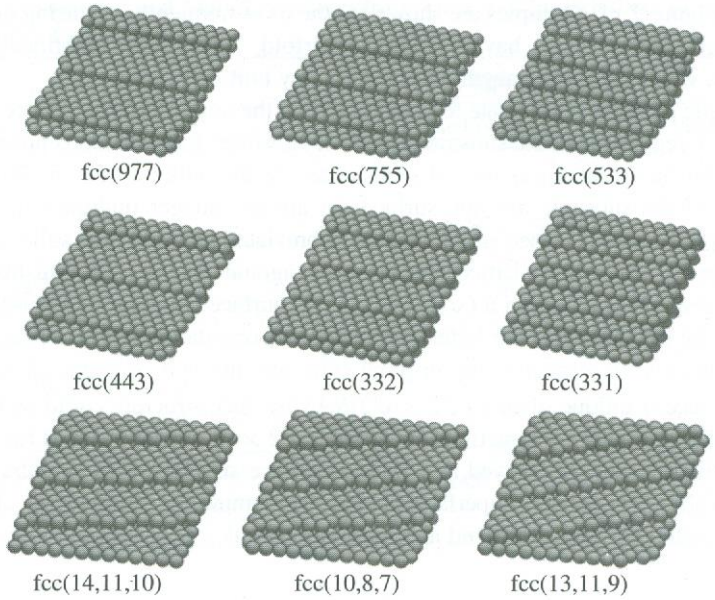

Figure 2.13. Schematic representation of the surface structures of several stepped (the first two rows) and kinked (the bottom row) crystal faces deduced from the bulk unit cell. Contraction of interlayer spacing and other modes of restructuring that are commonly observed are not shown.

TABLE 2.2 Correspondence between the Miller-Index and Stepped-Surface Notation

Miller Index	Stepped-Surface Designation
(544)	(S)-[9(111) × (100)]
(755)	(S)-[6(111) × (100)]
(533)	(S)-[4(111) × (100)]
(211)	(S)-[3(111) × (100)]
(311)	(S)-[2(111) × (100)]
	(S)-[2(100) × (111)]
(511)	(S)-[3(100) × (111)]
(711)	(S)-[4(100) × (111)]
(665)	(S)-[12(111) × (111)]
(997)	(S)-[9(111) × (111)]
(332)	(S)-[6(111) × (111)]
(221)	(S)-[4(111) × (111)]
(331)	(S)-[3(111) × (111)]
	(S)-[2(110) × (111)]
(771)	(S)-[4(110) × (111)]
(610)	(S)-[6(100) × (110)]
(410)	(S)-[4(100) × (110)]
(310)	(S)-[3(100) × (110)]
(210)	(S)-[2(100) × (110)]
	(S)-[2(110) × (100]]
(430)	(S)-[4(110) × (100)]
(10,8,7)	(S)-[7(111) × (310)]

Bimetallic surfaces

Unique properties of a surface composed of two metals

e.g. AuNi, $Pt_3Sn(111)$, $Cu_3Au(100)$

Lower surface energy → more stable → more likely to be observed

Low surface energy species preferentially segregates to the surface → enrichment in the surface as compared to the bulk

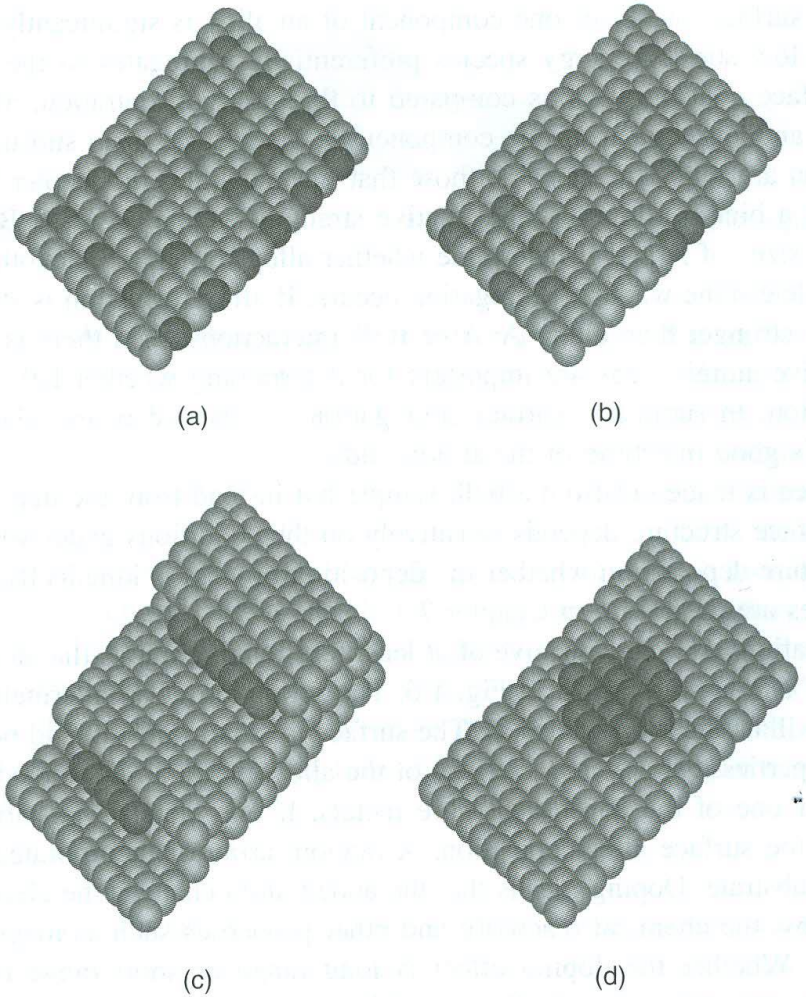

Figure 1.6 *Four limiting cases of the structure of a bimetallic surface prepared by metal-on-metal adsorption: (a) the formation of an intermetallic compound with a definite stoichiometry; (b) random absorption of a miscible metal; (c) segregation of an immiscible metal to the step edges; (d) segregation of an immiscible metal into islands*

Oxide and compound semiconductor surfaces

Insulator oxides (> 6 eV band gap): SiO_2, Al_2O_3, MgO
Conductor or semiconductor oxides (< 4 eV): CeO_2, In_2O_3, SnO_2, ZnO

Ionic crystals

Type 1,2: stable surfaces that exhibit a good balance of charge at the surface

Type 3: polar surface, large surface energies and unstable, extensive reconstruction

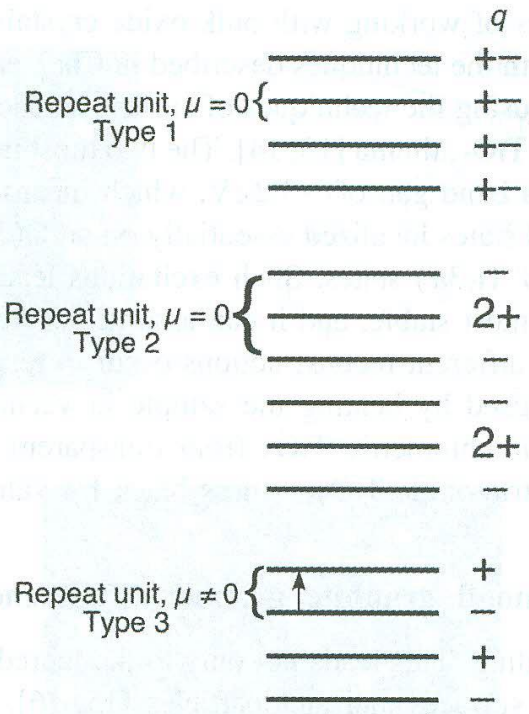

Figure 1.7 *Three types of planes formed by ionic crystals. q, ionic charge in layer; μ electric dipole moment associated with the lattice repeat unit.*

TABLE 6.2.1. Energy Gaps (E_g) of Selected Materials

Substance	E_g (eV)	Substance	E_g (eV)
Ge	0.67	Fe_2O_3	~2.3
$CuInSe_2$	0.9	CdS	2.42
Si	1.12	ZnSe	2.58
WSe_2	~1.1	WO_3	2.8
$MoSe_2$	~1.1	TiO_2 (rutile)	3.0
InP	1.3	TiO_2 (anatase)	3.2
GaAs	1.4	ZnO (zincite)	3.2
CdTe	1.50	$SrTiO_3$	3.2
CdSe	1.74	SnO_2	3.5
GaP	2.2	ZnS (zinc blende)	3.54
		C (diamond)	5.4

Carbon family: diamond, graphite, graphene, etc

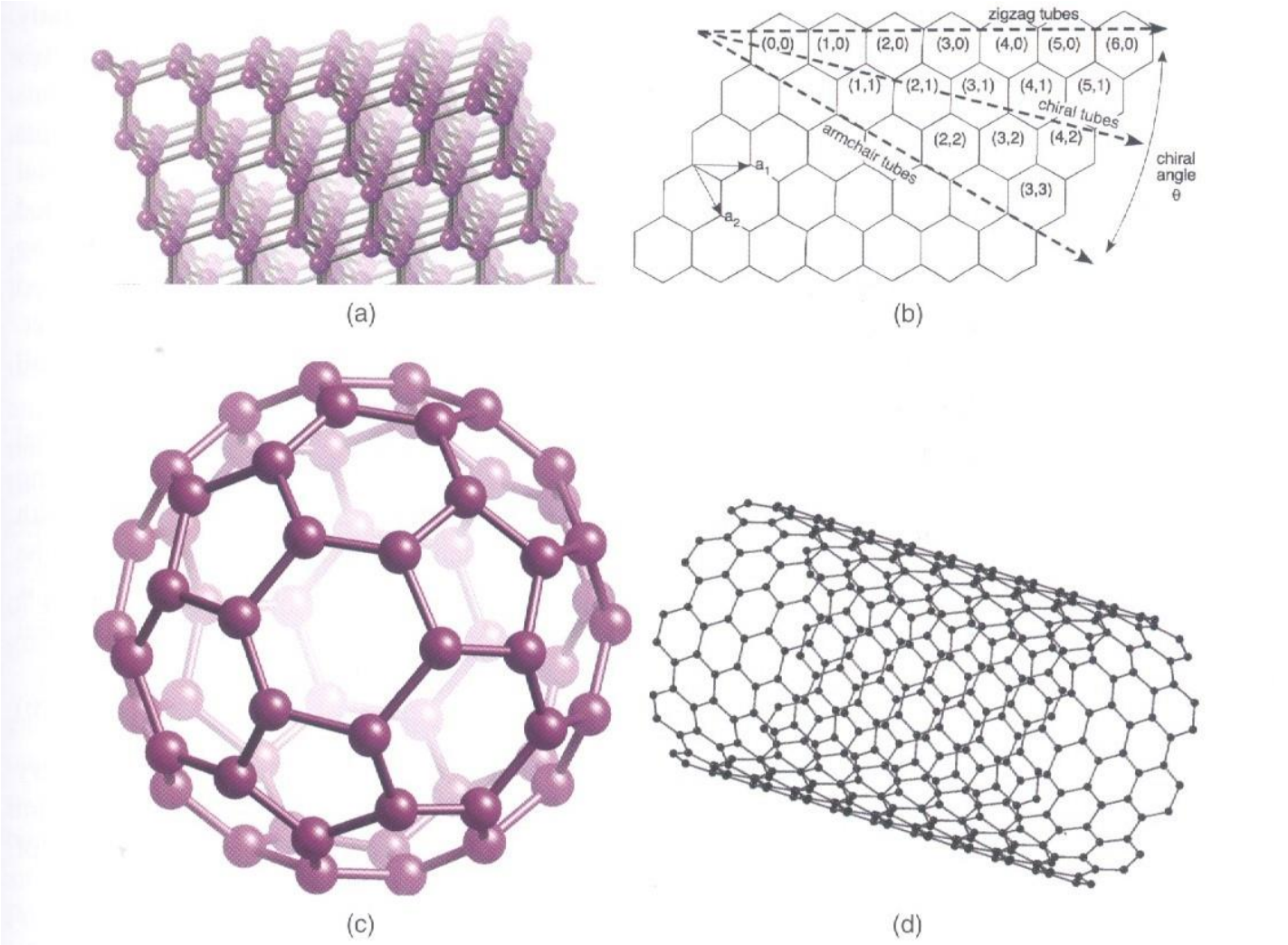

Figure 1.8 (a) A ball and stick model of the diamond lattice with the unreconstructed (111) surface shown at the top. (b) The six-membered ring structure that defines the basal plane of graphite or a graphene sheet. $\mathbf{a}_1$ and $\mathbf{a}_2$ are the surface lattice vectors. When rolled to form a seamless structure, the resulting nanotube has either a zigzag, chiral or armchair configuration depending on the value of the chiral angle. (c) The structure of the fundamental fullerene, that of C_{60}. (d) An example of a single-walled carbon nanotube.

Kolasinski

-3 types of orbital hybridization:
  sp (triple bond)
  sp^2 (double bond → planar structure: graphite, graphene, fullerenes, CNT)
  sp^3 (tetrahedral → diamond lattice)

-graphite or graphene: weak van der Waals forces → layer-layer
-CNT can be characterized by its chiral vector **C** given by

$$\mathbf{C} = n\,\mathbf{a}_1 + m\,\mathbf{a}_2 \tag{1.1.6}$$

where n and m are integers, and $\mathbf{a}_1$ and $\mathbf{a}_2$ are the unit vectors of graphene. The hexagonal symmetry of graphene means that the range of m is limited by $0 \le |m| \le n$. The values of n and m determine not only the relative arrangement of the hexagons along the walls of the nanotube, but also the nature of the electronic structure and the diameter. The diameter of a SWNT is given by

$$d = \frac{a}{\pi}\sqrt{n^2 + m\,n + m^2} \tag{1.1.7}$$

where the magnitude of the surface lattice vector $a = |a_1| = |a_2| = 0.246$ nm. The chiral angle, which can assume values of $0 \le \theta \le 30°$, is related to n and m by

$$\theta = sin^{-1}\left(\frac{m}{2}\sqrt{\frac{3}{n^2 + mn + m^2}}\right). \tag{1.1.8}$$

The translation vector **T** is the unit vector of the CNT. It is parallel to the tube axis but perpendicular to the chiral vector.

When $m = 0$, $\theta = 0°$. This leads to the formation of nanotubes in which the hexagonal rings are ordered in a zigzag structure. Most zigzag nanotubes are semiconducting, except for those with an index n divisible by 3, which are conducting (metallic). When $n = m$, $\theta = 30°$ and armchair tubes are formed. All armchair tubes are conducting. Chiral tubes are formed in between these extremes. Most chiral tubes are semiconducting; however, those with $n - m = 3q$ with an integer q are conducting.

-Fullerenes: bending graphene (1996 Nobel Prize), C_{60}(diameter 0.7 nm)

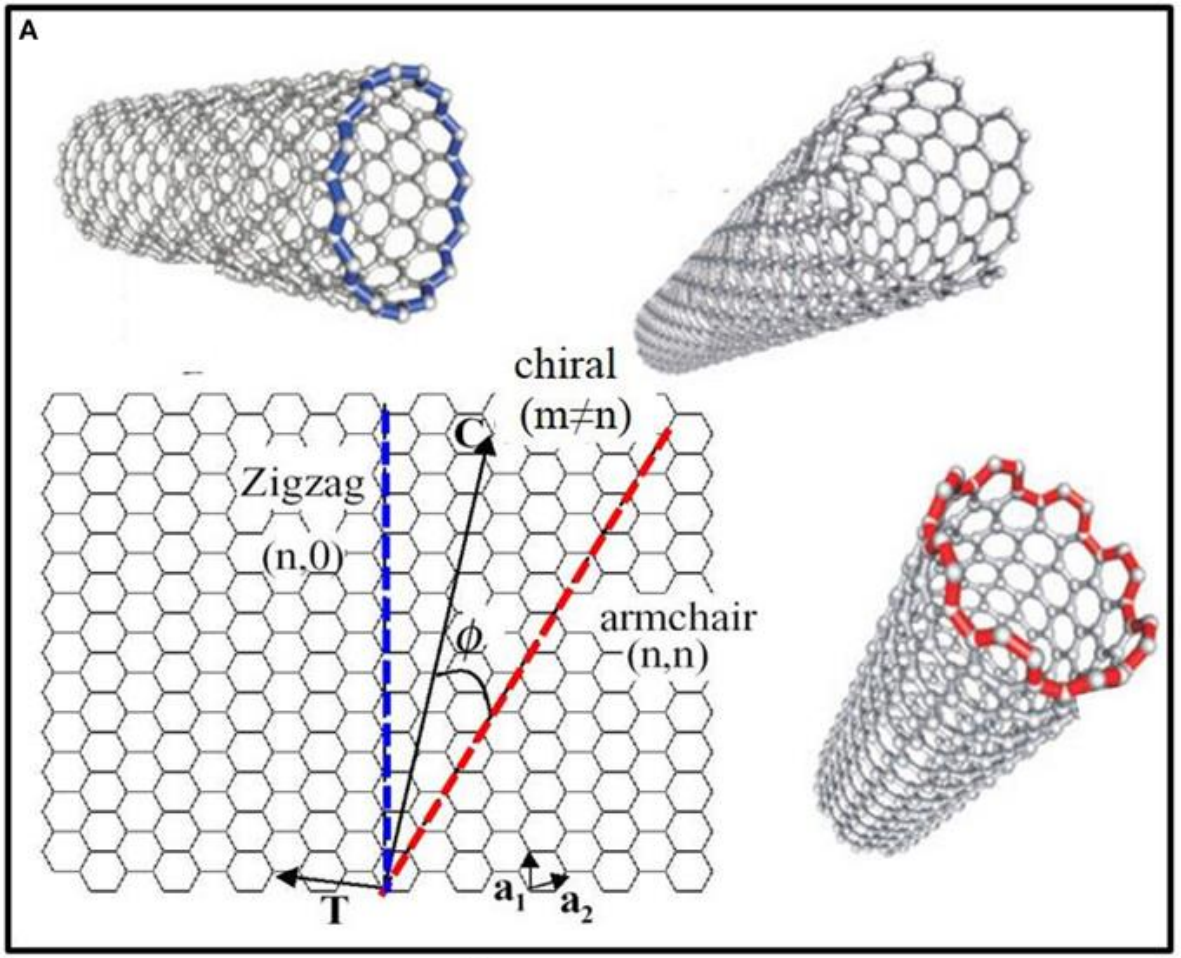

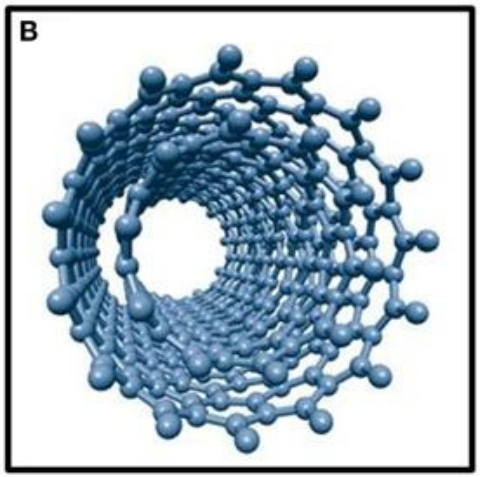

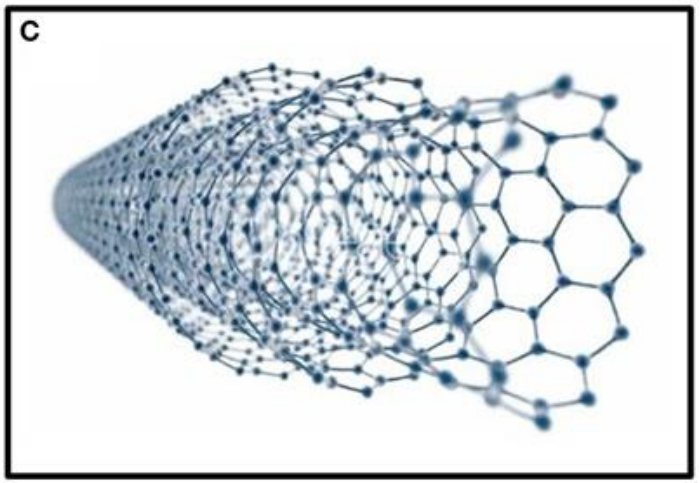

Structure and models of carbon nanotubes in function of their number of walls. (A) Single-walled carbon nanotubes (SWNTs) structures in function of their chirality (zigzag, armchair, and chiral). (B) Model of double-walled carbon nanotubes (DWNTs). (C) Structure of multi-walled carbon nanotubes (MWNTs) made up of several concentric shells.

May C. Morris *et al.*, Frontiers in Chemistry 3(63), 2015.

-Graphene (2010 Nobel Prize)

Production
1. Mechanical exfoliation (by adhesive tape) → size limit
2. Chemical exfoliation by intercalating a chemical species between graphene layers → large quantity, industrial use
3. Using precursors of organic molecules or graphene oxides → chemical reactions into graphene
4. Chemical vapor deposition for the production of graphene

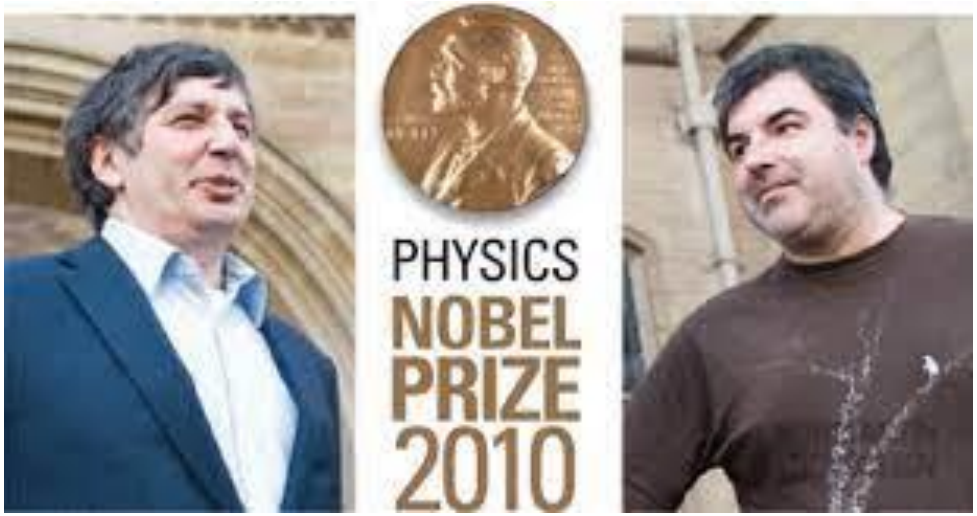

Two-dimensional solids (2D solids)

Table 1.2 *A list of selected two-dimensional materials and the methods used to produce monolayer or few-layer samples of these.*

Name/Formula	Material type	Preparation
Atomic		
Graphene, C	Semimetal, topological insulator	ME [32], CVD, LMCVD [33], segregation [27]
Silicene	Semiconductor, topological insulator	
Germanene	Semiconductor	
Phosphorene	Semiconductor	ME [34]
Monochalcogenides		
SnS, Se	Semiconductor	CVD, ME [35]
GeS, GeSe	Semiconductor	CVD, ME [35]
GaS, GaSe, GaTe	Semiconductor	
InS, InSe, InTe	Semiconductor	
Transition metal dichalcogenide (TMD or TMDC)		
MoS_2	Semiconductor	ME [32], LIC, LE [36], LMCVD [33], CVD [35]
WS_2	Semiconductor	LIC, LE [36], LMCVD [33], CVD [35]
WSe_2		LMCVD [33], MBE [37]
$MoSe_2$		LE [36], LMCVD [33], vdW epitaxy [38], MBE [37]
$TiSe_2$	Superconductor, $T_c \leq 3$ K	[39]
$MoTe_2$		LE [36], MBE [37]
VSe_2, $HfSe_2$		MBE [37]
$NbSe_2$	Metal	ME [32], LE [36], vdW epitaxy [38]

Kolasinski

M_2X_3/other		
Hexagonal boron nitride, *h*-BN	Wide band gap semiconductor	ME [32], LE [36], LMCVD [33], CVD [40], segregation [40]
Bi_2Te_3	Thermoelectric, topological insulator	LE [36], MBE [37]
Bi_2Se_3	Topological insulator	MBE [37]
Sb_2Se_3	Topological insulator	MBE [37]
GaSe		LMCVD [33]
$Ga_xIn_{1-x}Se$		LMCVD [33]
Transition metal oxides (TMOs)/Layered oxides		
HfO_2	Insulator	LMOS [41], LMCVD [33]
Al_2O_3	Insulator	LMOS [41], LMCVD [33]
Gd_2O_3		LMOS [41], LMCVD [33]
$Bi_2Sr_2CaCu_2O_x$		ME [32]
La_2CuO_4		
MoO_3		
V_2O_5		
P_2O_5	Insulator	
Transition metal carbide (TMC)		
WC		LMCVD [33]
Mo_2C		LMCVD [33]
TaC		LMCVD [33]
MXene		Etching [42, 43]

ME = mechanical exfoliation, LE = liquid exfoliation, LIC = lithium intercalation, CVD = chemical vapour deposition, LMOS = liquid metal oxide segregation, LMCVD = liquid metal chemical vapour deposition, MBE = molecular beam epitaxy.

Durable nanoparticles

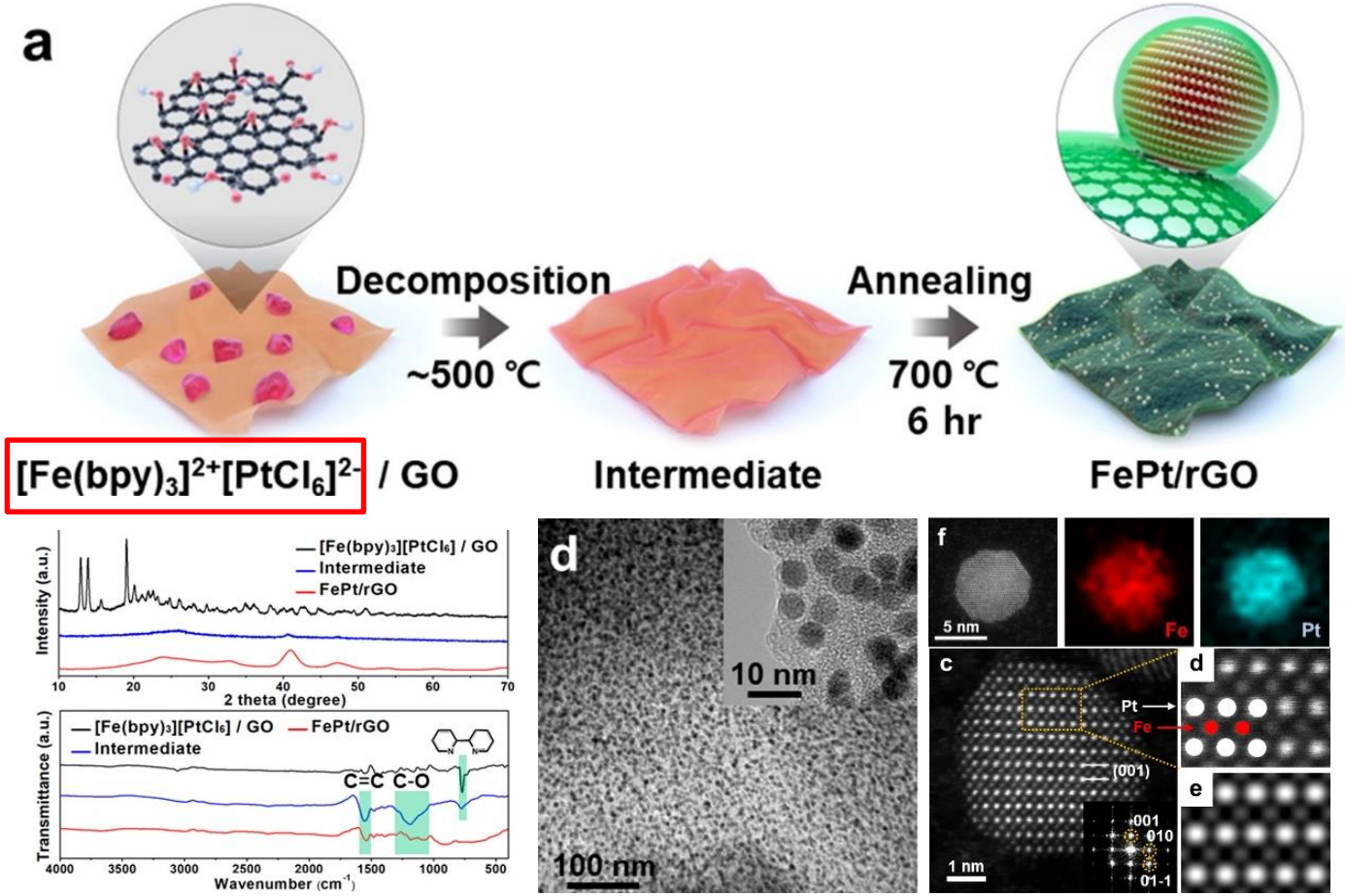

Molecular engineering approach on Fe-Pt bimetallic precursor with bipyridine ligands for small-sized and highly uniform ordered intermetallic Fe-Pt nanocrystals

➔ *in situ* bipyridine-derived carbon shell as physical protective layer, leading to highly uniform and atomically ordered Fe-Pt nanostructure

J. Am. Chem. Soc., 142 (**2020**) 14190

Co-N-C catalyst for H_2O_2 production

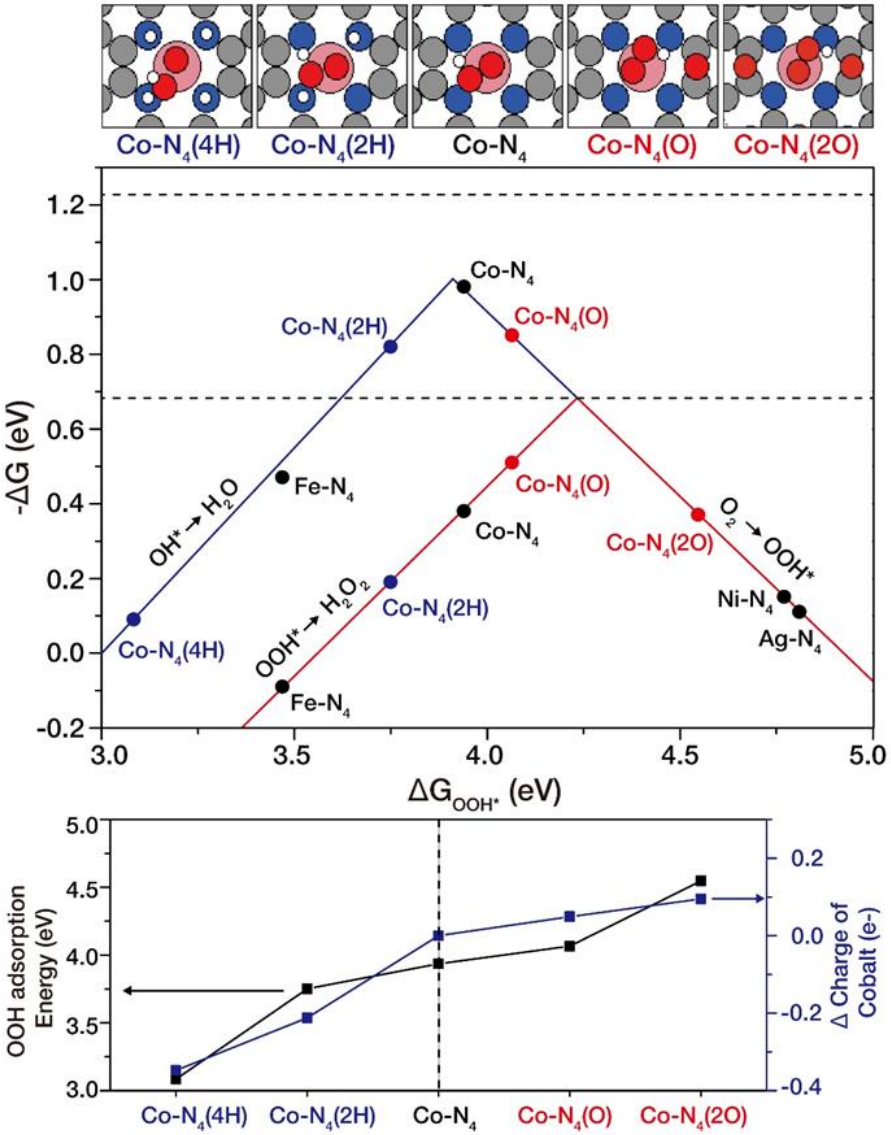

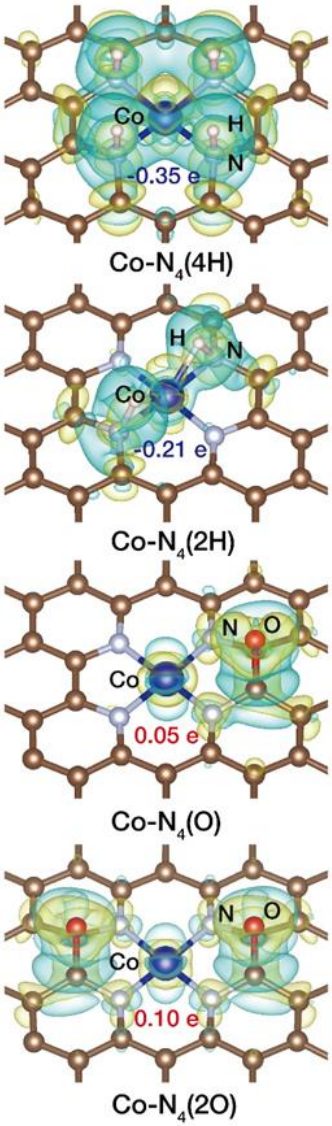

An electron-rich species such as O* is adsorbed near the Co-N_4 moiety (Co-N_4(O)),

ΔG_{OOH^*} increases from 3.9 to 4.1 eV getting very close to the optimal value for the H_2O_2 production.

Site specific single atom catalyst on graphene for H_2O_2 production

Nature Materials, 19 (2020) 436

Carbon-encapsulated Pt NPs for durable fuel cell

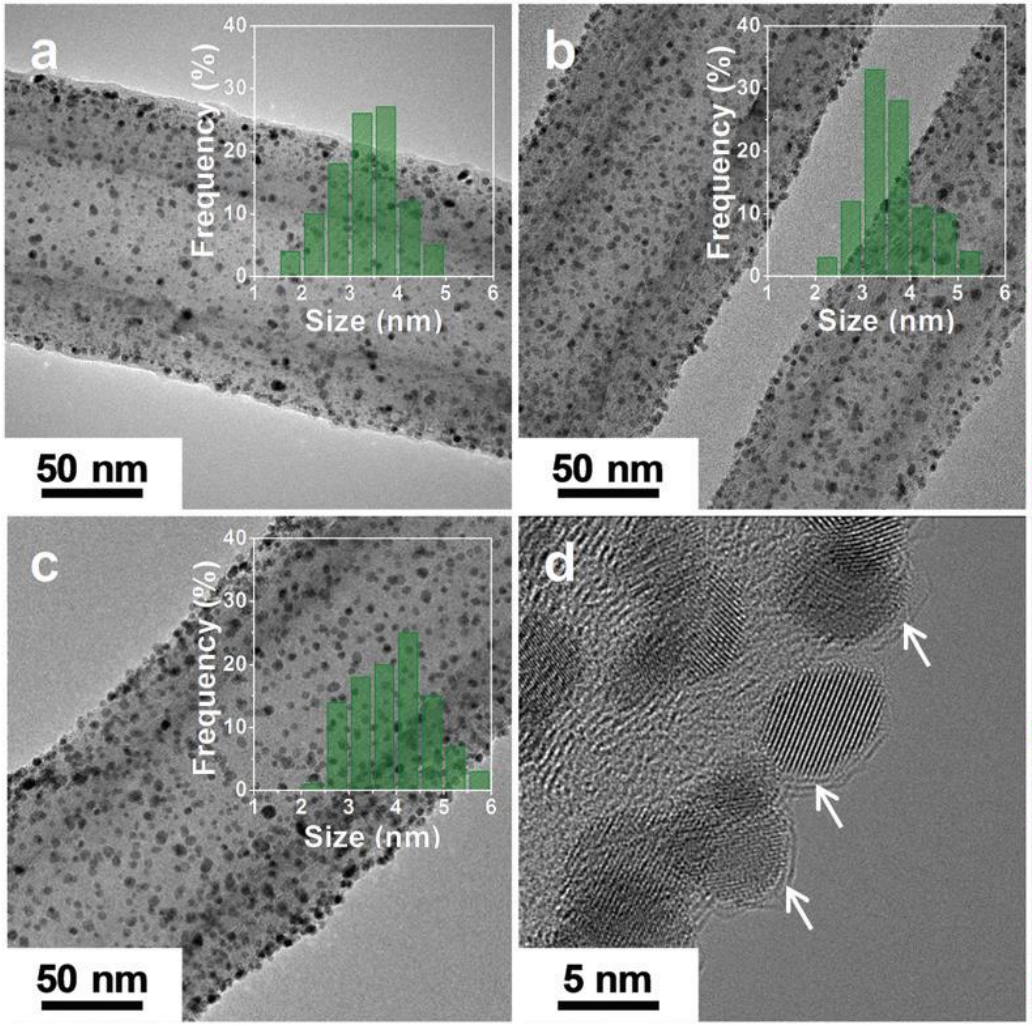

Pt–aniline complex as the source of the Pt and carbon shell

0.125 mgPt/cm^2 (lower than 2020 DOE target)

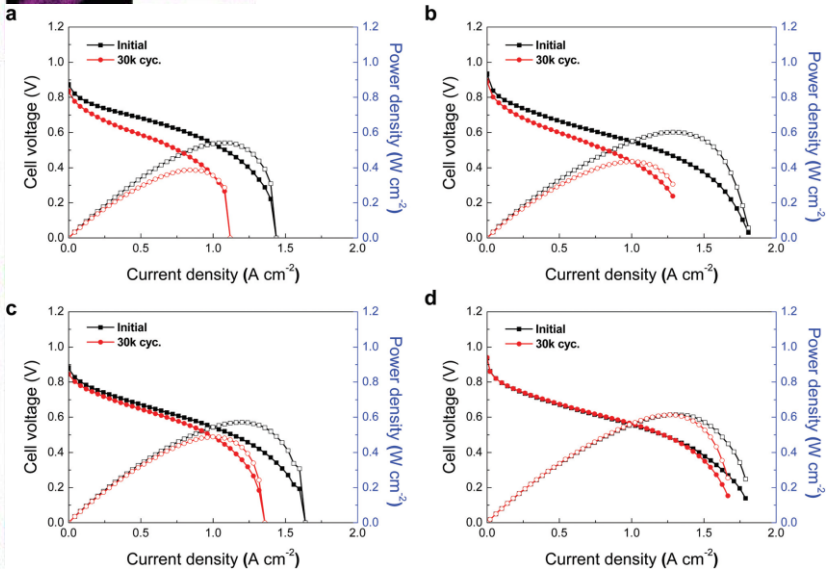

Stable after 30,000 accelerated stability test cycles

Energy & Environ. Sci. 12 (2019) 2820

Li-sulfur battery

Encapsulation method for preventing dissolution

❖ **Introduction of graphene quantum dots**

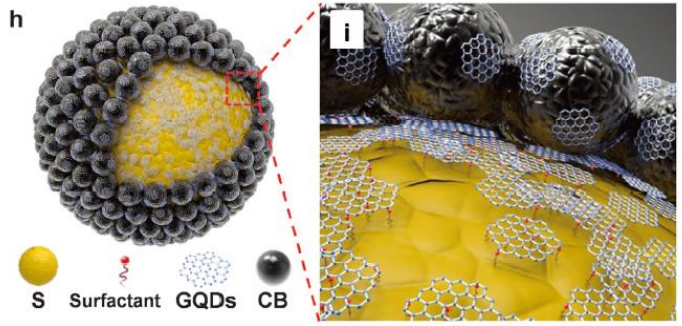

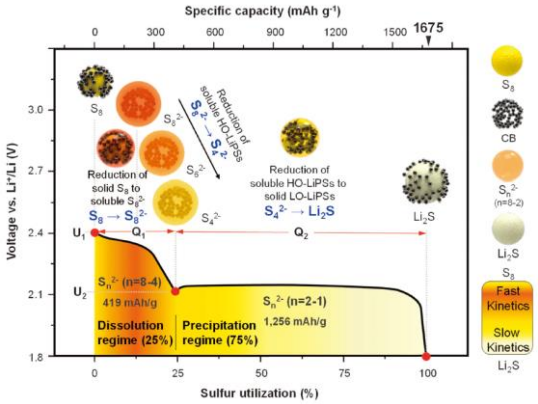

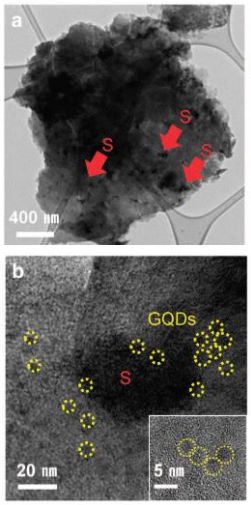

Mitigated polysulfide dissolution

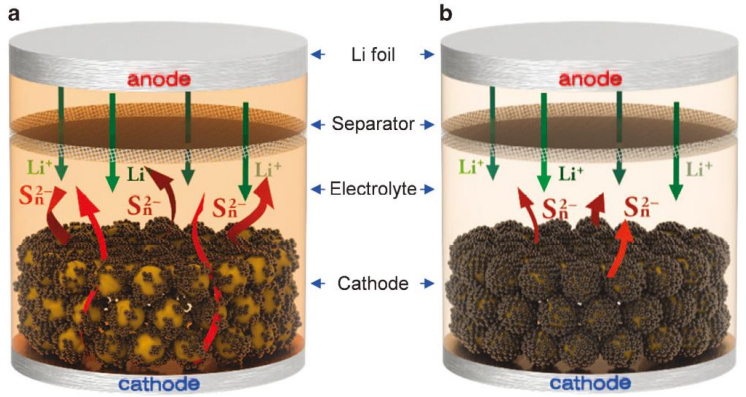

Enhanced battery performance

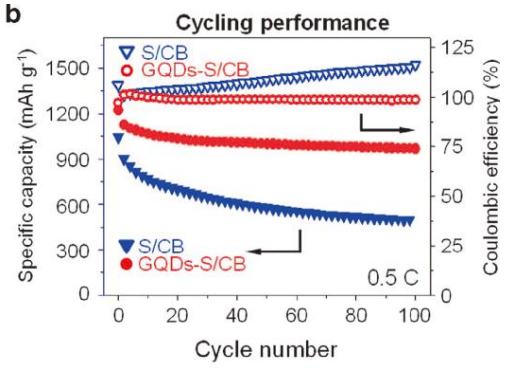

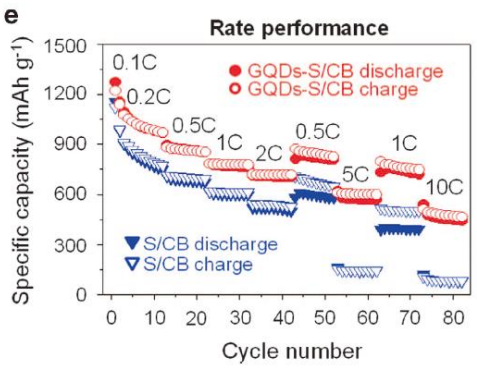

Y.-E. Sung and B. H. Hong group. *NPG Asia Mater.* 2016, **8**, e272

Porous solids

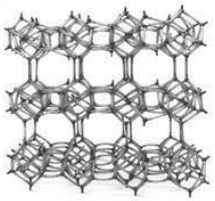

-Pore diameter

microporous < 2 nm, mesoporous 2 < d < 50 nm

macroporous > 50 nm, nanoporous ??

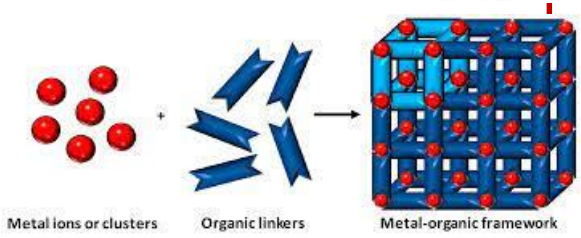

-Porosity(ε): amount of empty space in the material

$$\varepsilon = V_p/V, \quad V_p: \text{pore volume, V: apparent volume}$$

-exterior surface(outside surface) and interior surface(inside pore) → accessible area per unit mass (specific area of porous material), a_p

$$a_p = \text{exterior surface area + interior pore area}$$

-porous solids: deposition, etching, template use

-oxides: Al_2O_3, SiO_2, MgO

-Zeoilites: microporous (and mesoporous) aluminosilicates, aluminium phosphates, metal aluminium phosphates, silicon aluminium phosphates

-MOF(metal-organic frameworks): pores < 2nm. Crystal solids that are assembled by the connection of metal ions or clusters through molecular bridges → control void space by controlling the size of the molecular bridges

Adsorbate structures (Overlayer structures)

Wood's notation: simple but limited

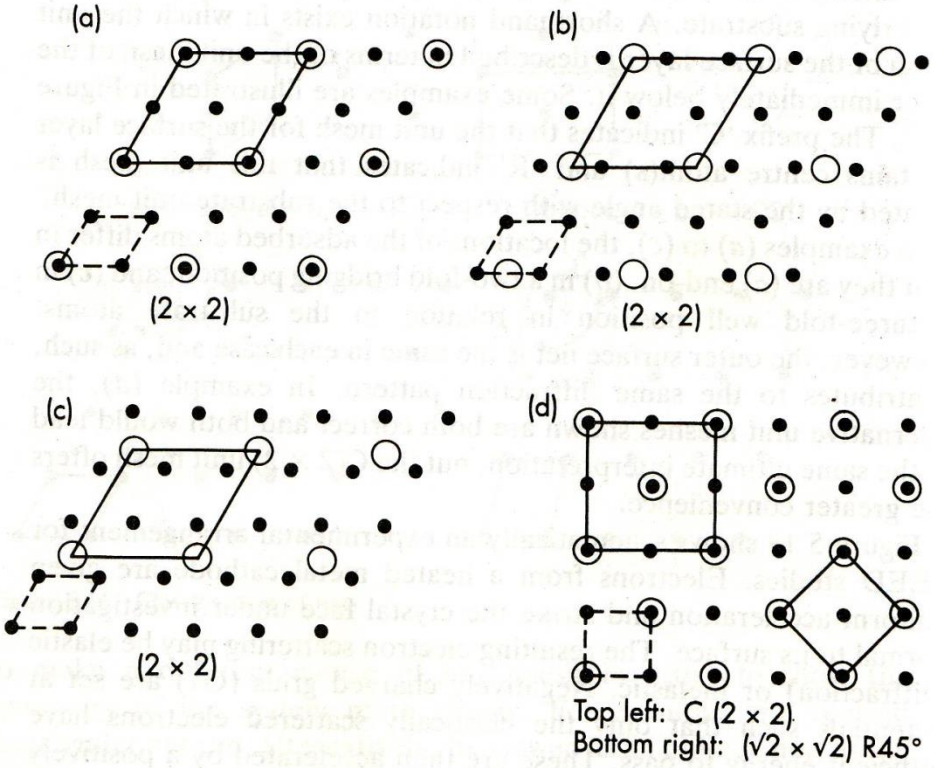

Figure 5.17 Examples and nomenclature of surface layers. Substrate atoms are represented by dots and adatoms by circles. The unit (1×1) mesh of the substrate is shown bottom left

P: primitive
C: centered
R: rotation angle

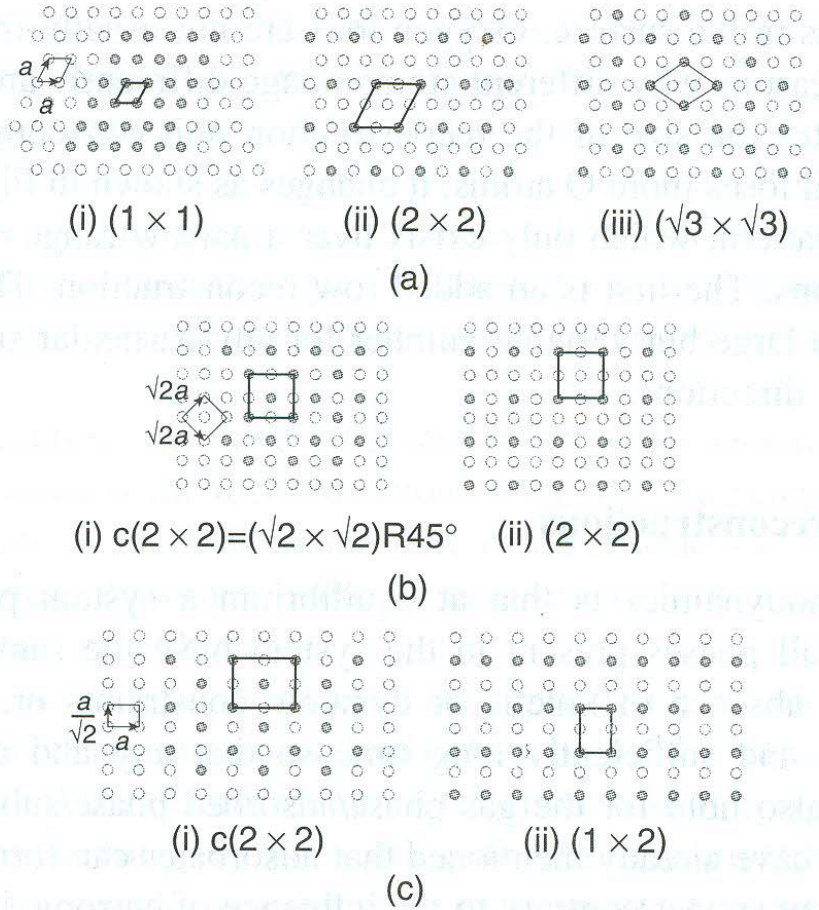

Figure 1.9 *Some commonly observed adsorbate structures on low index face-centred cubic (fcc) planes. (a) fcc(111), (i) (1 × 1), (ii) (2 × 2), (iii) (√3 × √3). (b) (i) fcc(100)–c(2 × 2), (ii) fcc(110)–c(2 × 2). (c) (i) fcc(100)–(2 × 2), (ii) fcc(110)–(1 × 2).*

Notation of surface structures

- Ideal structure of low-Miller-index surfaces of face-centered cubic (fcc)

Surface unit-cell vectors **a'** and **b'** can be expressed by bulk **a** and **b**

$$\mathbf{a}' = m_{11}\mathbf{a} + m_{12}\mathbf{b}$$
$$\mathbf{b}' = m_{21}\mathbf{a} + m_{22}\mathbf{b} \qquad (2.4)$$

where the coefficients m_{11}, m_{12}, m_{21}, and m_{22} define a matrix

$$M = \begin{pmatrix} m_{11} & m_{12} \\ m_{21} & m_{22} \end{pmatrix} \qquad (2.5)$$

that defines any unit cell unambiguously. For example, for all of the unit cells in Figure 2.8,

$$M = \begin{pmatrix} 1 & 0 \\ 0 & 1 \end{pmatrix} \qquad (2.6)$$

Let us consider the surface structure of an adsorbate that has a unit cell twice as long as the substrate unit cell and parallel to it. This structure [e.g., fcc(111)-(2 × 2)] is shown in Figure 2.11. The coefficients of its unit-cell vectors define the matrix

$$M = \begin{pmatrix} 2 & 0 \\ 0 & 2 \end{pmatrix} \qquad (2.7)$$

→ superlattice: unit cell different from substrate unit cell: p as primitive, c as centered

Matrix notation: can represent any structure (universal notation)

$b_1 = m_{11} a_1 + m_{12} a_2$

$b_2 = m_{21} a_1 + m_{22} a_1$

in matrix notation, $b = \mathfrak{M} \cdot a$ $\quad \mathfrak{M} = \begin{pmatrix} m_{11} & m_{12} \\ m_{21} & m_{22} \end{pmatrix}$

a: substrate, b: adsorbate

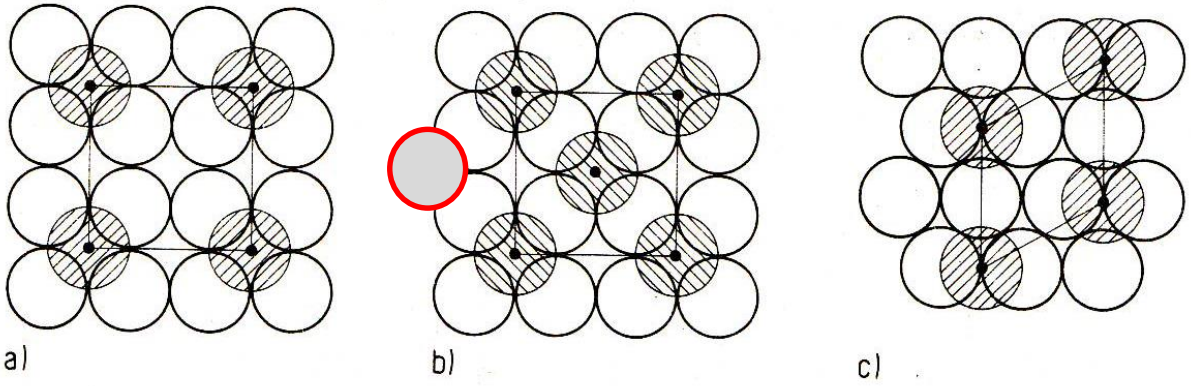

Fig. 9.2. Examples for overlayer structures. a) 2×2, b) $c(2 \times 2)$, c) $\sqrt{3} \times \sqrt{3}/R\,30°$.

$\mathfrak{M} = \begin{pmatrix} 2 & 0 \\ 0 & 2 \end{pmatrix}$, $\begin{pmatrix} 1 & 1 \\ -1 & 1 \end{pmatrix}$ and $\begin{pmatrix} 1 & 1 \\ -1 & 2 \end{pmatrix}$

Coherent vs. incoherent structures

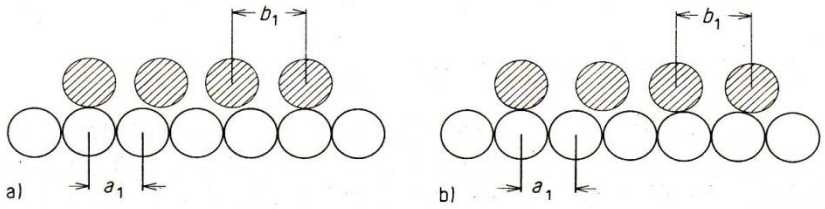

$m\ a_1 = n\ b_1$

n/m = rational # : coherent

irrational # : incoherent

- Surface structure of adsorbate (superlattice)

(1 x 1): surface atoms identical to the bulk unit cell → substrate structure
e.g., Pt(111)-(1 x 1)
(= fcc(111)-(1 x 1)

R: rotation angle

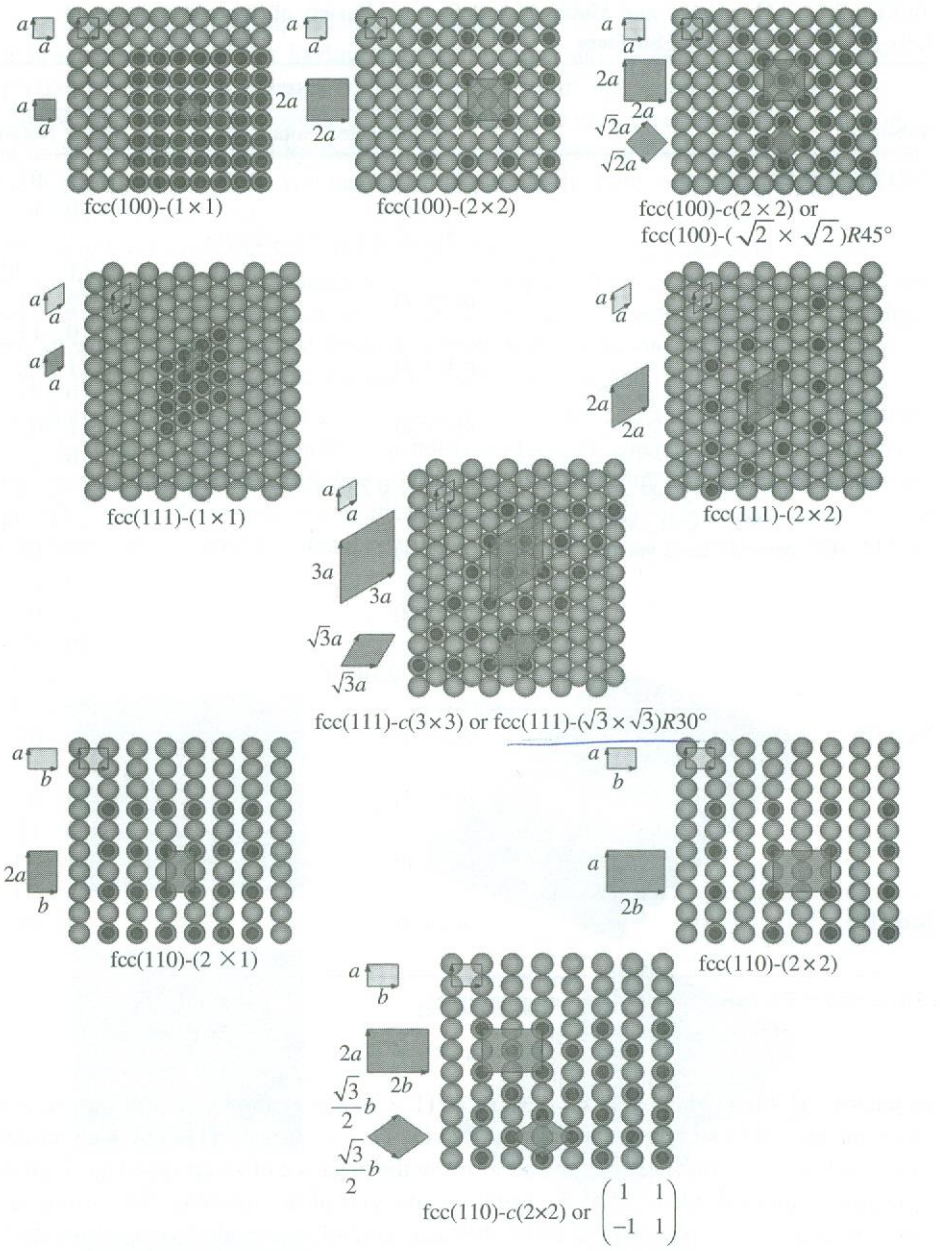

Figure 2.11. Commonly observed unit cells of adsorbate surface structures on fcc(100), (110), and (111) surfaces. (See color insert.)

TABLE 2.1 Abbreviated and Matrix Notations for a Variety of Superlattices on Low-Miller-Index Crystal Surfaces

Substrate	Superlattice Unit Cell: Abbreviated Notation[a]	Superlattice Unit Cell: Matrix Notation
fcc(100), bcc(100)	$p(1 \times 1)$	$\begin{vmatrix} 1 & 0 \\ 0 & 1 \end{vmatrix}$
	$c(2 \times 2) = (2\sqrt{2} \times \sqrt{2})R45^\circ$	$\begin{vmatrix} 1 & -1 \\ 1 & 1 \end{vmatrix}$
	$p(2 \times 1)$	$\begin{vmatrix} 2 & 0 \\ 0 & 1 \end{vmatrix}$
	$p(1 \times 2)$	$\begin{vmatrix} 1 & 0 \\ 0 & 2 \end{vmatrix}$
	$p(2 \times 2)$	$\begin{vmatrix} 2 & 0 \\ 0 & 2 \end{vmatrix}$
	$(2\sqrt{2} \times \sqrt{2})R45^\circ$	$\begin{vmatrix} 2 & 2 \\ -1 & 1 \end{vmatrix}$
fcc(111) (60° between basis vectors)	$p(2 \times 1)$	$\begin{vmatrix} 2 & 0 \\ 0 & 1 \end{vmatrix}$
	$p(2 \times 2)$	$\begin{vmatrix} 2 & 0 \\ 0 & 2 \end{vmatrix}$
	$(\sqrt{3} \times \sqrt{3})R30^\circ$	$\begin{vmatrix} 2 & 2 \\ -1 & 2 \end{vmatrix}$
fcc(110)	$p(2 \times 1)$	$\begin{vmatrix} 2 & 0 \\ 0 & 1 \end{vmatrix}$
	$p(3 \times 1)$	$\begin{vmatrix} 3 & 0 \\ 0 & 1 \end{vmatrix}$
	$c(2 \times 2)$	$\begin{vmatrix} 1 & -1 \\ 1 & 1 \end{vmatrix}$
bcc(110)	$p(2 \times 1)$	$\begin{vmatrix} 2 & 0 \\ 0 & 1 \end{vmatrix}$

[a]The parameter R is the orientation of the surface structures.

HW #2(4)

- Adsorption of atoms (e.g., Na, S, Cl): high coordination surface sites on metal surfaces
- Smaller atomic adsorbates (H, C, N, O): high coordination + penetration within substrate

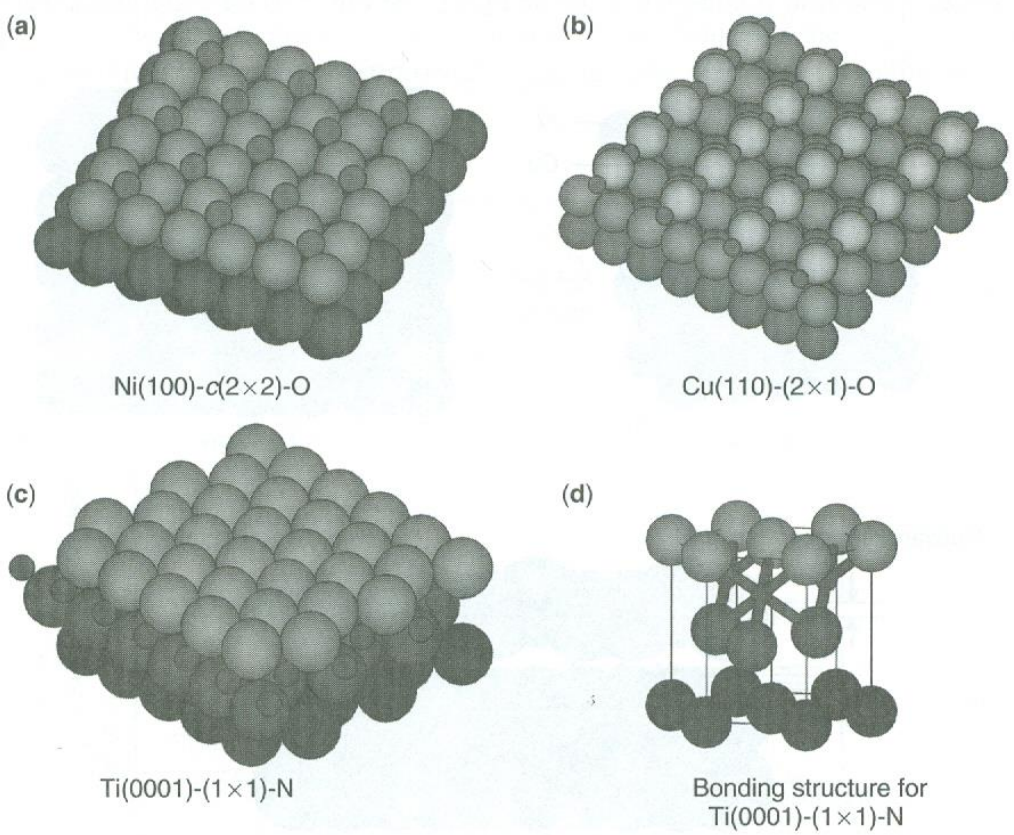

Figure 2.26. (a) The O surface structure on Ni(100) [23]; (b) the O chemisorption induced surface structure on Cu(110) [23]; (c) the N surface structure on Ti(0001) [24]; (d) the bonding structure for N on Ti (0001). All of these structures were obtained by LEED surface crystallography. (See color insert.)

Relaxation

- Relaxation: contraction of the interlayer distance at a clean surface between the first and second layer of atoms

When atoms or molecules adsorb, the surface atoms again relocate to optimize the strength of the adsorption-substrate bond

To minimize the surface energy (surface area)

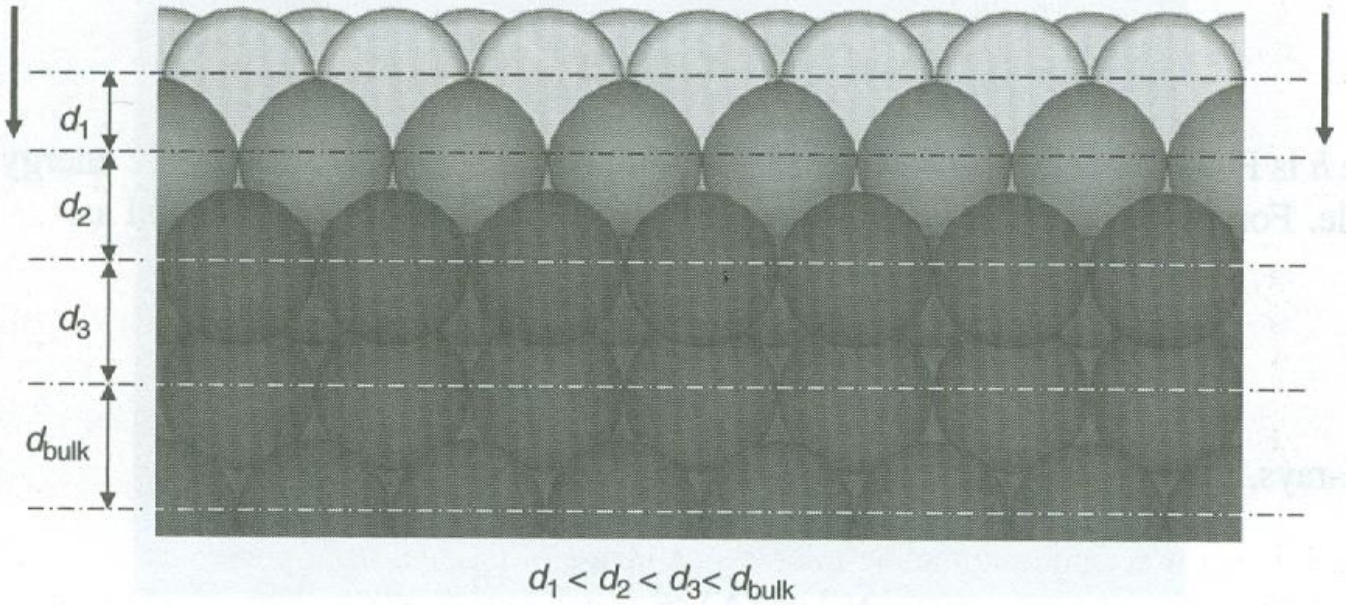

Figure 2.6. Schematic representation of the contraction in interlayer spacing usually observed at clean solid surfaces.

- Bond-length contraction or relaxation: in vacuum, all surface relax → reduced spacing between the 1st and 2nd atomic layers

The lower atomic packing/density, the larger the inward contraction

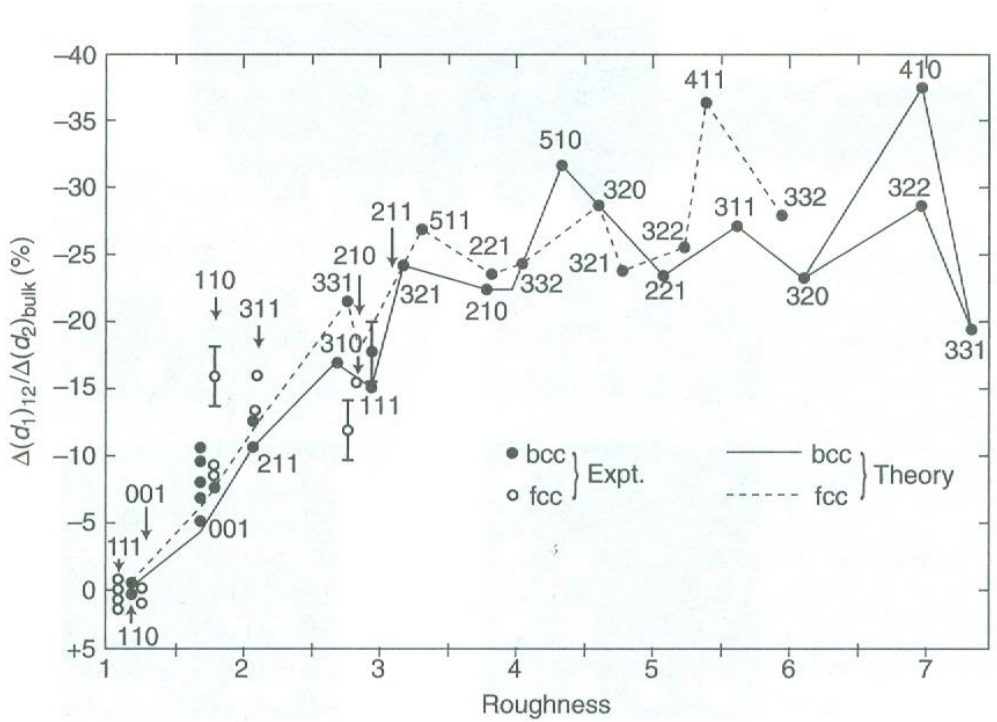

Figure 2.14. Contraction of interlayer spacing as a function of surface roughness (defined as 1/packing density) for several fcc and bcc metal surfaces. The points indicate experimental data, and the lines are theoretical fits [4].

Table 1.1 *Surface atom densities. Data taken from [2] except Si values from [3]. Diamond, Ge, GaAs and graphite calculated from lattice constants*

fcc structure							
Plane	(100)	(110)	(111)	(210)	(211)	(221)	
Density relative to (111)	0.866	0.612	1.000	0.387	0.354	0.289	
Metal	Al	Rh	Ir	Ni	Pd	Pt	Cu
Density of (111)/cm^{-2} $\times 10^{-15}$	1.415	1.599	1.574	1.864	1.534	1.503	1.772
Metal	Ag	Au					
Density of (111)/cm^{-2} $\times 10^{-15}$	1.387	1.394					
bcc structure							
Plane	(100)	(110)	(111)	(210)	(211)	(221)	
Density relative to (110)	0.707	1.000	0.409	0.316	0.578	0.236	
Metal	V	Nb	Ta	Cr	Mo	W	Fe
Density of (100)/cm^{-2} $\times 10^{-15}$	1.547	1.303	1.299	1.693	1.434	1.416	1.729
hcp structure							
Plane	(0001)	$(10\bar{1}0)$	$(10\bar{1}1)$	$(10\bar{1}2)$	$(11\bar{2}2)$	$(11\bar{2}2)$	
Density relative to (0001)	1.000	$\frac{3}{2r}$	$\frac{\sqrt{3}}{(4r^3+3)^1}$	$\frac{\sqrt{3}}{(4r^3+12)}$	$\frac{1}{r}$	$\frac{1}{2(r^3+1)^1}$	
Metal	Zr	Hf	Re	Ru	Os	Co	Zn
Density of (0001)/cm^{-2} $\times 10^{-15}$	1.110	1.130	1.514	1.582	1.546	1.830	1.630
Axial ratio $r = c/a$	1.59	1.59	1.61	1.58	1.58	1.62	1.86
Metal	Cd						
Density of (0001)/cm^{-2} $\times 10^{-15}$	1.308						
Axial ratio $r = c/a$	1.89						

	Diamond lattice			Zincblende	Graphite
Element	C	Si	Ge	GaAs	C
Areal Density/cm^{-2} $\times 10^{-15}$					basal plane
(100)	1.57	0.6782	0.627	0.626	3.845
(111)	1.82	0.7839	0.724	0.723	

Reconstruction

- The forces that lead to surface relaxation → reconstruction of surface layer

e.g., dangling bonds in semiconductor

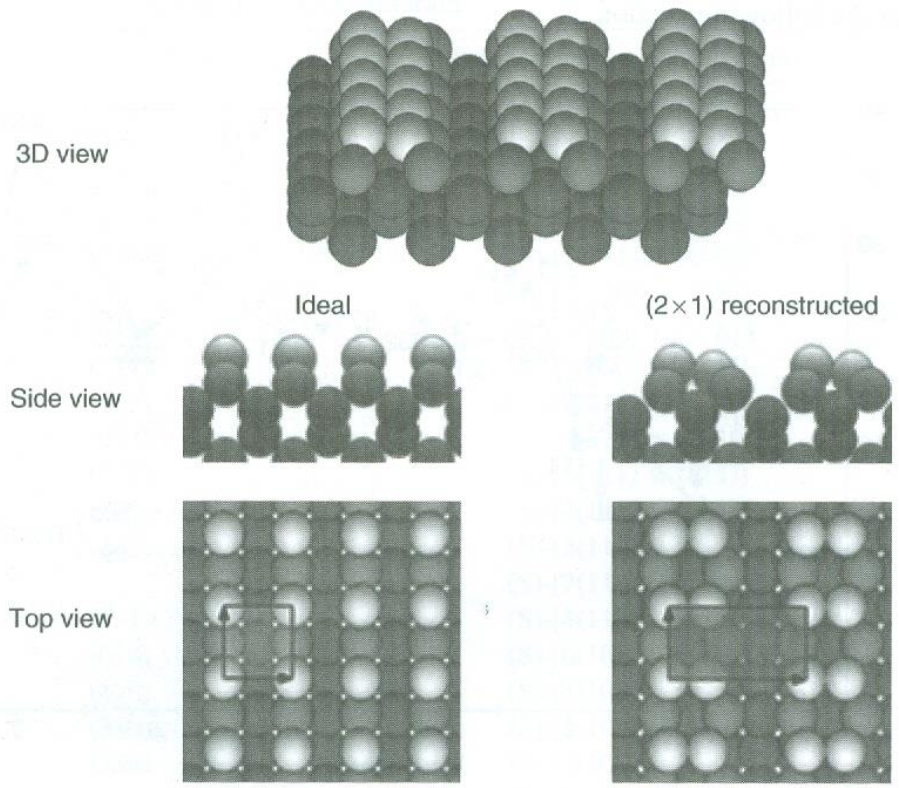

Figure 2.15. The reconstructed Si(100) crystal face as obtained by LEED surface crystallography The upper layer is indicated by a lighter color. Note that surface relaxation extends to three atomic layers into the bulk [8].

Loss of nearest neighbors at the surface → drastic rearrangements of these atoms, rebonding between surface atoms

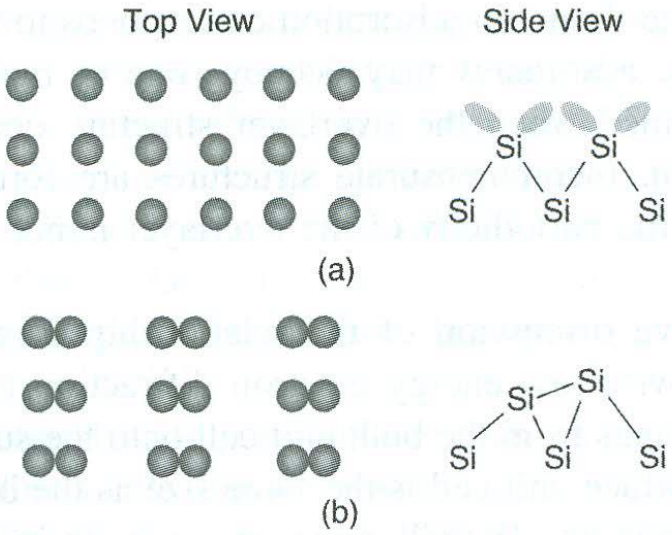

Figure 1.10 *The Si(100)–(2 × 1) reconstruction: (a) unreconstructed clean Si(100)–(1 × 1); (b) reconstructed clean Si(100)–(2 × 1).*

- Reconstruction in metal surfaces: several % in Pt, Au, Ir and so on

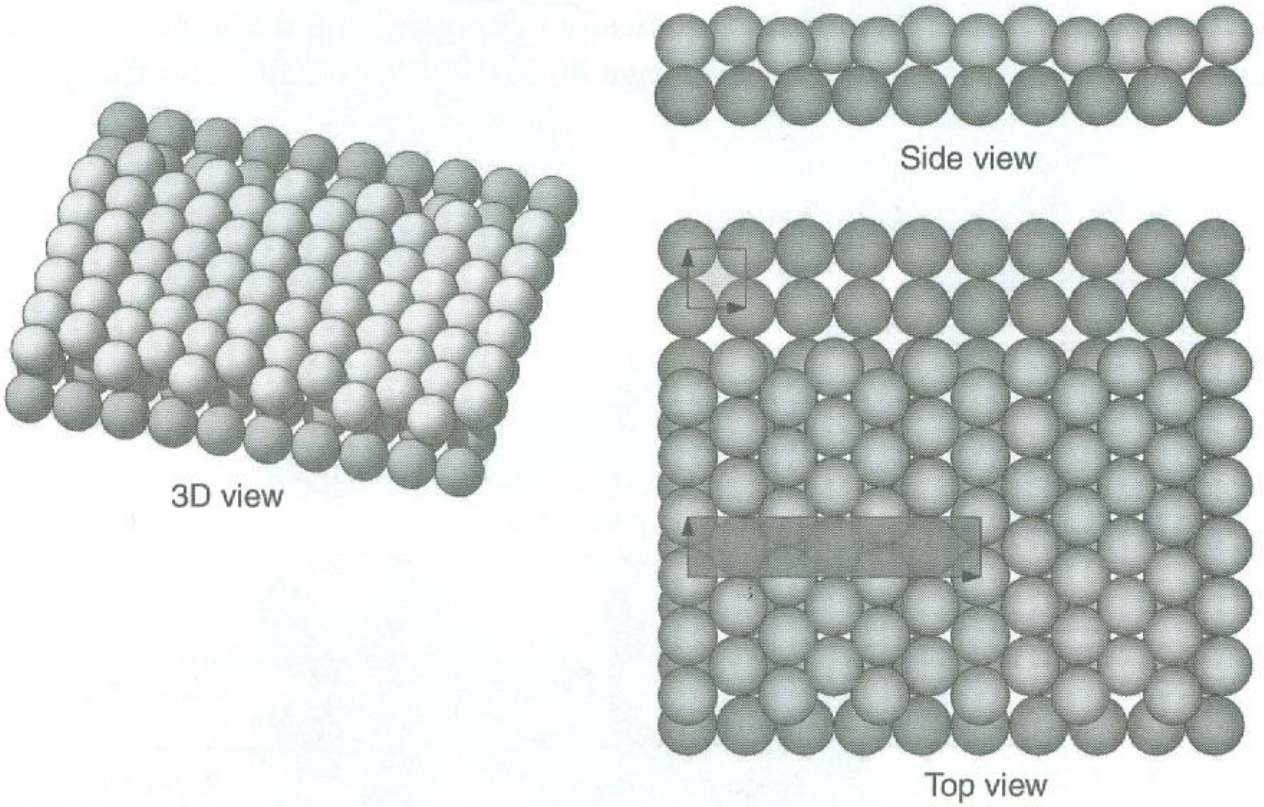

Figure 2.17. The structure of the reconstructed Ir(100) crystal face obtained from LEED surface crystallography. The first layer is indicated by a lighter color. Hexagonal packing in the surface layer induces buckling. The second layer retains its square unit cell. (See color insert.)

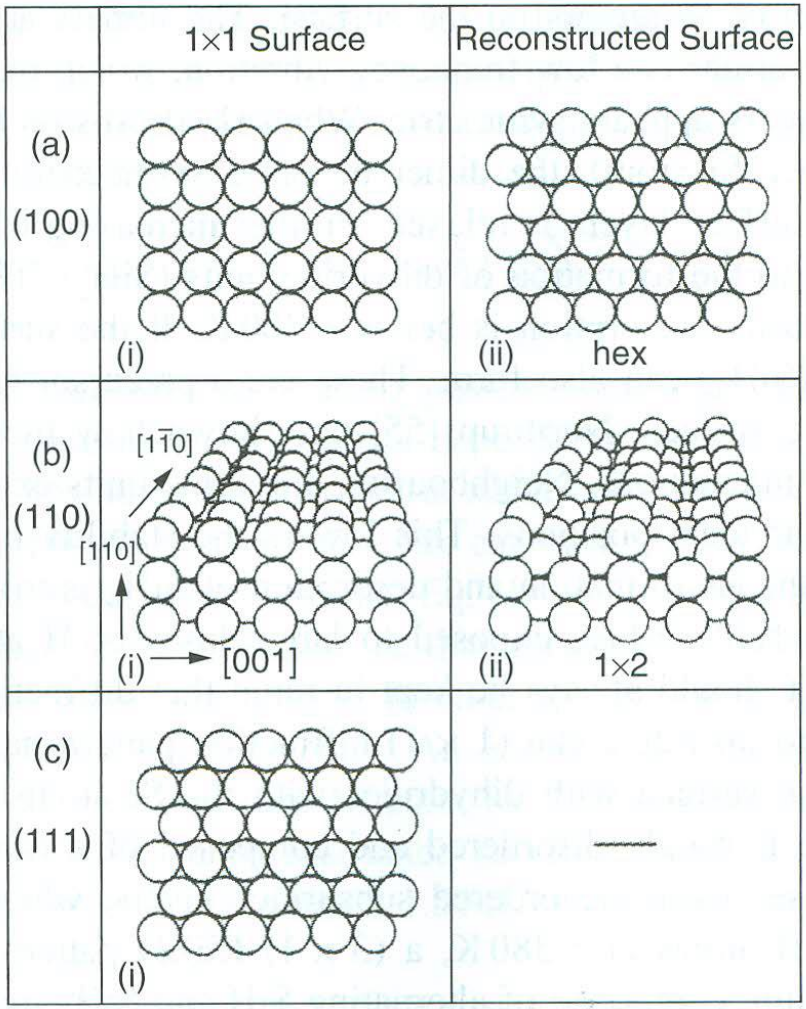

Figure 1.13 *Reconstructed and unreconstructed surfaces for the three low index planes of Pt: (a) (100) plane, (i) (1 × 1) unreconstructed surface, (ii) quasi-hexagonal (hex) reconstructed surface; (b) (110) plane, (i) (1 × 1) unreconstructed surface, (ii) missing row (1 × 2) reconstructed surface; (c) (111) plane, (i) (1 × 1) unreconstructed surface (Pt(111) is stable against reconstruction). Reproduced from R. Imbihl and G. Ertl,* Chem. Rev. *95, 697.*

- Reconstruction of high-Miller-index surfaces: roughening transition

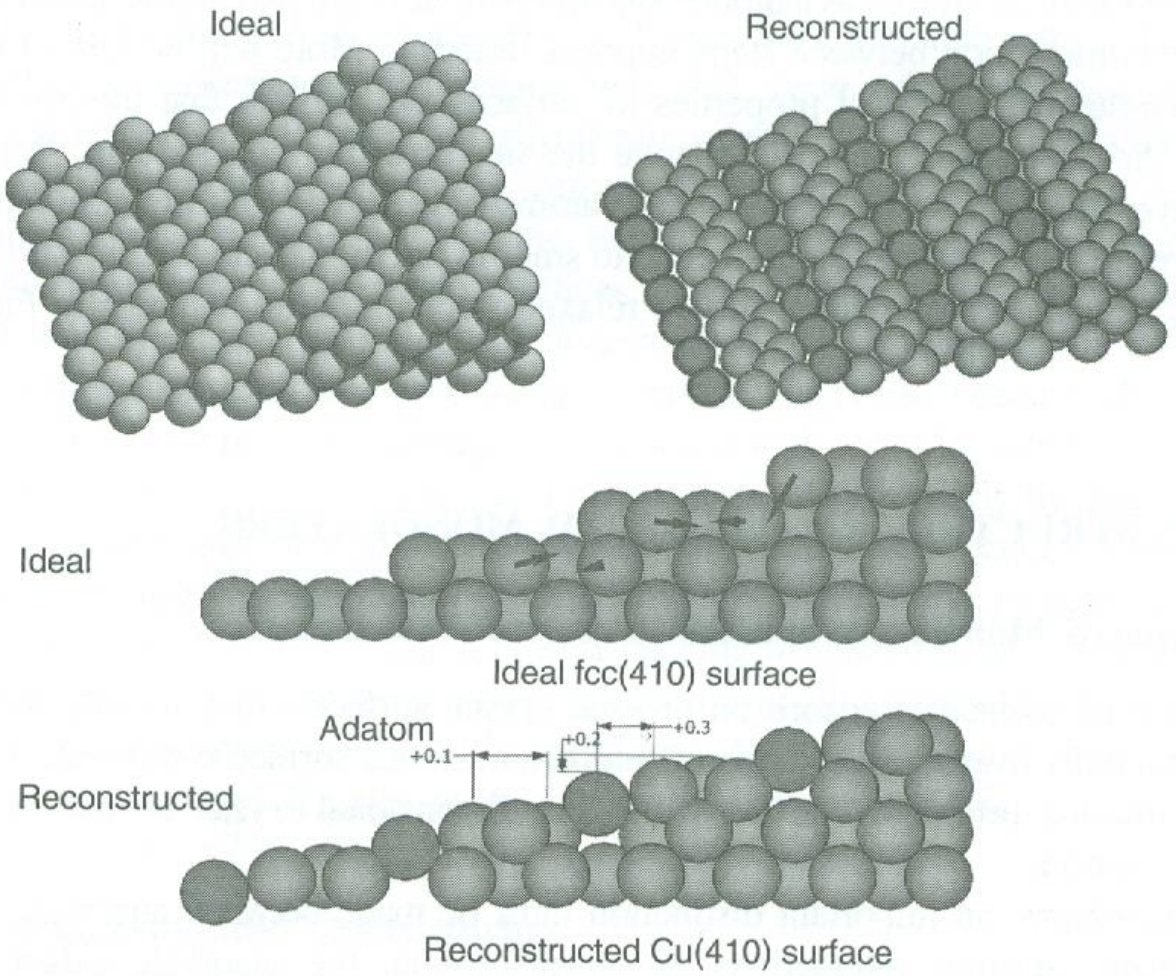

Figure 2.20. Relaxation at a Cu(410) stepped surface [21]. The relative displacements (in Angstrom) of atoms are shown in the side view of the bulk surface. Atoms in the first row at the each step become adatoms that are pointed out in the side view of the reconstructed surface. (See color insert.)

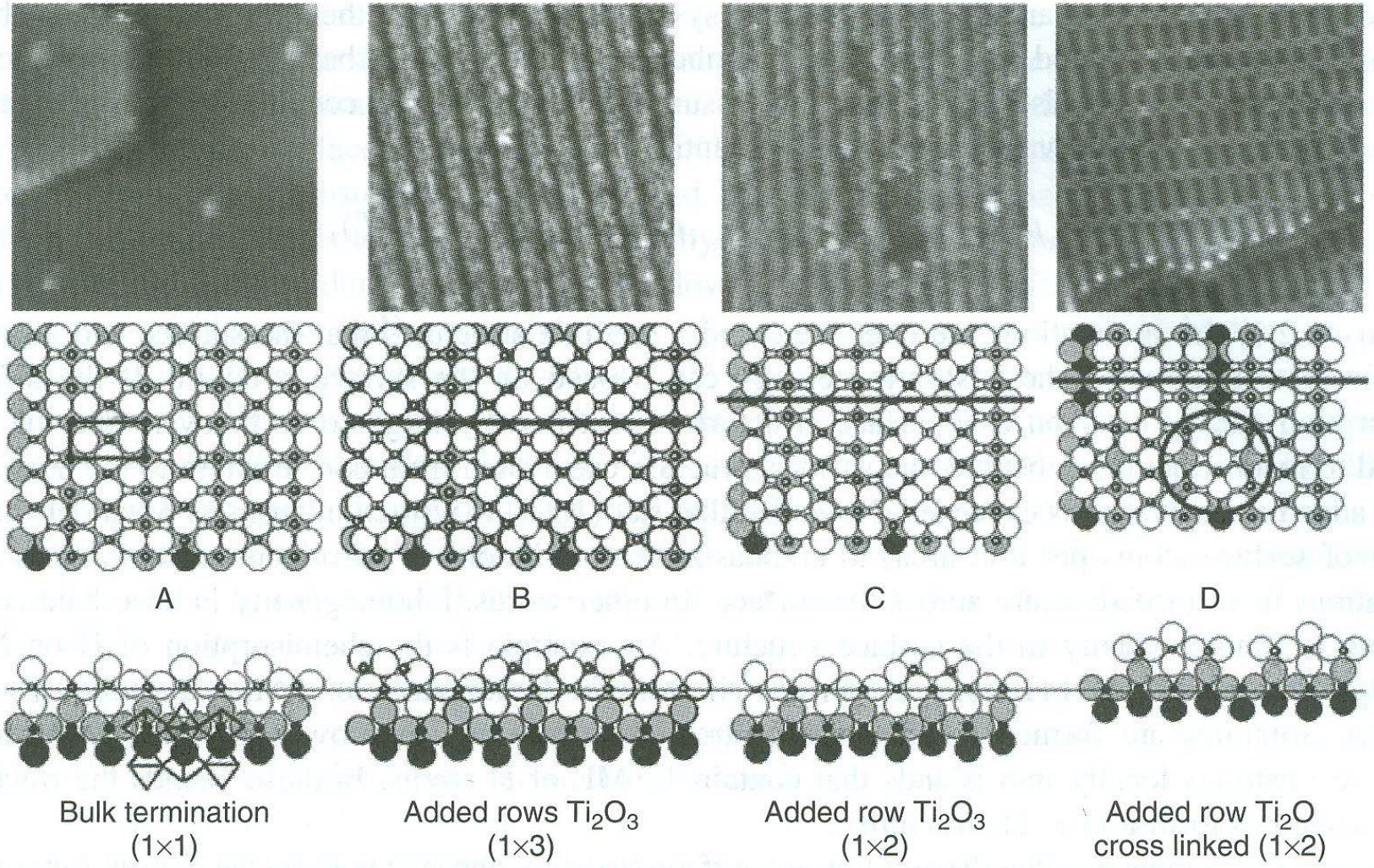

Figure 1.11 *The surface structures observed on TiO_2(110) as a function of increasing bulk reduction of the crystal. Upper panels are scanning tunnelling microscope images with 20 nm scan size. The lower two panels display the proposed surface structures. Reproduced from M. Bowker,* Curr. Opin. Solid State Mater. Sci. *10, 153. (2006) with permission from Elsevier.*

Adsorbate induced reconstructions

Adsorbate → strong adsorbate-substrate bond → chemisorbed layer removes the relaxation and reconstruction → surface return to bulk-like

However, adsorbate can also induce a new surface restructuring

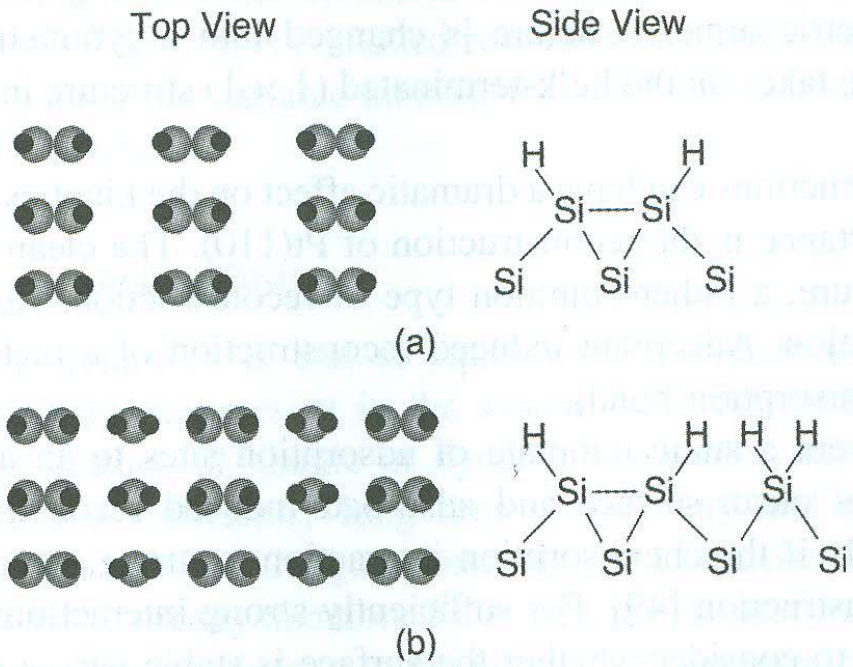

Figure 1.12 *The adsorption of H on to Si(100): (a) Si(100)–(2 × 1):H, θ (H) = 1 ML; (b) Si(100)–(3 × 1):H, θ (H) = 1.33 ML. Note: the structures obtained from the adsorption of hydrogen atoms on to Si(100) are a function of the hydrogen coverage, θ (H). 1 ML = 1 monolayer as defined by 1 hydrogen atom per surface silicon atom.*

Chiral surfaces

-Great challenge in heterogeneous catalyst → to develop catalysts for asymmetric synthesis (catalyst that accelerate the rate of reaction for only one of a pair of enantiomers → mirror image structure with the same chemical formula (D, L))
-Chiral recognition: to form a porous solid, the pores or porewalls of which are chiral. e.g. chiral silicate zeolites, chiral metal-organic frameworks
-2-D structure for chiral interactions: left-handed

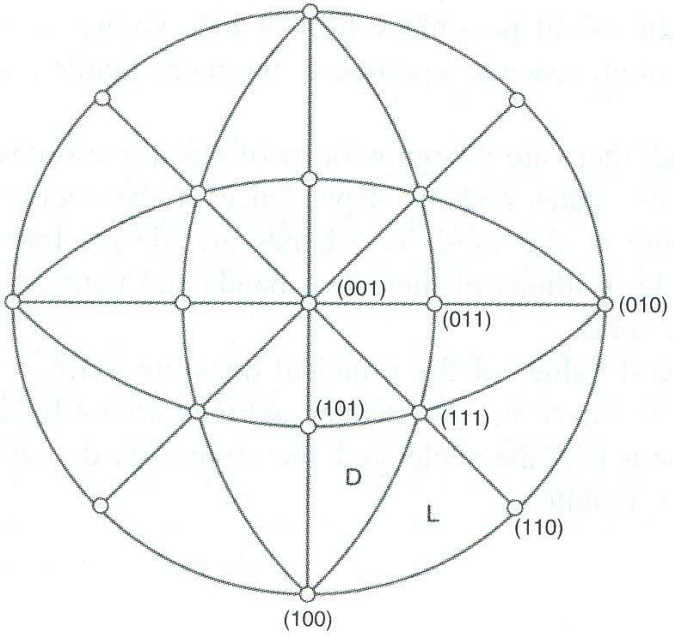

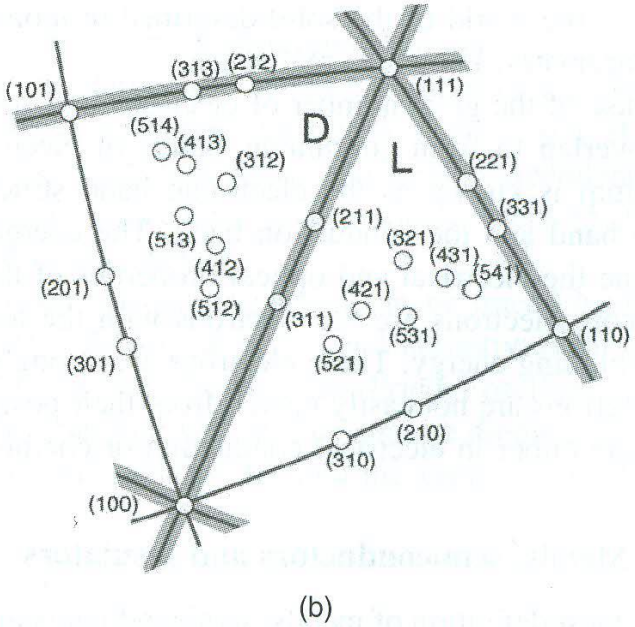

Clockwise: D
Anti-clockwise: L

Figure 1.14 *Stereogram projected on (001) showing the mirror zones relevant to primitive fcc, bcc and simple cubic crystal surfaces. Note that right-handed axes are used. The chiralities of two triangles are labelled D and L according to symmetry-based convention of Pratt et al. [63]. Reproduced from S.J. Pratt, S.J. Jenkins, D.A. King,* Surf. Sci., *585, L159. © (2005), with permission from Elsevier.*

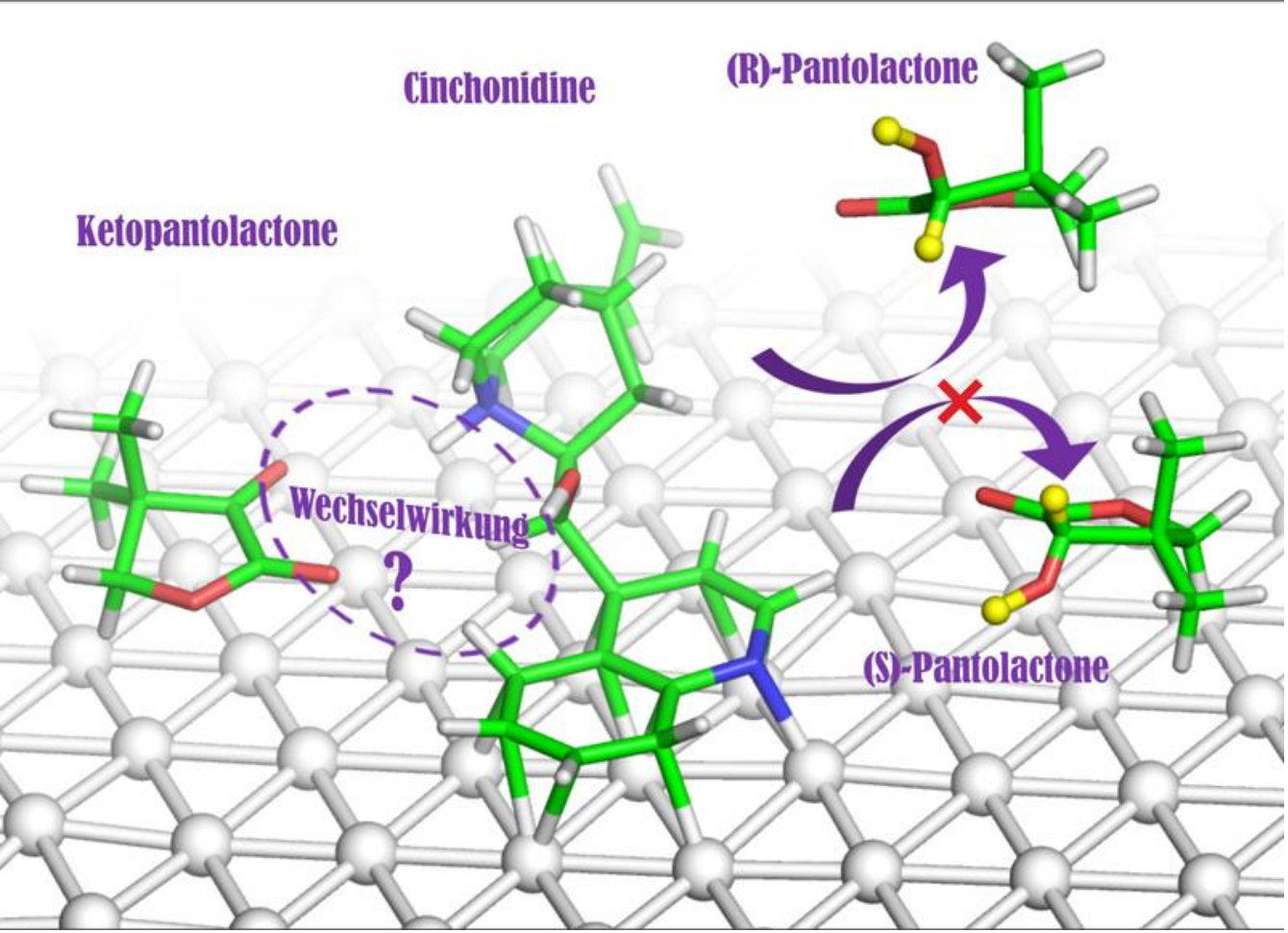

Model of the reaction steps on the chirally modified platinum surface. (Illustration: Prof. A. Baiker's group / ETH Zurich)

ethlife.ethz.ch

Chiral molecules exist in two mirror forms, so-called enantiomers. Because the two enantiomers differ in terms of their biological effect, it is crucial that only one of two possible forms is produced in the production of fine chemicals, pharmaceuticals, flavours and fragrances, or even fertilisers, for instance. One way of achieving this is to use certain catalysts, which create a particular reaction centre to determine the chirality (handedness) of a product in a controlled fashion. Experts refer to this as "asymmetric catalysis".

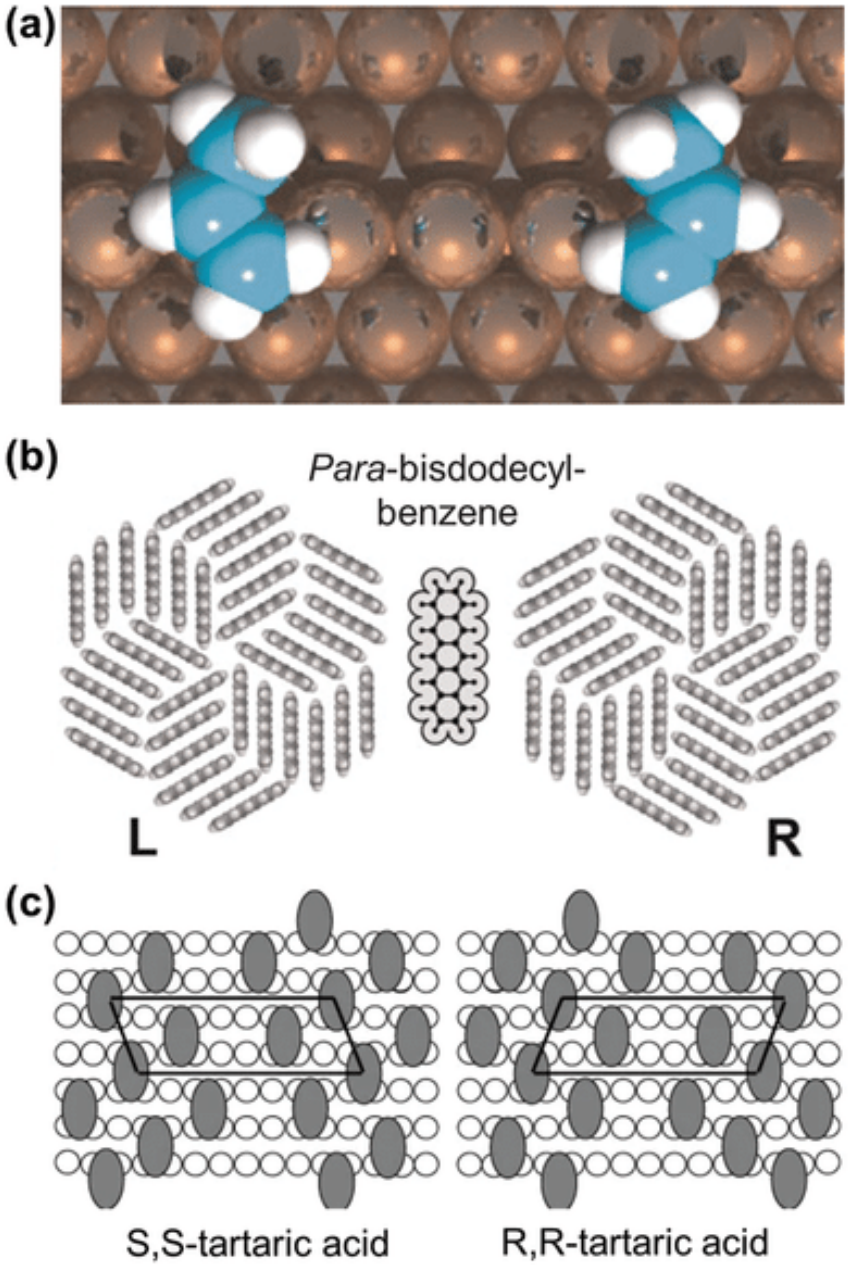

Surface chirality induced by molecular adsorption. a) Enantiomeric states of propene molecules adsorbed on a copper (211) surface. Despite the achiral molecular structure, adsorbed propene molecules on stepped copper surface can create chiral motif. b) Pentacene molecules assembled into L- and R-pinwheel cluster. Forty four pentacene molecules are close-packed together by the intermolecular interactions. c) (S,S)-Tartaric acid molecule (left) and (R,R)-tartaric acid molecule (right) adsorbed on Cu(110) surface. Supramolecular assembly of tartaric acid exhibits different orientation depending on the chirality of molecules. a) Reproduced with permission.85 Copyright 2009, Wiley-VCH. b) Reproduced with permission.71 Copyright 2012, Wiley-VCH. c) Reproduced with permission.93 Copyright 2000, Springer Nature.

Ki Tae Nam group, *Adv. Mat*. (2020)

Co_3O_4 cubic spinel (a = b = c = 8.084 Å)

Tetragonal Mn_3O_4 (a = b = 5.765 Å, c = 9.442 Å) a spinel structure elongated along the *c*-axis

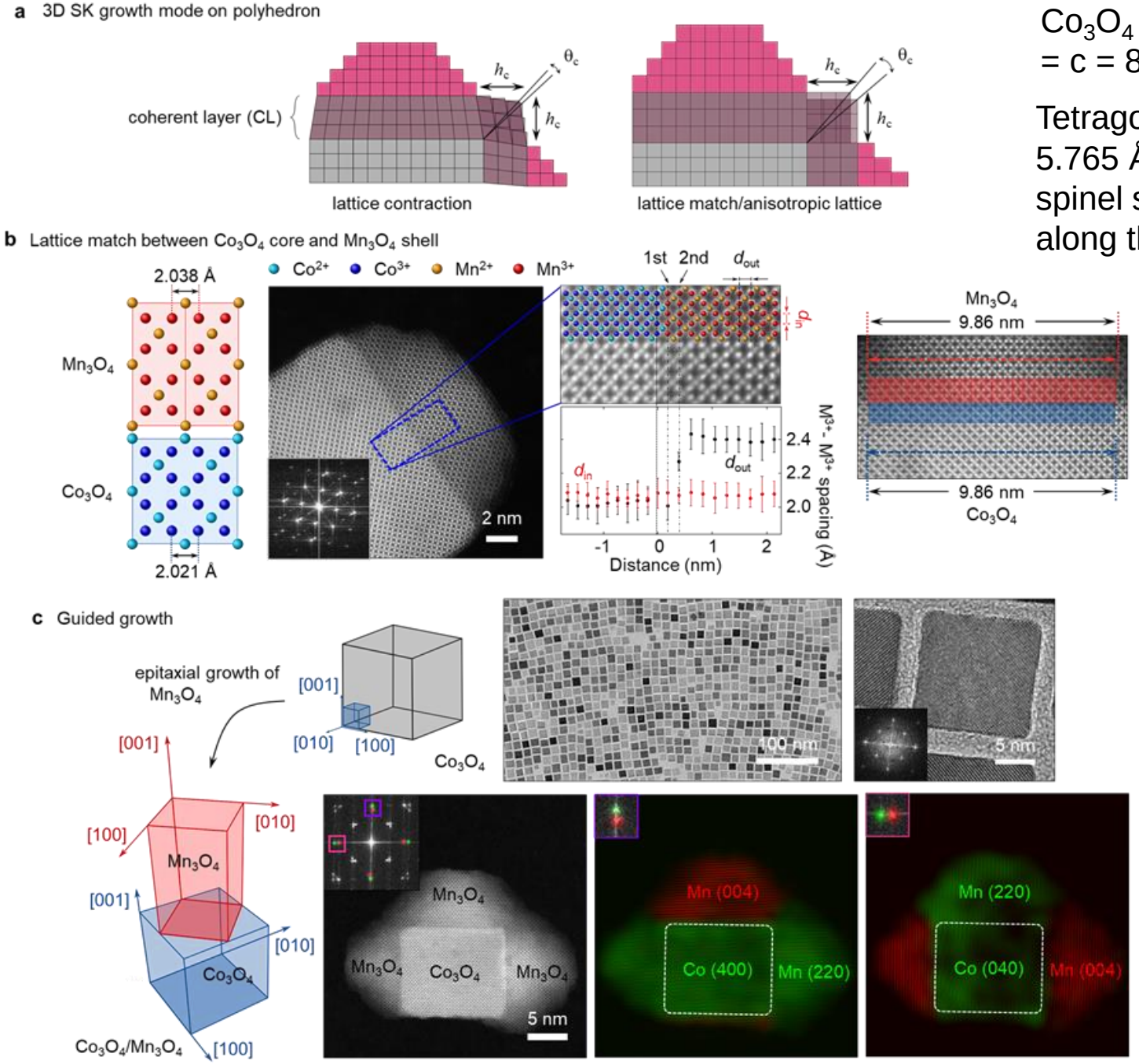

Nature **2020**, *577*, 359–363.

Additional Note

(This content is not the scope of the exam.)

*I will record and provide video file in new ETL for students in need.

2. Surface electronic structure

Metals, semiconductors and insulators

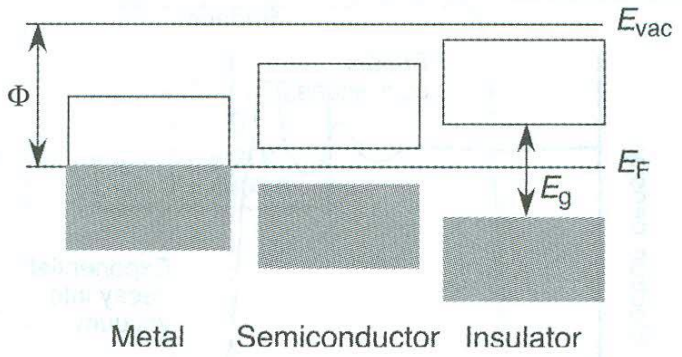

Figure 1.15 *Fermi energies, vacuum energies and work functions in a metal, a semiconductor and an insulator. The presence and size of a gap between electronic states at the Fermi energy, E_F, determines whether a material is a metal, semiconductor or insulator. E_g, band gap; Φ work function equal to the difference between E_F and the vacuum energy, E_{vac}.*

Fermi level (E_F): the energy of the highest occupied electronic state (at 0 K)
At higher T, e^--h^+ pair formation
Vacuum energy (E_{vac}): the energy of a material and an e^- at infinite separation
Work function (Φ):

$$e\Phi = E_{vac} - E_F$$

e: the elementary charge
→ minimum energy to remove one e- from the material to infinity at 0 K.
actual min. ionization energy is great than Φ due to no state at E_F for SC & insulator

Band model

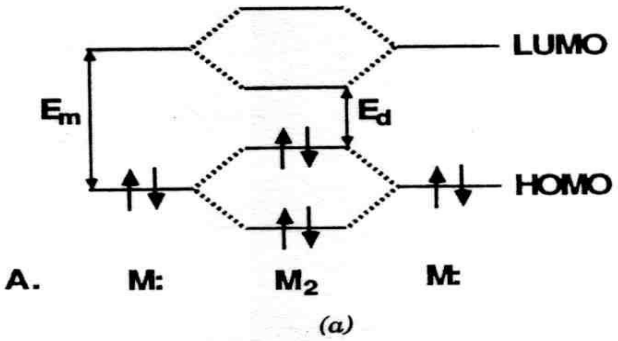
LUMO
E_m
E_d
HOMO
A.
M:
M_2
M:
(a)

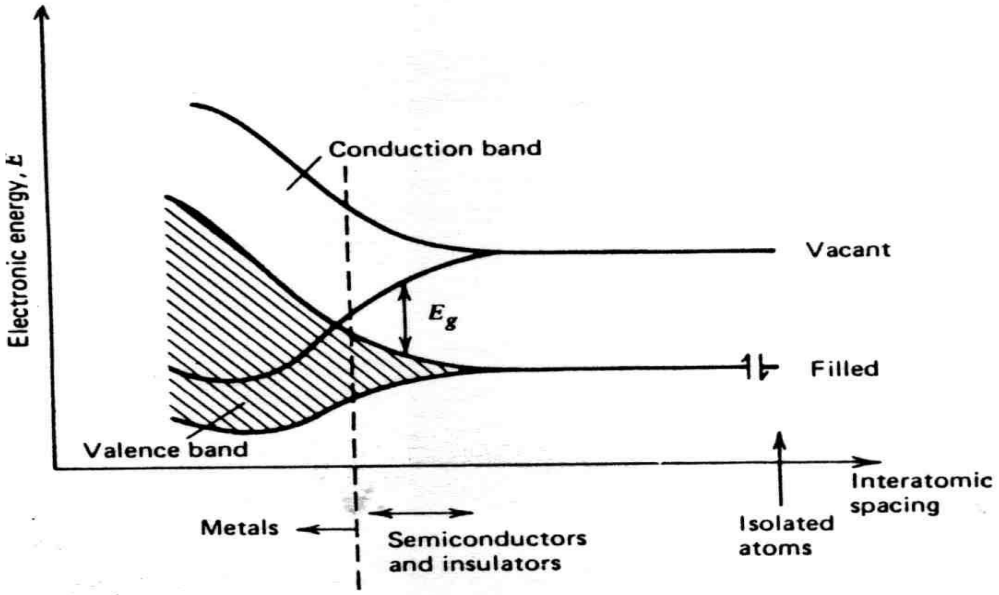
Electronic energy, E
Conduction band
Vacant
E_g
Filled
Valence band
Interatomic spacing
Metals
Semiconductors and insulators
Isolated atoms

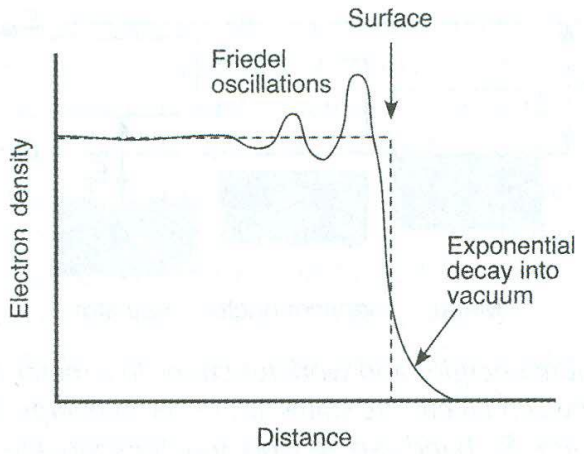

Figure 1.16 *Friedel oscillations: the electron density near the surface oscillates before decaying exponentially*

Dependence of the work function (Φ) on surface properties
→ e^- density does not end abruptly at the surface (Fig.1.16), instead, it oscillates near the surface (Friedel oscillation)

probability that an electronic level at energy E is occupied by an electron at thermal equilibrium f(E) → Fermi-Dirac distribution function

$$f(E) = \frac{1}{1 + \exp\left[(E - E_F)/kT\right]}$$

Fermi level E_F; value of E for which f(E) = 1/2 (equally probable that a level is occupied or vacant)
At T = 0, all levels below E_F ($E < E_F$) are occupied ($f(E) \rightarrow 1$); all levels $E > E_F$ vacant

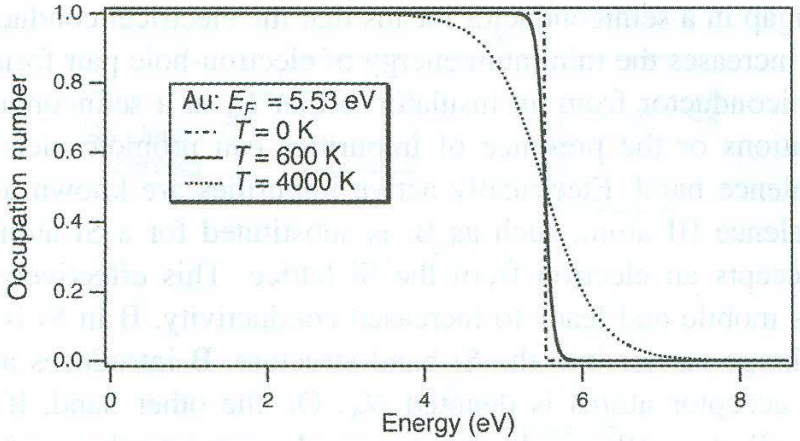

Figure 1.17 *Fermi-Dirac distribution for gold at three different temperatures, T, E_F, Fermi energy.*

Band gap (E_g), $E_g = E_c - E_v$

Fermi level of intrinsic semiconductor

$$E_F = E_i = \frac{E_C + E_V}{2} + \frac{k_B T}{2} \ln\left(\frac{N_V}{N_C}\right) \qquad (1.3.10)$$

The position of the Fermi energy in a doped semiconductor depends on the concentration and type of dopants. E_F is pushed upward by n-type dopants according to

$$E_F = E_i + k_B T \ln\left(\frac{N_D}{n_i}\right). \qquad (1.3.12)$$

In a p-type material, E_F is pulled towards the valence band

$$E_F = E_i - k_B T \ln\left(\frac{N_A}{n_i}\right). \qquad (1.3.13)$$

-Insulator: large band gap (typically > 3eV), diamond ~5.5 eV
-Solar wavelength 600~1000 nm → 1.5~0.5 eV (← $\lambda(nm) = 1240/E_g(eV)$)

TiO_2 (3 eV) ~400 nm(UV), Si(1.1 eV)~1130 nm(IR)

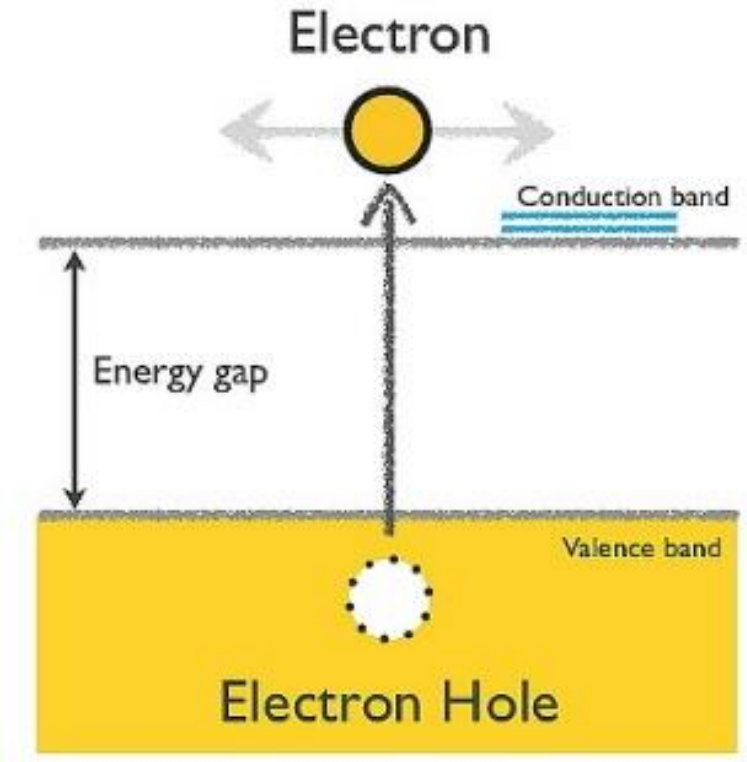

Energy levels at metal interfaces

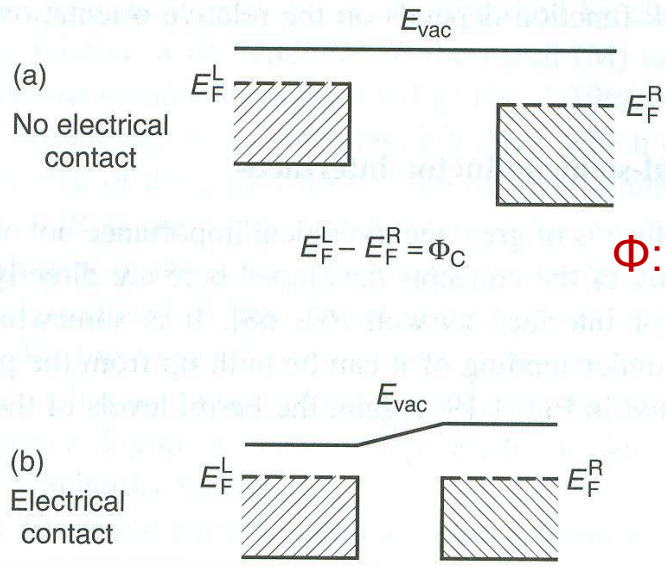

Φ: work function

Figure 1.18 *Electronic bands of metals (a) before and (b) after electrical contact. The Fermi energies of the two metals align at equilibrium when electrical contact is made. E_{vac}, vacuum energy; E_F, Fermi energy; subscripts L and R refer to left-hand and right-hand metal, respectively.*

Contact → electron flow left to right due to Fermi level difference → equal E_F
→ slightly depleted of electron in left, excess in right → dipole develops
→ contact potential

$$\Delta\varphi = \Phi_R - \Phi_L$$

→ Electron flow: R to L due to electric field by the sloping vacuum level

Energy levels at metal-semiconductor interfaces

$\Phi_S > \Phi_M$
Charge transfer: M → S

Ohmic contact

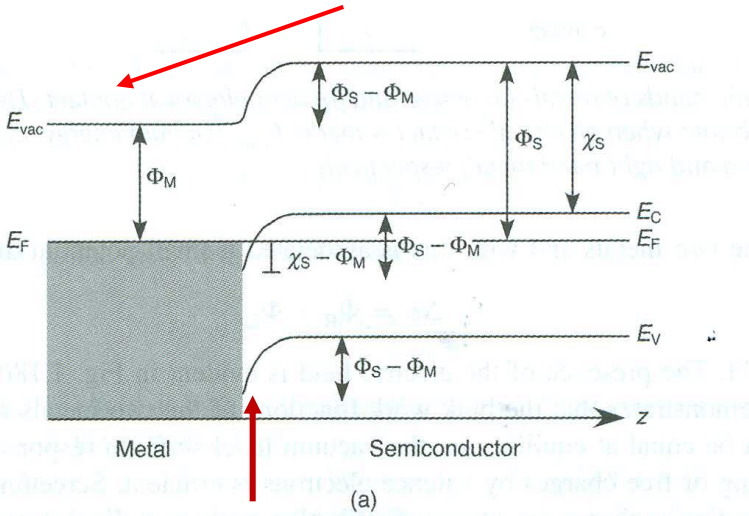

Space charge region → band bending

$\Phi_S < \Phi_M$
Charge transfer: S → M

Schottky barrier

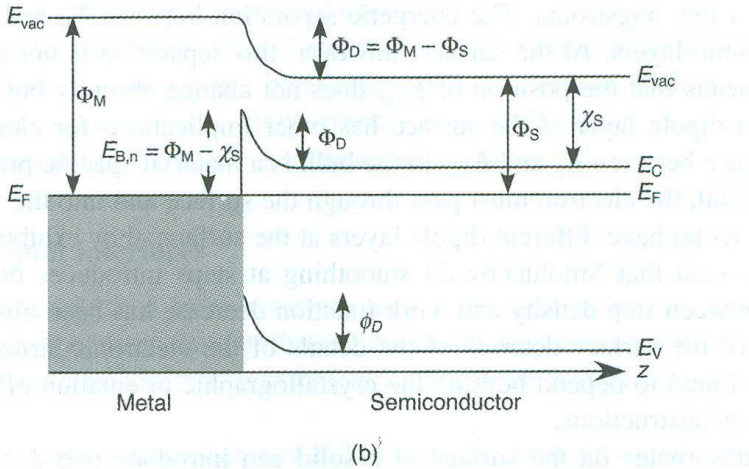

Figure 1.19 *Band bending in an n-type semiconductor at a heterojunction with a metal. (a) Ohmic contact ($\Phi_S > \Phi_M$). (b) Blocking contact (Schottky barrier, $\Phi_S < \Phi_M$). The energy of the bands is plotted as a function of distance z in a direction normal to the surface. Φ_S, Φ_M work function of the semiconductor and of the metal, respectively; E_{vac}, vacuum energy; E_C, energy of the conduction band minimum; E_F, Fermi energy; E_V energy of the valence band maximum; E_g band gap. Reproduced from S. Elliott,* The Physics and Chemistry of Solids, *John Wiley, New York. © (1998), with permission from John Wiley & Sons, Ltd.*

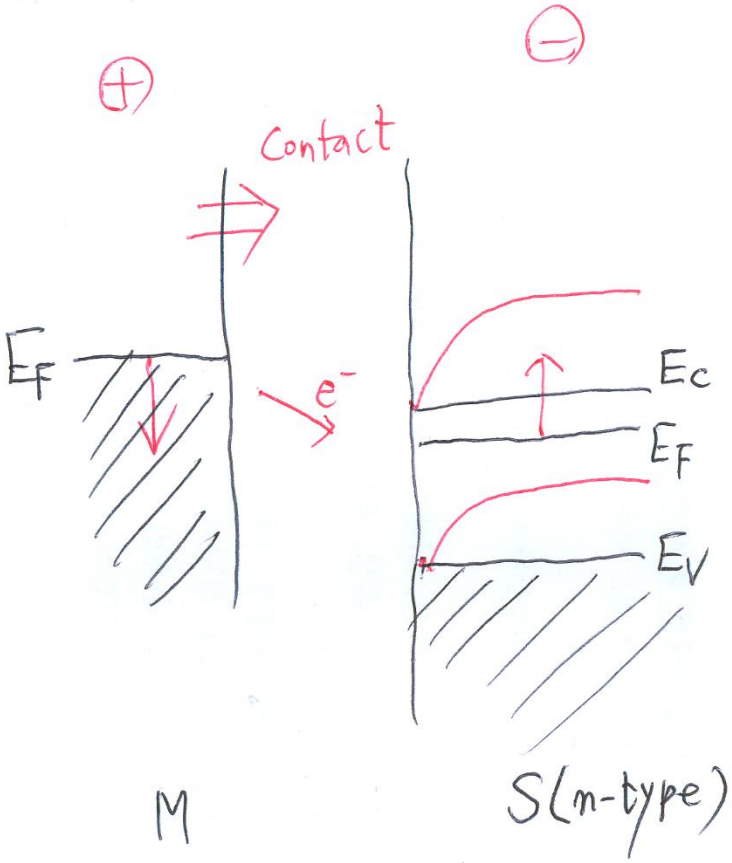

Ohmic contact

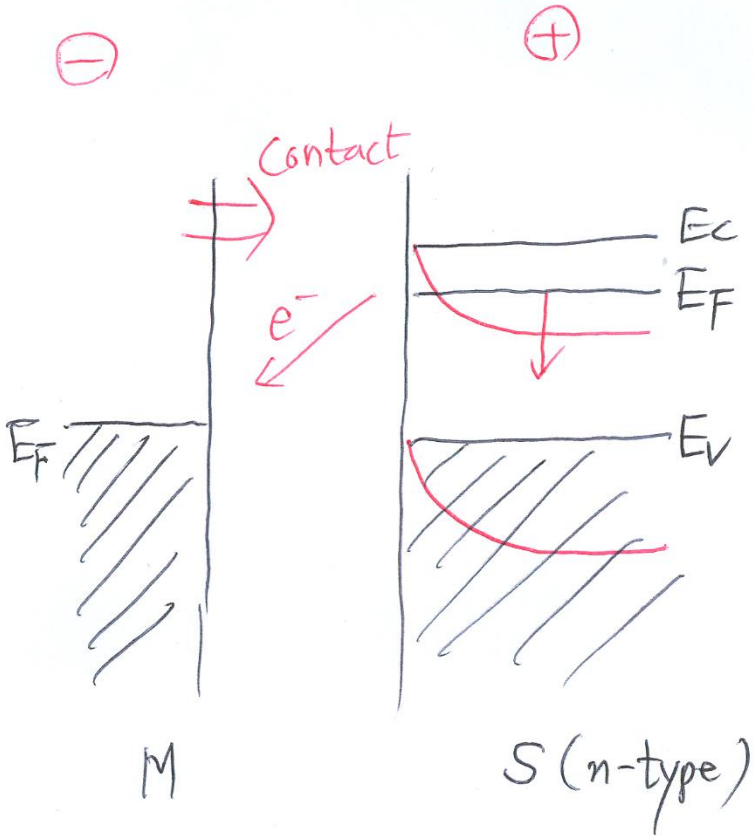

Schottky barrier

Semiconductor/solution interface

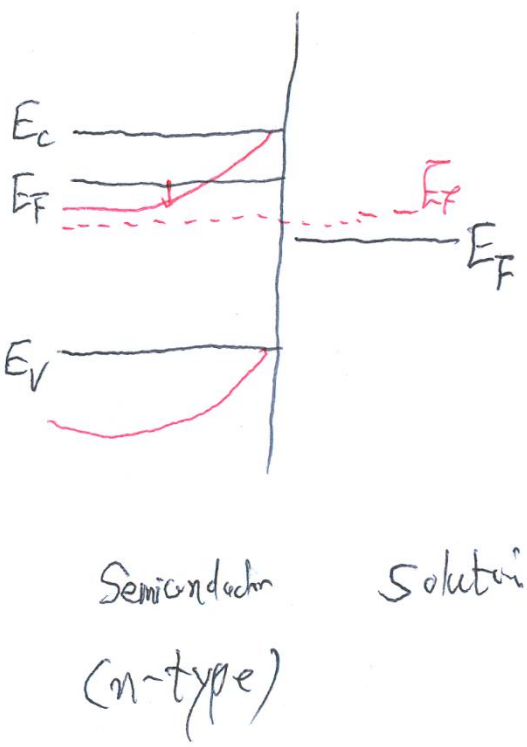

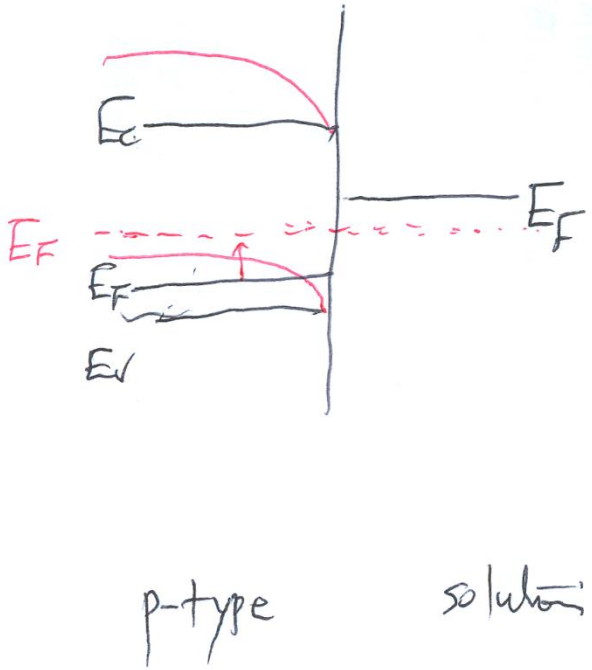

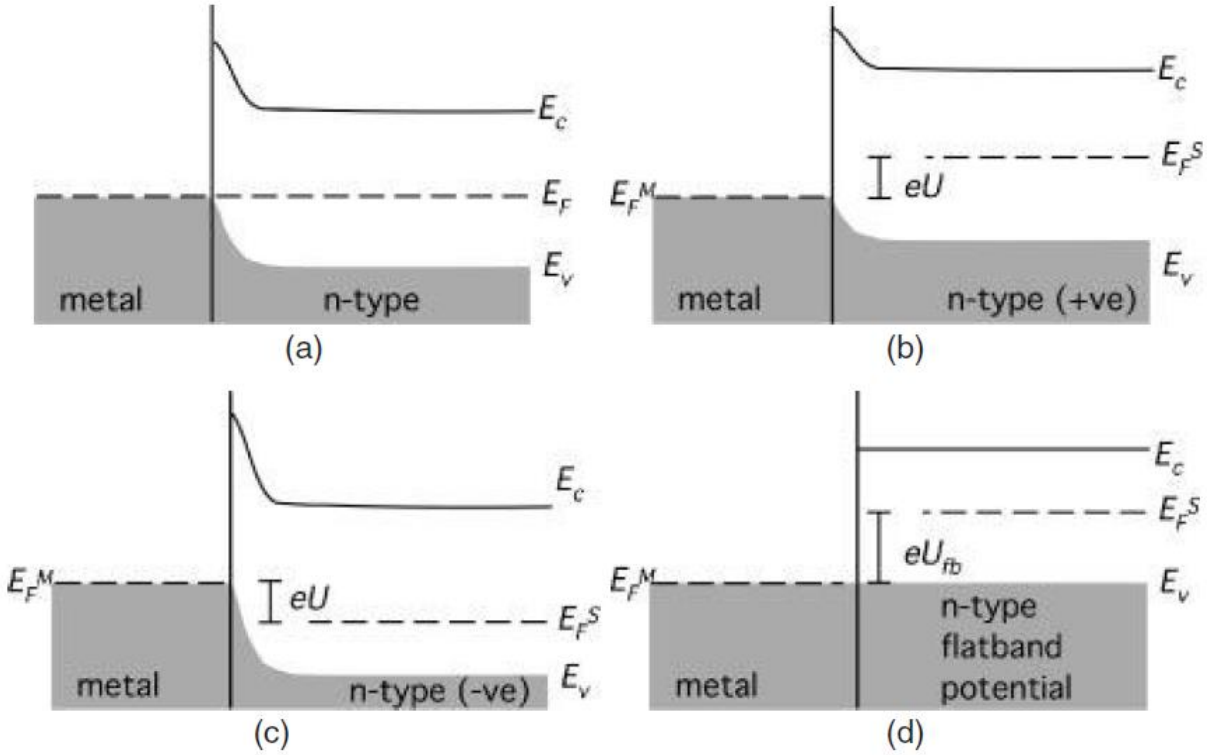

Figure 1.20 *The electrochemical potential and the effects of an applied voltage on a metal/semiconductor interface. (a) No applied bias. (b) Forward bias. (c) Reverse bias. (d) Biased at the flatband potential, U_{fb}. E_C, energy of the conduction band minimum; E_F, Fermi energy; E_V, energy of the valence band maximum; superscripts M and S refer to the metal and the semiconductor, respectively.*

Surface electronic states

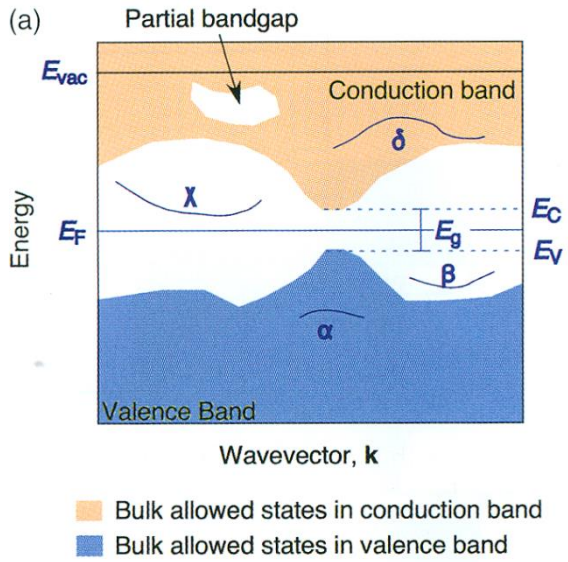

Figure 1.23 *(a) The band structure of a semiconductor, including an occupied surface resonance (α), an occupied surface state (β), a normally unoccupied surface state (χ), and a normally unoccupied surface resonance (δ). (b) The band structure of a topological insulator.* E_{vac}*, vacuum energy;* E_F *Fermi energy;* E_V*, energy of the valence band maximum;* E_C*, the conduction band minimum.*

-Surface vs. bulk → surface atoms can be thought of as impurity → localized electronic states

(i) Overlap with bulk states (overlapping states): surface resonance

(ii) Exist in a band gap: surface state

-Structural defects or adsorbates → also surface states

-Surface states can act as donor or acceptor states → strong influence on electronic properties of devices

Size effects in nanoscale systems

Table 1.2 *Clusters can be roughly categorized on the basis of their size. The properties of clusters depend on size. For clusters of different composition the boundaries might occur as slightly different values. The diameter is calculated on the assumption of a close packed structure with the atoms having the size of a Na atom*

	Small	Medium	Large
Atoms (N)	2–20	20–500	500–10^6
Diameter/nm	≤ 1.1	1.1–3.3	3.3–100
Surface/Bulk (N_s/N)	Not separable	0.9–0.5	$\leq 0.5 \sim 0.2$ for N = 3 000 $\ll 1$ for $N \geq 10^5$
Electronic states	Approaching discrete	Approaching bands	Moving toward bulk behaviour
Size dependence	No simple, smooth dependence of properties on size and shape	Size dependent properties that vary smoothly	Quantum size effects may still be important but properties approaching bulk values

-Surface vs. bulk(=infinite solids) → bulk to shrinked a finite cluster of atoms (Table 1.2)

-Small cluster are close to molecular in their electronic states that are discrete(i.e., orbital, not band structure)

-What separates clusters → “nanoparticles”: their properties are “size-dependent”

The reasons of size-dependent

(i) Relative large number of surface atoms to bulk atoms → surface contribution↑

(ii) Quantum confinement: a phenomenon that occur when particle senses the size of container it is in size of particle is given by its de Broglie wavelength

$\lambda = h/p$ (h: Planck constant, p = mv (linear momentum))

e.g., Si, onset size of size-dependent electronic structure is ~5 nm (Table 1.4)
(e^--h pair (exciton): radius of exciton = size of the particle → size-dependent)

Easiest example is a particle-in-a-box

$E_n = n^2h^2/8mL^2$, n = 1,2,….

→ energy is quantized, $\Delta E \propto 1/m, 1/L^2, \Delta E \propto 1/mL^2$
→ sufficiently small particles exhibit quantum effects

Table 1.4 *Bohr exciton radius r_{ex} for selected semiconductors.*

Semiconductor	Si	Ge	SiC	GaAs	GaP	InP	CdS	InSb	MoS_2
r_{ex} (nm)	4.9	17.7	2.7	14	1.7	9.5	3.0	69	1.61

Source: Values taken from [114] except MoS_2 [115].

3. Surface vibrational structure

Solids: vibration of atoms(lattices) and electrons
How atoms vibrate about their equilibrium surface sites (surface atom vibrations)
→ phonon (lattice vibration), plasmon (electron vibration)
→ quantized mode of a vibration according in a rigid crystal lattice

At T > 0K, atoms vibrate about the equilibrium positions, and their expansion will cause displacement of these positions themselves → thermally induced vibrations → heat capacity, thermal expansivity

Harmonic oscillator model: 1-D harmonic oscillators
→ phonon band structure

$E_v = (v + ½)\hbar\omega_o$
v: vibrational quantum number,
ω_0: fundamental radial frequency of the oscillator

→ not allowed all energies
→ quantized “phonon”

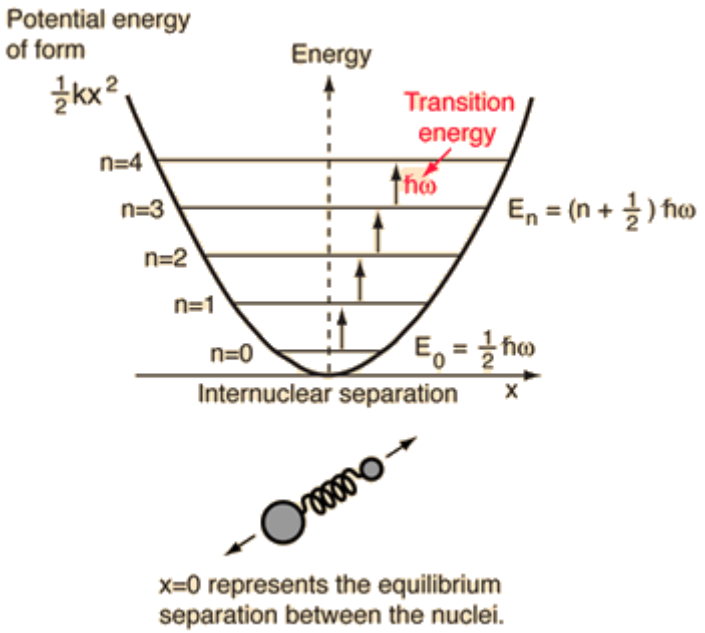

hyperphysics.phy-astr.gsu.edu

Debye frequency(ω_D or ν_D): maximum frequency for the phonons of solids → a measure of the rigidity of the lattice

ω_D or ν_D: Au 14.3 meV (115 cm^{-1}), W 34.5 meV (278 cm^{-1}), Si 55.5 meV (448 cm^{-1}),
Stepped Pt surface 25 meV (205 cm^{-1}, 4 x 10^{-21} J),
Diamond (most rigid lattice) 192 meV (1550 cm^{-1}),
→ slightly higher ω in real crystal than Debye model, Si 520 cm^{-1}

Debye temperature(T_D or θ_D) vs. Debye frequency

$$T_D = \hbar\omega_D/k_B$$

T_D: Pt(111): 110K(surface), 234K(bulk), Ni(110): 220K

-Inelastic He scattering to determine the vibrational spectrum of surface atoms at solid surfaces
-HREELS(high-resolution electron energy loss spectroscopy): surface atom vibration

-surface phonon is different from bulk
-phonon in nanoscale system → vibrational Raman spectrum depends on nano size and shape → no comprehensive theory yet!

Surface plasmon resonance (SPR)

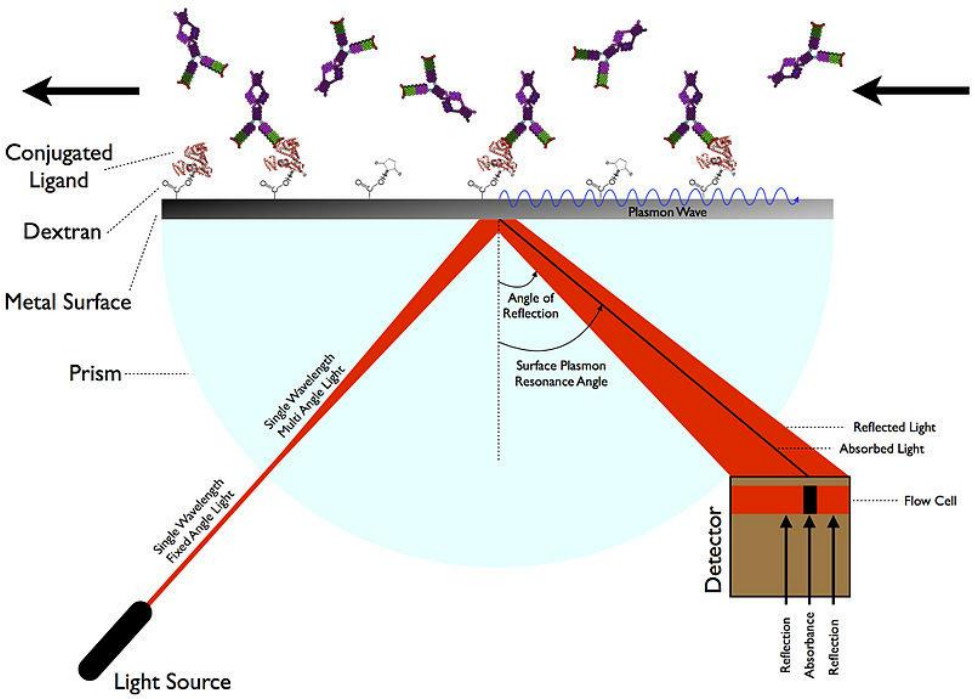

Surface plasmon resonance (SPR) is the collective oscillation of valence electron in a solid stimulated by incident light. The resonance condition is established when the frequency of light photons matches the natural frequency of surface electrons oscillating against the restoring force of positive nuclei. SPR in nanometer-sized structures is called **localized surface plasmon resonance**. SPR is the basis of many standard tools for measuring adsorption of material onto planar metal (typically gold and silver) surfaces or onto the surface of metal nanoparticles. It is the fundamental principle behind many color-based biosensor applications and different lab-on-a-chip sensors. (from Wikipedia)

Surface plasmon

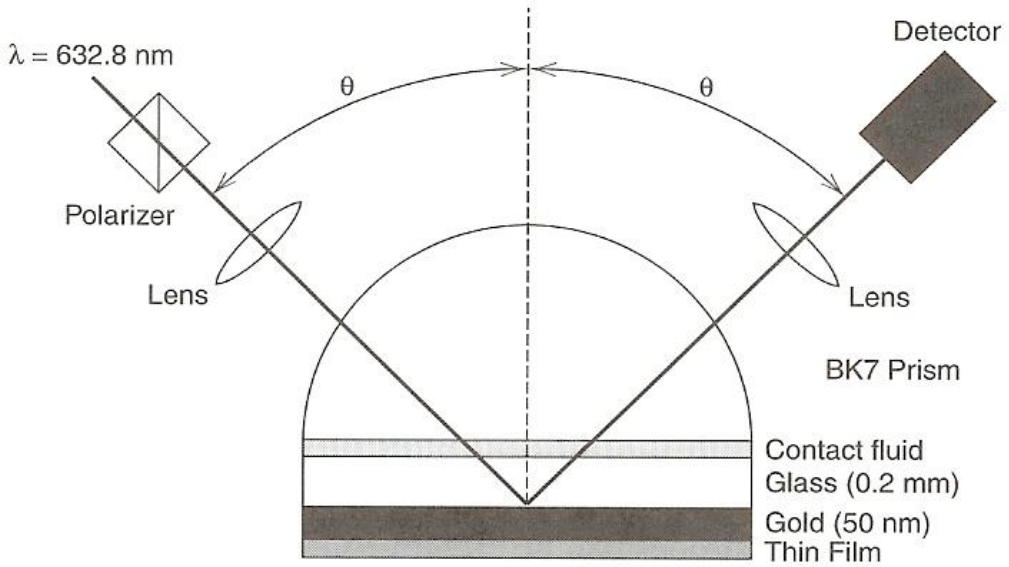

플라스몬(plasmon)이란 금속 내의 자유전자가 집단적으로 진동하는 유사 입자를 말한다. 금속의 나노 입자에서는 플라스몬이 표면에 국부적으로 존재하기 때문에 표면 플라스몬(surface plasmon)이라 부르기도 한다. 그 중에서도 금속 나노 입자에서는 가시~근적외선 대역 빛의 전기장과 플라스몬이 짝지어지면서 광흡수가 일어나 선명한 색을 띠게 된다. (이 경우, 플라스몬과 광자가 결합되어 생성하는 또다른 유사 입자를 플라스마 폴라리톤이라고 한다.) 이 현상을 표면 플라스몬 공명(surface plasmon resonance)이라 하며, 국소적으로 매우 증가된 전기장을 발생시킨다. (위키백과)

Summary

- Ideal flat surface is composed of regular arrays of atoms with an areal density on the order of 10^{15} cm^{-2} (10^{19} m^{-2}).
- Surfaces expose a variety of potential high-symmetry binding sites of different co-ordination numbers.
- Real surfaces always have a number of defects (steps, kinks, missing atoms, etc.).
- Clean surfaces can exhibit either relaxations or reconstructions.
- Relaxations are modest changes in bond lengths and angles.
- Reconstructions are changes in the periodicity of the surface compared to the bulk-terminated structure.
- Two-dimensional solids are materials that are essentially all surface because they are composed of only a single atomic layer, as in graphene, nor a single formula unit, as in MoS_2.
- The properties of 2D solids differ from those of 3D solids composed of multiple layers of 2D materials.
- Porous materials can have internal surface areas that are orders of magnitude larger than their exterior surface areas.
- Adsorbates can form ordered or random structures, and may either distribute themselves homogeneously over the surface or in islands.
- Adsorbates can also cause changes in the surface structure of the substrate inducing either a lifting of the clean surface reconstruction or the formation of an entirely new surface reconstruction.
- The occupation of electronic states is defined by the Fermi-Dirac distribution, Eq. (1.3.5).
- Surface electronic states exist in a bulk band gap.
- A surface resonance has a wavefunction that is concentrated at the surface, but it does not exist in a band gap and, therefore, interacts strongly with bulk states.
- Vibrations in solids are quantized and form bands analogous to the band structure of electronic states.
- The mean phonon occupation number follows the Planck distribution law, Eq. (1.4.7).
- Properties of matter become size dependent as the contributions of surface atoms start to outweigh those of bulk atoms and as quantum confinement effects set in.
- Both the electronic structure and the phonon spectrum change as particle size approaches the nanoscale.